Assessing small-scale degradation patterns in a heterogeneous semi-arid landscape using aerial imagery

A case study in the Sneeuberg rangelands, South Africa

Inauguraldissertation

zur

Erlangung der Würde eines Doktors der Philosophie

vorgelegt der

Philosophisch-Naturwissenschaftlichen Fakultät der Universität Basel

von

Juliane Krenz

aus Frankfurt (Oder), Deutschland

Basel, 2020

Genehmigt von der Philosophisch-Naturwissenschaftlichen Fakultät
auf Antrag von

Prof. Dr. Nikolaus J. Kuhn, Universität Basel
Fakultätsverantwortlicher & Dissertationsleiter

Dr. Holly Croft, Universität Sheffield
Korreferent

Basel, den 25. Juni 2019

Prof. Dr. Martin Spiess
Dekan der Philosophisch-Naturwissenschaftlichen Fakultät

"At first encounter the Karoo may seem arid, desolate and unforgiving, but to those who know it, it is a land of secret beauty and infinite variety."

(Palmer, E., The Plains of Camdeboo. SA Penguin, 2011.)

SUMMARY

Land degradation in drylands is recognised as a global environmental problem that affects ecosystem services negatively. It is mostly prominent in the form of soil degradation, which is defined as a decline in soil quality, caused by soil erosion, contamination, acidification, or salinisation amongst other processes. Despite the vast area covered by drylands and its crucial impact on the environment and human wellbeing, only limited information about the spatial extent of degradation is available. Drylands are characterised by a sparse vegetation cover that is often arranged in a regular or irregular heterogeneous pattern of vegetated and bare soil patches. This is also reflected in heterogeneous chemical, structural, and textural soil properties. Conventional landscape mapping is very time- and labour intense, and this highly dynamic spatial heterogeneity is not depictable on soil maps. Also emerging technologies, as satellite imagery, are not sufficient to detect the small-scale patterns in these heterogeneous landscapes yet. Hence, detailed spatial data on soil types or degradation features are missing. However, it is crucial to evaluate the relevance of processes affecting soil quality, soil redistribution, and biogeochemical cycling in semi-arid landscapes. To address these knowledge gaps, the following three questions frame this research:

1. Is land use-induced patchiness of soil and vegetation a prevalent feature in the Karoo landscape?
2. How can remote sensing products represent the heterogeneity of soil degradation in drylands accurately?
3. Which information from remote sensing products is needed to improve conventional field mapping in heterogeneous landscapes?

A small catchment area in the Karoo rangelands of South Africa was chosen as a representative of a semi-arid ecosystem. The widespread erosional features of various shapes and degrees, such as silted-up reservoirs, incised sediment, badland and gully formation, make this area an ideal study site, where soil redistribution through erosion and deposition has happened and is still on-going. The objectives of the thesis are the documentation of small-scale heterogeneity of a semi-arid rangeland to assess the relevance of human-induced degradation and the development of a method for mapping and quantifying degradation. Soil samples were collected throughout the study site, from areas of various degrees of soil and vegetation degradation, to identify differences in soil properties. The results confirm the patchiness of the soil properties. Soil property patterns do not coincide with the vegetation cover but show a high degree of variability within the same landscape units, especially soil nutrients and total organic carbon. Apart from soil degradation by erosion, sediments trapped behind dams can be identified as a depositional substrate and show strong potential for formation of anthropogenic soils new to rangelands. The derived GIS analysis based on high-

resolution unmanned aerial vehicle (UAV) imagery and data products generated with them proved that this data can contribute to identifying soil degradation with similar accuracy to conventional field mapping. Additionally, UAV derived data was evaluated regarding its suitability to assess badlands as sediment sources. The developed workflow enabled to quantify badlands and obtain best volume estimations for deeply incised badland systems that ideally would have a low amount of vegetation cover.

The lack of globally consistent information on the extent of dryland degradation is a major source of uncertainty in assessing their current role within the global carbon cycle and projecting drylands' future change. The results of this study demonstrate that UAVs provide a valuable tool for low-cost and rapid assessment of soil degradation, particularly in heterogeneous landscapes where manual field sampling is very time consuming and limited to subjective assessments by the surveyor. Substantial improvements in degradation mapping can be achieved, if multispectral UAV imagery is combined with topographic information. Collecting local high-resolution data is needed for the validation and the upscaling to regional or global biogeochemical models. It improves the understanding of the relevance of spatial and temporal dynamics in heterogeneous landscapes under global change.

Keywords

drylands, erosion, landscape mapping, small-scale spatial heterogeneity, soil degradation, reservoir siltation, soil mapping, unmanned aerial vehicle (UAV)

ZUSAMMENFASSUNG

Trockengebiete zeichnen sich neben den geringen unregelmäßigen Niederschlägen durch eine spärliche Vegetationsbedeckung und infolgedessen durch heterogene chemische und strukturelle Bodeneigenschaften aus. Außerdem vereinnahmen sie große Flächen der Erde. Ein globales Umweltproblem, dass sich negativ auf die Ökosystemfunktionen auswirkt, ist die Landdegradierung in Trockengebieten. Die hauptsächlich in Form von Bodenerosion auftretende Verschlechterung der Bodenqualität wird u.a. durch Kontamination, Versauerung und Versalzung verursacht. Trotz der globalen Relevanz des bestehenden Problems gibt es nur begrenzte Informationen über das Ausmaß der Degradierung, da die traditionelle Landschaftskartierung es aufgrund der zeit- und arbeitsintensiven Methoden noch nicht vermag, diese hochdynamischen und räumlichen Heterogenitäten auf herkömmlichen Bodenkarten abzubilden. Auch neue Technologien wie die Kartierung mithilfe von Satellitenbildern sind noch nicht in der Lage, die kleinräumigen Muster in diesen heterogenen Landschaften abzubilden. Aufgrund der fehlenden Daten können keine räumlichen Analysen zu Bodentypen und Degradierungsmustern gemacht werden, die jedoch für die Bewertung der Bodenqualität, die Umverteilung des Bodens und den biogeochemischen Kreislauf in semiariden Landschaften beeinflussenden Prozesse relevant sind. Aus der beschriebenen Situation heraus ergeben sich folgende Forschungsfragen, um die bestehenden fachwissenschaftlichen Lücken zu schließen:

1. Welche Relevanz besitzen die kleinräumigen Muster der Vegetations- und Bodendegradierung in Trockenlandschaften?
2. Wie können Methoden der Fernerkundung die Heterogenität der Bodendegradation in Trockenlandschaften genau darstellen?
3. Welche Informationen von Fernerkundungsprodukten sind für die Verbesserung der traditionellen Feldkartierung in heterogenen Landschaften notwendig?

Als Untersuchungsgebiet wurde – stellvertretend für semiaride Ökosysteme – ein kleines Einzugsgebiet in den Weideländern der Karoo-Halbwüste in Südafrika gewählt. Mit den für dieses Ökosystem charakteristischen Erosionsmerkmalen und Zerstörungsgraden wie versandete Reservoirs, eingeschnittene Sedimente sowie Ödland und Rinnenbildung ist das Gebiet ein geeigneter Untersuchungsort, an dem die Umverteilung des Bodens durch Erosion und Ablagerung bereits stattfand und weiterhin andauert.

Ziel der vorliegenden Arbeit ist die Dokumentation der kleinräumigen Heterogenität des spezifischen semiariden Weidelands, um die Relevanz der anthropogen verursachten Degradierung zu bewerten. Parallel dazu wird eine Methode zur Kartierung und Quantifizierung der Degradierung entwickelt. Für die Identifikation der Unterschiede der Bodeneigenschaften wurden innerhalb des gesamten Untersuchungsgebietes Bodenproben mit unterschiedlicher Intensität der Boden- und Vegetationsdegradierung genommen und das

Untersuchungsgebiet mit einer Drohne überflogen. Wie die Ergebnisse bestätigen, existiert – besonders bei den Bodennährstoffen und dem organischen Kohlenstoff – eine Heterogenität der Bodenparameter. Während die Bodenbeschaffenheit keine signifikanten Differenzen zwischen den verschiedenen Vegetationsbedeckungen zeigt, besitzt sie allerdings ein hohes Maß an Variabilität innerhalb der gleichen Einheiten. Neben der Bodendegradierung durch Erosion wurden akkumulierte Sedimente hinter den Dämmen als neues Substrat identifiziert. Sie zeigen ein starkes Potential für die Bildung neuer anthropogener Böden. Eine weitere Erkenntnis ist, dass die hochauflösenden Drohnenbilder mithilfe einer entwickelten GIS-basierten Analyse zur Identifikation von Bodendegradierung genutzt werden können, wobei die Genauigkeit der Daten mit denen der traditionellen Feldkartierung vergleichbar ist. Außerdem wurden die gewonnen Daten zur Bestimmung der Volumina der Ödlandflächen und deren Beitrag als Sedimentquellen verwendet. Einschränkend ist festzuhalten, dass die Methode zur Quantifizierung nur auf Flächen mit tiefen Sedimenteinschnitten und geringer Vegetationsbedeckung nutzbar ist. Der Mangel an weltweit konsistenten Informationen über das Ausmaß der Degradierung von Trockengebieten ist eine Hauptursache für die Unsicherheiten bei der Beurteilung ihrer aktuellen Rolle im globalen Kohlenstoffkreislauf und bei der Prognose ihrer zukünftigen Veränderungen.

Die Ergebnisse der Studie zeigen, dass Drohnen ein wertvolles Werkzeug für die kostengünstige und schnelle Beurteilung der Bodenverschlechterung – insbesondere in heterogenen Landschaften – sind. Da in diesen Gebieten die Feldkartierung einerseits zeitaufwändig und andererseits bedingt durch subjektive Beurteilungen des Vermessens negativ geprägt sind, können durch den Einsatz multispektraler Daten und topographischer Informationen Verbesserungen bei der Degradierungskartierung erreicht werden. Das Erfassen lokaler hochauflösender Daten für die Validierung und die Hochskalierung auf regionale und globale biogeochemische Modelle ist zwingend notwendig, um das Verständnis für die Bedeutung der räumlichen und zeitlichen Dynamik in heterogenen Landschaften im globalen Wandel zu beurteilen.

Schlagworte

Bodendegradierung, Bodenkartierung, Drohnen, Erosion, kleinräumige Heterogenität, Landschaftskartierung, Trockengebiete, Versandung

CONTENTS

ABBREVIATIONS AND ACRONYMS

a.s.l.	Above sea level
appr.	Approximately
C	Carbon
DEM	Digital Elevation Model
DSM	Digital Surface Model
DTM	Digital Terrain Model
FAO	Food and Agriculture Organization of the United Nations
GIS	Geographic Information System
GLADA	Global Assessment of Land Degradation and Improvement
GLASOD	Global Assessment of Human-induced Soil Degradation
GSD	Ground Sampling Distance
ISRIC	International Soil Reference and Information Centre
LSU	Livestock Unit/Large Stock Unit
LU	Landscape Unit
MTP	Manual Tie Point
NDVI	Normalised Difference Vegetaion Index
NPP	Net Primary Production
Pg	Pentagram
RC	Reservoir Capacity
RGB	Red, Green and Blue
RUSLE	Revised Universal Soil Loss Equation
SOC	Soil Organic Carbon
SOM	Soil Organic Matter
SVM	Support Vector Machine
TIC	Total Inorganic Carbon
TLS	Terrestrial Laser Scanner
TN	Total Nitrogen
TOC	Total Organic Carbon
UAV	Unmanned Aerial Vehicle
UN	United Nations
UNCCD	United Nations Convention to Combat Desertification
US EPA	United States Environmental Protection Agency
vis-NIR	Visible near-infrared
yr	Year

LIST OF FIGURES

LIST OF TABLES

CHAPTER 1

Introduction

1.1 LAND DEGRADATION IN DRYLANDS

1.1.1 THE GLOBAL RELEVANCE OF LAND DEGRADATION

Land degradation can be defined as a temporary or permanent reduction in the capacity of land to perform ecosystem functions and services that support society and development (FAO, 2019; UNCCD, 1994) as for instance agricultural productivity, loss of biodiversity, disruption or alteration of biological cycles, and a decline in water quality (Foley et al., 2005). Despite the high value of ecosystems for human beings, land degradation is primarily caused by human activities (FAO, 2019; UNCCD, 1994), such as deforestation, overgrazing, mismanagement of agricultural land, overexploitation, or industrial activities (Oldeman et al., 1991). These causative factors can influence the ecosystem in three major ways: physically (erosion by wind or water, crusting, compaction, and sealing), chemically (salinisation, sodication, acidification, and pollution), and/or biologically (decline in biodiversity, natural vegetation or organic matter) (Ponce-Hernandez et al., 2004). Soil degradation is a major form of land degradation and refers to the decline of soil quality which has usually negative effects on ecosystem services (FAO et al., 1994; Lal and Stewart, 1990). It can be caused by soil erosion, contamination, acidification, or salinisation amongst other processes (Oldeman et al., 1991).

By releasing carbon (C) sequestered in soil, land degradation contributes significantly to climate change (Dregne, 2002; Lal, 2001a; Montanarella et al., 2018). Mainly induced by deforestation, forest degradation, drying or burning of peatlands, and the decline of carbon in cultivated soils and rangelands, land degradation was estimated to be responsible for releasing 3.6-4.4 billion tonnes of CO_2 annually between 2000 and 2009 (Montanarella et al., 2018). These values are projected to increase further, as soil erosion will accelerate as a result of climate change and anthropogenic pressure. Economically, the loss of biodiversity and ecosystem services will cost more than 10% of the annual global gross product (Montanarella et al., 2018). Hence, there is a widespread desire to map the exact location and severity of degradation for policymakers across authority levels to make better-informed land management decisions, to develop restoration plans e.g. to enhance C sequestration in soils, but also to reduce human migration caused by poor livelihoods and violent conflict over natural resources.

1.1.2 THE IMPORTANCE OF DRYLANDS AND RANGELANDS

Land degradation can occur in any climate zone, however it is mostly attributed to arid, semi-arid and dry sub-humid areas, the so called “drylands” (Hoffman and Ashwell, 2001), where it is referred to as desertification (UNCCD, 1994). Drylands are characterised as areas where the ratio of long-term annual precipitation to potential evapotranspiration is less than 0.65 (UN EMG, 2011). They cover about 40% of the Earth’s land and are home to approximately 40% of the world’s population (Cherlet et al., 2018). Soil degradation affects mostly marginal

semi-arid lands that are used for cultivation. Temperature rises and rainfall pattern changes will enhance the climatic pressure on the dryland ecosystems. In combination with population growth and intensified agricultural activities to meet global food demands, the vulnerability to land degradation in these areas will increase further (FAO, 2004).

As with drylands, rangelands are similarly affected by future climate change and population growth and hence threatened by land degradation and the loss of ecosystem services (Safriel and Adeel, 2005). Rangelands are areas dominated by native vegetation suitable for grazing and browsing, and extensively used by ungulates (US EPA, 2016). They account for 65% of the world's drylands (an area of about 40 Mio km^2), support about 50% of the world's livestock (Safriel and Adeel, 2005), and provide a various number of ecosystem and socio-economic services, such as food supply, recreational opportunities, or biofuel (Gyde Lund, 2007). Although there is disagreement about the proportion of globally degraded rangelands, estimates vary from 18% (Blench and Sommer, 1999) to 73% (Dregne and Chou, 1992), it is acknowledged that many rangelands are in a critical condition (Dregne and Chou, 1992; Gibbs and Salmon, 2015) – which affects the livelihood of millions of people (Montanarella et al., 2018; Safriel and Adeel, 2005). Degradation processes in rangeland systems are still poorly understood and estimates on rangeland health vary widely. Major challenges are inconsistent definitions of degradation, limited spatial extents of field studies, and the complexity of underlying ecological processes, their dynamics, and interrelationships (Jamsranjav et al., 2018).

1.1.3 CARBON CYCLING IN DRYLANDS

The primary degradation hazards are wind and water erosion since they can cause irreversible degradation (Dregne, 2002) which leads inevitably to changes in the carbon cycle and balances (Lal, 2002a). Carbon enters the biosphere mainly via photosynthesis. During gross primary production about 100-150 Pg C are taken up by plants per year (Randerson et al., 2002). The incorporated C is partly lost via natural processes such as plant respiration, litter or soil organic matter (SOM) decomposition, and fires or anthropogenic processes such as deforestation or erosion (FAO, 2004). Dryland soils are generally characterised by low (< 1%) soil organic carbon (SOC) contents, low nutrient reserves, and frequent water stress (Lal, 2002b). Their limited nutrient and water availability constrain their biomass production and lead to a low net primary production (NPP). The sparse and dispersed vegetation can only provide little litter input to increase the amount of sequestered carbon (Figure 1-1). Despite the low C input, dryland soils contain about 241 Gt of SOC (Eswaran et al., 2000). Rangelands store about 30% of the world's terrestrial C (Derner and Jin, 2012; Neely et al., 2009). Unlike croplands, they receive no input of fertilisers that could compensate for damages and losses from degradation, in particular soil erosion (Powell et al., 1996). Consequently, their degradation reduces the ecosystems' C pool and leads to C emissions (Lal, 2004). In addition,

soil redistribution affects SOC quantity and quality (Doetterl et al., 2016). Given the vast area covered by rangelands, enhanced C fluxes linked to land use and cover changes could greatly influence the global C cycle. However, many studies on degradation induced changes in the C cycle focus on water and tillage erosion in agricultural systems (Govers et al., 1996; Gregorich et al., 1998; McCarty and Ritchie, 2002; Van Oost et al., 2007, 2005; Wang et al., 2010; Zhang et al., 2006) and the importance of studies on C fluxes in rangelands is neglected.

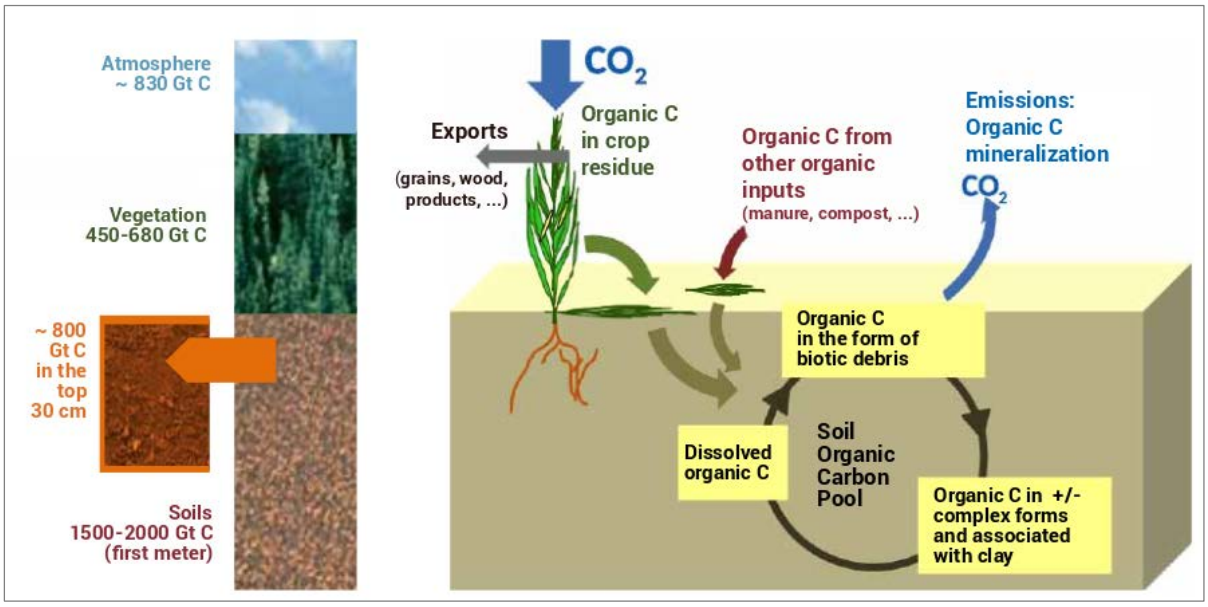

Figure 1-1 Simplified representation of the soil carbon cycle. Soils represent the largest organic carbon pool of the biosphere. Soil erosion and subsequent sediment transport and depositional processes lead to SOC redistribution. Sustainable land management can reduce SOC loss but also increase the stored carbon (UNCCD, 2015).

1.1.4 SPATIAL HETEROGENEITY IN DRYLANDS

Drylands are characterised by a sparse vegetation cover that is often reflected in a regular or irregular heterogeneous pattern of vegetated and bare soil patches (Cammeraat and Imeson, 1999; Deblauwe et al., 2008; Dunkerley and Brown, 1999; Maestre and Cortina, 2002; Valentin et al., 1999). The so called two-phase mosaics of vegetation alternating with bare soil can have various scales and shapes (Rietkerk et al., 2002), such as labyrinths (Rietkerk et al., 2002), gaps (Deblauwe et al., 2008; Rietkerk et al., 2002), spots (Aguiar and Sala, 1999; Couteron and Lejeune, 2001; Soriano et al., 1994), or bands (Cammeraat and Imeson, 1999; Galle et al., 1999; Saco et al., 2007; Valentin et al., 1999). Water dynamics, sediment and nutrient fluxes between the different patches strongly influence the formation, preservation, and alteration of these patchworks (Aguiar and Sala, 1999; Ludwig et al., 2005; Rietkerk et al., 2002; Schlesinger et al., 1990). The vegetation mosaic is also reflected in heterogeneous chemical, structural, and textural soil properties (Schlesinger et al., 1996, 1990), that introduce spatial variations in

factors such as infiltration capacity (Bochet et al., 2000; Cammeraat and Imeson, 1999; Cerdá, 1997), soil nutrient content (Rietkerk et al., 2000; Schlesinger et al., 1996), and soil erodibility (Castillo et al., 1997; Cerdá, 1997; Wynn and Mostaghimi, 2006), and can indicate soil degradation. Not only natural causes, like a change in rainfall can influence these patterns but also anthropogenic pressure. Land use affects surface processes, vegetation cover, and soil properties of drylands, often leading to redistribution of soil through erosion and deposition and thus creating a patchwork of soils different from their natural conditions (Ludwig et al., 2005; Rietkerk et al., 2002). The spatial heterogeneity of dryland landscapes is highly dynamic and indicates that the underlying soil types are inherently complex and often show a higher variability than can be depicted on soil maps. This underlines the demand for more detailed studies of rangeland soil systems. It is important to document and understand small-scale variability in rangeland soils to assess how different processes affect soil quality.

1.1.5 MONITORING AND ASSESSING LAND DEGRADATION

Although land degradation is recognised as a global environmental and development issue (Cherlet et al., 2018), there is still a lack of understanding about the spatial extent. Estimations of degraded land vary from 1 billion ha (Oldeman et al., 1991) up to extreme estimates of 6 billion ha (Bot et al., 2000) due to different used methodological approaches (Gibbs and Salmon, 2015). Assessing land degradation depends on the type of degradation (physical, chemical, biological), and the methods range from simple qualitative field observations to modelling of complex ecological processes.

Conventional methods for land degradation assessment are often based on expert or land user's opinions (Aber et al., 2010; Kapalanga, 2008), such as the Global Assessment of Human-induced Soil Degradation (GLASOD) (Oldeman et al., 1991). The GLASOD report is up to date the only complete globally consistent information source on land degradation. Despite its drawbacks, such as the dependence on local expert knowledge and hence introduced subjectivity, or the coarse spatial resolution of the produced 1:10 million map, the results have been widely used in other studies (Batjes, 2019; Pimentel et al., 1995; Sonneveld and Dent, 2009). The Land Degradation Assessment in Drylands (LADA) executed by the FAO (FAO 2011a, 2011 b) tries to close the gap between policy and institutional barriers to sustainable land use and management practices at the local level. It provides a monitoring and assessment system that can be used at various levels, from global to local scale (Nachtergaele and Licona-Manzur, 2009), thanks to its multi-disciplinary approach based on field surveys and remote sensing analysis.

For soil degradation assessment at a local or catchment scale, field surveys, including observations, monitoring and measurements are needed. Field surveys using diagnostic criteria are the easiest to apply but they are very time-consuming. Their subjective rating, even if assessment forms are used, make it difficult to compare assessments produced by multiple

surveyors. Field measurements such as erosion pins (Boardman et al., 2015) or sediment traps (Luce and Black, 1999) can be used to calculate erosion rates but need a large amount of measurements. They are time- and labour-intense and therefore only suitable for assessing small areas. Terrestrial laser scanning or total stations can be used to generate high-precision terrain models for small-scale detailed erosion mapping (Eitel et al., 2011; Stöcker et al., 2015; Vinci et al., 2015). These methods are very expensive, time-taking, labour-intensive and depend on the accessibility of the geomorphic features. The dissected character of degraded drylands complicates ground-based terrain mapping and often requires positional changes of the devices to recover obstructions from the laser's field view (Brodu and Lague, 2012). Recently developed methods such as remote sensing and unmanned aerial vehicles (UAVs) offer a promising approach to overcome constraints faced with traditional field methods.

1.1.6 THE ROLE OF REMOTE SENSING AND UAVS

Several efforts over the past two decades have attempted to move beyond subjective assessments to more quantitative approaches of soil degradation. The development of geographical information system (GIS) tools and the relative ease in accessing satellite imagery has enabled researchers to study land use and land cover change across space and time (Joshi et al., 2016; Rogan and Chen, 2004). The value of remote sensing for mapping landscape attributes is clear, since it offers objective, repeated measurements over wide areas at reasonable costs (Lobell, 2010). Studies on monitoring and assessing dryland ecosystems (Geerken et al., 2005; Geerken and Ilaiwi, 2004; Rango et al., 2009), their vegetation change (Andela et al., 2013; Wingate et al., 2018, 2016) or environmental properties such as biological crusts (Rodríguez-Caballero et al., 2015) have increased rapidly in the last decades. Besides the wide field of applications, the use of remote sensing in soil sciences is limited since they cannot directly measure traditional indicators of soil quality, such as soil organic carbon (SOC) content (Lobell, 2010). To address this problem, vegetation indices are often used as proxies for local soil measurements. An equivalent to the expert-opinions based GLASOD study is the Global Assessment of Land Degradation and Improvement project (GLADA). GLADA is the first quantitative assessment of land degradation. It is based on the remotely-sensed normalised difference vegetation index (NDVI) (Bai et al., 2010, 2008a, 2008b) which has been suggested as a proxy for land degradation among others by Wessels et al. (2007, 2004). NDVI is sensitive to the green vegetation components, since it is derived from the reflectance of the red and near-infrared bands (Tucker, 1979). A large proportion of dryland vegetation is non-photosynthetic, either dead, woody or dormant between rainfall events. Hence, NDVI assessments in drylands are complicated by the sparse vegetation, depend on the phenological cycle and fluctuate seasonally (Schmidt and Karnieli, 2000).

Considering the heterogeneity of drylands, spatial patterns are much smaller than what can be pictured on commonly available satellite images, and the resolution is usually not

sufficient to calculate sediment losses accurately (Laliberte et al., 2011; Mondal et al., 2017a, 2017b). In the last decade, UAVs have gained increasing popularity among scientists in remote sensing because they offer new opportunities for collecting spatial environmental data at high-resolution, especially for study areas in rough and remote terrain (Griffiths, 2006) UAVs allow fast data acquisition and generation of user-specific data products, such as digital surface or terrain models (DSM/DTM), orthomosaics, or NDVI maps. Several studies have investigated the use of UAVs in degrading landscapes to monitor or assess the extent of gullies (d'Oleire-Oltmanns et al., 2012; Marzolff and Poesen, 2009; Stöcker et al., 2015; Wang et al., 2016), rills and interill erosion (Eltner et al., 2015a), or badlands (d'Oleire-Oltmanns et al., 2012; Neugirg et al., 2016; Nobajas et al., 2017). In combination with terrestrial images, UAVs can fill data gaps of missing information such as from overhanging gully walls (Stöcker et al., 2015). Workflows for remote sensing of rangelands have been described amongst others by Laliberte et al.(2011) and Rango et al. (2009).

Land degradation mapping studies based on aerial photographs (from satellites or UAVs) focus mainly either on a change in vegetation (Dube et al., 2017; Jong et al., 2011; Laliberte et al., 2011; Wessels et al., 2008) or major soil degradation features (Mararakanye and Roux, 2012; Wang et al., 2016), but do not consider the actual identification of small-scale degradation hotspots and their potential relevance for soil degradation.

1.1.7 LAND DEGRADATION IN SOUTH AFRICA

South Africa comprises up to 99% of drylands (Hoffman and Ashwell, 2001), making it very susceptible to land degradation. About 29% of the land are already degraded (Bai and Dent, 2007), and 81% are considered to be affected by land degradation, making it to one of the most severe environmental problems in the country (Hoffman and Ashwell, 2001; Hoffman and Todd, 2000). About 17 million people (38% of the population) live in degrading, mainly communal, areas (Bai and Dent, 2007).

Research on land degradation has a long history in South Africa (Acocks, 1975; Hoffman and Cowling, 1990). There is considerable evidence that South African soils are deteriorating due to poor land management practices (du Preez et al., 2018) and suffering an average NPP loss of 29 kg C ha^{-1} yr^{-1} (Bai and Dent, 2007). Severely degraded areas as mapped by Hoffman and Ashwell (2001) are often characterised by a communal land tenure system and have been part of the former "homelands" during the Apartheid, such as the former Ciskei, Transkei, and KwaZulu and the communally farmed areas in the Limpopo and North-Western Province. These areas are significantly more degraded than commercial areas according to the assessment of their soil and vegetation degradation, probably as a result of precipitation changes and geomorphological factors (Meadows and Hoffman, 2003). Apart from land management and overstocking, the abandonment of marginal cultivated land seems to be another major driver of land degradation in the country (Kakembo and Rowntree, 2003).

In the Karoo, land degradation results in enhanced soil erosion by overland flow and the development of gullies (dongas) (Boardman, 2014; Boardman et al., 2003), by sediment export through river systems (Foster et al., 2012, 2008), or by deflation as in the Free State (Wiggs and Holmes, 2011). The Karoo occupies about one third of the total area of South Africa (Dean et al., 1995) and is a hotspot of degradation (Hoffmann et al., 1999) due to its semi-arid nature and the associated rainfall variability (Knight and Holmes, 2018). Large parts of the landscape are dissected by ephemeral drainage lines that are episodically active after heavy infrequent storms (Knight and Holmes, 2018) and increase the sediment yield to downstream areas (Foster et al., 2012). Net erosion rates are high and far above the suggested tolerable soil loss rate of 10 t ha^{-1} yr^{-1} and the predicted national average of 12.6 t ha^{-1} yr^{-1} (Le Roux et al., 2008). Boardman et al. (2017, 2015) calculated rates in the range of 41-145 t ha^{-1} yr^{-1} based on erosion pin measurements over ten sites for the Sneeuberg region.

1.2 THE KAROO RANGELANDS AS A DYNAMIC AND VULNERABLE LANDSCAPE

1.2.1 PAST RESEARCH CONDUCTED

The Sneeuberg Mountains north of Graff-Reinet have been in focus of land degradation and geormorphological research since the late 1990s (Fox and Rowntree, 2013). Holmes et al. (2003) and Holmes (2001, 1998) studied the palaeoenvironments of Great Karoo headwater catchments and proposed that incision of Sneeuberg valley-fills appeared to post-date European colonisation. Boardman and other colleagues intensively study land degradation in the Sneeuberg uplands since 2001. They started a long-term erosion experiment and are since then measuring erosion pins on badlands annually (Boardman et al., 2015). Various studies have been conducted on the environmental history of the Sneeuberg uplands looking at badland and gully erosion and their changes (Boardman et al., 2003; Boardman and Foster, 2008; Rowntree, 2014). Others have paid attention on land degradation with a focus on sediment dynamics in small farm dams (Foster et al., 2012, 2008, 2005; Keay-Bright and Boardman, 2009; Rowntree and Foster, 2012). Dickie and Parsons (2012) studied the heterogeneity of soil parameters between grassland and shrub communities and their influence to the susceptibility of soil erosion. They concluded that the self-perpetuating nature of semi-arid shrubs caused a redistribution in soil parameters which can exacerbate soil erosion. A mixture of land management (Keay-Bright and Boardman, 2007, 2006; Mighall et al., 2012), climate, and changes in connectivity between sediment source and storage areas and reservoirs are generally believed as drivers of land degradation in this area (Foster et al., 2012). In sum, erosion studies in the Sneeuberg area mostly looked at amounts of total soil loss and/or deposition of entire catchments (Boardman et al., 2015) while within-catchment spatial patterns of erosion and accumulation have not yet been examined in detail.

1.2.2 ENVIRONMENTAL AND HISTORICAL SETTINGS IN THE KAROO RANGELANDS

The study area (31.69899°S, 24.587650°E) is located in the Klein Seekoei River basin in the northern Great Karoo of South Africa, approximately 70 km north of the small town Graaff-Reinet. It is part of the Sneeuberg Range, a landscape of flat and gently sloping plains interspersed with hills and mountain ranges extending from 1650 up to 2502 m a.s.l. at the Compassberg, and forms part of the Great Escarpment.

The semi-arid landscape is particularly vulnerable to erosion due to the seasonality of rainfall, its impact on vegetation, and the occurrence of drought. Surveys using aerial photographs of the area estimated roughly 15 to 25% of the land as moderately to severely degraded (Boardman et al., 2003; Keay-Bright and Boardman, 2006). Landscape degradation is mainly characterised by the widespread presence of intensely dissected colluvial footslopes (badlands) and incised channels (dongas) in the valley bottoms (Boardman et al., 2003). Both presumably have reduced the agricultural productivity, altered the hydrological cycle, and increased the sediment yield in downstream areas (Foster et al., 2012). The sediment in the area largely leads to the siltation of reservoirs. Approximately half of the 106 storage reservoirs Boardman and Foster (2011) have located in the Sneeuberg area are full of sediment with little or no water storage capacity. These observations show that land degradation and soil redistribution are happening widely in the Sneeuberg area. Incision of these sediments has resulted in the formation of badlands and gullies (Boardman et al., 2003).

The Sneeuberg landscape has probably been modified since the establishment of European farmlands in the 1770s (Boardman et al., 2003). The primary land use was stock grazing of cattle, sheep, and goats (Boardman et al., 2003). Secondarily, alfalfa, potatoes, and rain-fed wheat were grown on the valley bottoms but droughts caused frequent crop failure (Boardman et al., 2003; Boardman and Foster, 2008). Stock densities varied widely across the region but peaked in the 1930s. Overall stock densities for the Middelburg District between 1865 and 1961 were two to three times higher than in 1995 (4.6 large stock units/km^2) and were above the average for the Karoo (Boardman et al., 2003). The high stock numbers and less appropriate management practices in the early 20th century coupled with droughts may have converted marginal grasslands to shrublands and presumably caused much of the land degradation seen nowadays (Boardman et al., 2003; Keay-Bright and Boardman, 2007). Today, domestic stock (sheep, cattle, and goats) have largely replaced the migratory herds of ungulates and some game farms have been established.

The study area was, unlike other catchments, only used for grazing and thus represents a simple environment to assess cause and effect of land degradation on soil properties. It is part of a watershed that covers a total area of 3.2 km^2 and drains into the filled reservoir labelled as Dam 53 (31.698558°S, 24.588183°E) by Boardman and Foster (2011). The reservoir is located at appr. 1740 m a.s.l. and surrounded by hills up to 2080 m a.s.l. An appr. 140 m long earth dam

wall was probably constructed in the 1930s and breached in 1974 (Boardman et al., 2017). A main gully up to 6 m deep and up to 10 m wide follows the thalweg of the catchment and forms the breach in the dam wall. The catchment has a clearly defined gully system and some badlands.

1.2.3 CLIMATE

The Sneeuberg Mountain range is situated within the Eastern part of the Warm Temperate Zone (Sugden, 1989). Due to its increased altitude, the Sneeuberg uplands are rather cooler and wetter than the Karoo plains. January is usually the warmest month but both diurnal and seasonal temperatures show large fluctuations (Boardman et al., 2003). Summer maxima can reach up to 40 °C and winter minima below -10 °C.

Average annual rainfall (1988-2007) at Compassberg farm is 498 mm (Boardman and Foster, 2008). A summer rainfall regime is characteristic, where approximately 70% of the annual precipitation is received between October and March (Keay-Bright and Boardman, 2007). Although the study area lies within the semi-arid climate region, extreme rainfall events are relatively frequent. Rainfall analysis from weather stations close to the study area showed a significant increase in extreme events between 1931 and 1990 (Mason et al., 1999). According to their estimations, the area experienced a 10-20% increase in intensity of 10-year rainfall events. Foster et al., (2012) showed a shift in the magnitude-frequency relationship of daily rainfall since 1950 for the Middleburg station (appr. 60 km Northeast of study area). Besides an extreme change between the analysed time-periods (1900 to 1950 and 1951 to 2000), where the daily rainfall that previously had an 80-year return-period now has a greatly increased frequency with a return period of only 6 years, the long term mean rainfall seems to be constant.

1.2.4 LITHOLOGY

The geology of the Sneeuberg area is dominated by the Karoo supergroup (Watkeys, 1999). Jurassic dolerite sills, sheets, and dykes have intruded the older sandstones from the Early Triassic Katberg formation (Upper Beaufort Group) and mudstones of the Late Permian Balfour Formation (Lower Beaufort) (Catuneanu et al., 2005; Viglietti et al., 2017). The dominant Compassberg Peak is a dolerite pluton. The headwater valley of the Klein Seekoei River is characterised by dolerite hills while valleys are comprised of less resistant Balfour Formation mudstones, shales, and sandstones covered with thin layers of unconsolidated Late Quaternary sediments (Boardman et al., 2003; Holmes et al., 2003).

1.2.5 SOILS

Soil formation in semi-arid environments is limited by water availability, if available only sparsely, which inhibits chemical weathering of rocks and decomposition processes (Fang and Moncrieff, 2001; Ravi et al., 2010; Sugden, 1989). Thus, Sneeuberg soils are shallow, weakly structured and usually comprise thin and coarse regolith components (Sugden, 1989). They are mainly derived from in situ weathering of the underlying doleritic material, silt, mud- or claystones (Watkeys, 1999). Valley bottoms are often in-filled with thick accumulations of alluvial and colluvial material (Keay-Bright and Boardman, 2006). According to the Soil and Terrain Database for South Africa soils are described as lithic leptosols, "very shallow soils on hard or weathered rock that limit root growth" (ISRIC, 2006). The soils often lack a modern A horizon presumably due to high erosion rates (Boardman et al., 2003). This is particularly true for badland and severely degraded areas with compacted surfaces. The study site is predominantly characterised by soils with a high sand content, such as sandy loam and loamy sand and low organic carbon content (< 2%).

1.2.6 VEGETATION

The Sneeuberg Mountain range is a meeting place of several biomes as a result of major climatic, topographic, and geological transitions (Cowling, 1983). It lies on the boundary between the Nama-Karoo biome and the Grassland biome. More specifically vegetation is classified as False Upper Karoo in the valleys and *Merxmuellera* Mountain Veld on the hillslopes (Acocks, 1975), or Karoo Escarpment Grassland, Eastern Upper Karoo and Upper Karoo Hardeveld on the slopes (Mucina and Rutherford, 2006). The grassland units are characterised as extensive semi-arid rangelands with a combination of grasses, annual forbs, and a few dwarf shrubs (< 1 m tall)(Mucina and Rutherford, 2006). The unpalatable *Merxmuellera disticha* is the dominant species in these grasslands (Palmer et al., 1999). However, pure grasslands are rare, shrubs are often interspersed and bare patches are common. Trees occur only along drainage lines (Esler and Archer, 2018). Clark et al. (2009) investigated the vegetation in the Sneeuberg region intensively and described it as a floristic centre of endemism on the Great Escarpment.

1.3 KNOWLEDGE GAPS AND RESEARCH QUESTIONS

Land degradation in drylands is recognised as a global environmental problem (Bai et al., 2008a; Berhe et al., 2005; FAO, 2004; Lal, 2001b; Oldeman et al., 1991). Despite emerging technologies, there is only limited information on its spatial extent, especially on small-scale patterns in these heterogeneous landscapes. Given the vast area covered by rangelands and their highly dynamic spatial heterogeneity, changes in nutrient and carbon fluxes could greatly influence the global carbon cycle (FAO, 2004; Lal, 2004). The underlying soil types are

inherently complex but their large variability is usually not depictable in conventional soil maps. Hence, detailed spatial data on the soil types or degradation features are missing, but would be crucial to evaluate the relevance of processes affecting soil quality, soil redistribution, and biogeochemical cycling in semi-arid landscapes. This indicates the need for detailed studies on rangeland soil systems and the development of methods to investigate degradation in these highly heterogeneous landscapes at a representative level.

The Karoo rangelands are representative of a semi-arid ecosystem. With their widespread erosional features of various shapes and degrees, such as silted-up reservoirs, incised sediments, badland, and gully formation they are an ideal study site where soil redistribution through erosion and deposition has happened and is still on-going. While many studies about erosion in the Karoo focused on the sediment yield of single catchments, within-catchment spatial patterns of erosion and accumulation have not yet been studied in detail.

Hence, the following research questions were defined:

1. Is land use-induced patchiness of soil and vegetation a prevalent feature in the Karoo landscape?
2. How can remote sensing products represent the heterogeneity of soil degradation in rangelands accurately?
3. Which information from remote sensing products is needed to improve or maybe even replace traditional field mapping in heterogeneous landscapes?

Based on the research questions, the primary objectives of this thesis are to (i) document small-scale spatial heterogeneity of an exemplary degraded semi-arid rangeland to assess the relevance of human-induced degradation and to (ii) develop a method for mapping and quantifying degradation.

Chapter 2 provides an overview of the current state of soil and degradation in the studied catchment. The spatial heterogeneity of soil and vegetation was mapped and investigated based on field observations and soil sampling. Subsequently, chapter 3, aims to evaluate the identified sediment sink and source areas quantitatively. Therefore, UAV imagery was used to generate high resolution DTMs of badland features to investigate the suitability and potentials of UAV imagery for erosion and deposition volume assessments. In chapter 4 the spatial extent of soil degradation was mapped using an UAV-derived orthomosaic and two approaches for the development of a representative degradation feature map were developed. Since traditional field surveys of degradation are very time-intensive, low-cost automated solutions that can deliver the same level of detail are needed. An inexpensive and commercially available UAV equipped with a conventional camera was chosen because it offers the greatest potential for wide application in soil and land management. Based on the aim to develop a method which can be easily adapted under multiple conditions and to be

independent of seasonal water availability and phenological cycles, the conventional camera of the UAV was preferred over a multispectral camera.

1.4 THESIS STRUCTURE

Chapter 2

1.4.1 RESEARCH PAPER I - SMALL-SCALE SOIL HETEROGENEITY ON DEGRADED RANGELANDS IN THE SOUTH AFRICAN GREATER KAROO

Authors: Juliane Krenz, Philip Greenwood & Nikolaus J. Kuhn

Status: in prep., target journal: Journal of Arid Landscapes

Short Abstract:

The study consists of a high-resolution field mapping of soil redistribution in a degraded Karoo rangeland, including a silted-up reservoir. In addition, soil sampling was used to assess the relevance of soil heterogeneity within the catchment. The results confirm the patchiness of the soil properties. Most notably, nutrient contents were significantly greater in vegetated (Grassland: TOC 1.10%, TN 0.10%, Mixed Vegetation: TOC 0.93%, TN 0.08%) than in degraded areas (TOC 0.47%, TN 0.4%). On the former reservoir, sediments differ remarkably from the surrounding soils due to their depth and texture, as well water supply, vegetation, and manure input. Consequently, the sediments show a strong potential for formation of anthropogenic soils new to rangelands.

Chapter 3

1.4.2 RESEARCH PAPER II - ASSESSING BADLAND SEDIMENT SOURCES USING UNMANNED AERIAL VEHICLES

Authors: Juliane Krenz & Nikolaus J. Kuhn

Status: Published in: Badland Dynamics in a Context of Global Change, 2018, ELSEVIER

Short Abstract:

This study investigates the use of UAVs for generating high resolution DTMs of badlands in a remote catchment in the Karoo highveld in South Africa. The catchment is affected by severe soil erosion and reservoir siltation, but the relevance of badlands as sediment source is unclear. The chapter describes UAV hardware, image capturing, DTM, and orthomosaic generation and a workflow for badland erosion estimation with the acquired imagery. The results show that erosion volumes in badlands accounted for only 17.2% of the reservoir storage capacity in the study area, which indicates that there are additional sediment sources within the catchment.

Chapter 4

1.4.3 RESEARCH PAPER III - SOIL DEGRADATION MAPPING IN DRYLANDS USING UAV DATA

Authors: Juliane Krenz, Philip Greenwood & Nikolaus J. Kuhn

Status: Published in Soil Systems, 2019

Short Abstract:

Arid and semi-arid landscapes often show a patchwork of bare and vegetated spaces. Their heterogeneous patterns can be of natural origin, but may also indicate soil degradation. This study investigates the use of UAV imagery to identify the degradation of soil, based on the hypothesis that vegetation cover can be used as a proxy for estimating the soils' health status. To assess the quality of the UAV-derived products, we compare a conventional field derived map with two modelled maps based on (i) vegetation cover, and (ii) vegetation cover, topographic information, and a flow accumulation analysis.

Chapter 5

1.4.4 SYNTHESIS AND OUTLOOK

The final chapter summarised the primary results from the different research papers and then discusses the major findings and limitations with reference to the research questions raised. As a last point, potential further research opportunities and improvements are debated.

1.5 REFERENCES

Aber, J.S., Marzolff, I., Ries, J.B., 2010. Chapter 17 - Soil Mapping and Soil Degradation, in: Small-Format Aerial Photography. Elsevier, Amsterdam, pp. 229–231. https://doi.org/10.1016/B978-0-444-53260-2.10017-1

Acocks, J.P.H., 1975. Veld types of South Africa. Botanical survey memoir, No. 40, Pretoria.

Aguiar, M.R., Sala, O.E., 1999. Patch structure, dynamics and implications for the functioning of arid ecosystems. Trends Ecol. Evol. 14, 273–277. https://doi.org/10.1016/S0169-5347(99)01612-2

Andela, N., Liu, Y.Y., Van Dijk, A., De Jeu, R.A.M., McVicar, T.R., 2013. Global changes in dryland vegetation dynamics (1988–2008) assessed by satellite remote sensing: combining a new passive microwave vegetation density record with reflective greenness data. Biogeosci Discuss 10, 8749–8797.

Bai, Z.G., de Jong, R., van Lynden, G.W.J., 2010. An update of GLADA—Global assessment of land degradation and improvement. ISRIC Rep. 8, 58.

Bai, Z.G., Dent, D.L., 2007. Land degradation and improvement in South Africa. 1. Identification by remote sensing. (No. 2007/03). ISRIC, Wageningen.

Bai, Z.G., Dent, D.L., Olsson, L., Schaepman, M.E., 2008a. Global assessment of land degradation and improvement. 1. Identification by remote sensing. (No. Report 2008/1). ISRIC, Wageningen.

Bai, Z.G., Dent, D.L., Olsson, L., Schaepman, M.E., 2008b. Proxy global assessment of land degradation. Soil Use and Manag. 24(3), 223-234.

Batjes, N.H., 2019. Technologically achievable soil organic carbon sequestration in world croplands and grasslands. Land Degrad. Dev. 30, 25–32. https://doi.org/10.1002/ldr.3209

Berhe, A.A., Harden, J.W., Harte, J., Torn, M.S., 2005. Soil Degradation and Global Change: Role of Soil Erosion and Deposition in Carbon Sequestration.

Boardman, J., 2014. How old are the gullies (dongas) of the Sneeuberg uplands, Eastern Karoo, South Africa? CATENA 113, 79–85. https://doi.org/10.1016/j.catena.2013.09.012

Boardman, J., Favis-Mortlock, D., Foster, I., 2015. A 13-year record of erosion on badland sites in the Karoo, South Africa: A 13-Year Record of Erosion on Badland Sites in the Karoo. Earth Surf. Process. Landf. 40, 1964–1981. https://doi.org/10.1002/esp.3775

Boardman, J., Foster, I., 2008. Badland and gully erosion in the Karoo, South Africa. J. Soil Water Conserv. 63, 121A-125A. https://doi.org/10.2489/jswc.63.4.121A

Boardman, J., Foster, I.D.L., 2011. The potential significance of the breaching of small farm dams in the Sneeuberg region, South Africa. J. Soils Sediments 11, 1456–1465. https://doi.org/10.1007/s11368-011-0425-5

Boardman, J., Foster, I.D.L., Rowntree, K.M., Favis-Mortlock, D.T., Mol, L., Suich, H., Gaynor, D., 2017. Long-term studies of land degradation in the Sneeuberg uplands, eastern Karoo, South Africa: A synthesis. Geomorphology 285, 106–120. https://doi.org/10.1016/j.geomorph.2017.01.024

Boardman, J., Parsons, A.J., Holland, R., Holmes, P.J., Washington, R., 2003. Development of badlands and gullies in the Sneeuberg, Great Karoo, South Africa. CATENA 50, 165–184. https://doi.org/10.1016/S0341-8162(02)00144-3

Bochet, E., Poesen, J., Rubio, J.L., 2000. Mound development as an interaction of individual plants with soil, water erosion and sedimentation processes on slopes. Earth Surf. Process. Landf. 25, 847–867. https://doi.org/10.1002/1096-9837(200008)25:8<847::AID-ESP103>3.0.CO;2-Q

Bot, A., Nachtergaele, F., Young, A., 2000. Land resource potential and constraints at regional and country levels. Food & Agriculture Org.

Brodu, N., Lague, D., 2012. 3D terrestrial lidar data classification of complex natural scenes using a multi-scale dimensionality criterion: Applications in geomorphology. ISPRS J. Photogramm. Remote Sens. 68, 121–134. https://doi.org/10.1016/j.isprsjprs.2012.01.006

Cammeraat, L.H., Imeson, A.C., 1999. The evolution and significance of soil–vegetation patterns following land abandonment and fire in Spain. CATENA 37, 107–127. https://doi.org/10.1016/S0341-8162(98)00072-1

Castillo, V.M., Martinez-Mena, M., Albaladejo, J., 1997. Runoff and Soil Loss Response to Vegetation Removal in a Semiarid Environment. Soil Sci. Soc. Am. J. 61, 1116–1121. https://doi.org/10.2136/sssaj1997.03615995006100040018x

Catuneanu, O., Wopfner, H., Eriksson, P.G., Cairncross, B., Rubidge, B.S., Smith, R.M.H., Hancox, P.J., 2005. The Karoo basins of south-central Africa. J. Afr. Earth Sci. 43, 211–253. https://doi.org/10.1016/j.jafrearsci.2005.07.007

Cerdá, A., 1997. The effect of patchy distribution of Stipa tenacissima L. on runoff and erosion. J. Arid Environ. 36, 37–51. https://doi.org/10.1006/jare.1995.0198

Cherlet, M., Hutchinson, C., Reynolds, J., Hill, J., Sommer, S., von Maltitz, G. (Eds.), 2018. World Atlas of Desertification, 3rd ed. Publication Office of the European Union, Luxembourg.

Clark, V.R., Barker, N.P., Mucina, L., 2009. The Sneeuberg: A new centre of floristic endemism on the Great Escarpment, South Africa. South Afr. J. Bot. 75, 196–238. https://doi.org/10.1016/j.sajb.2008.10.010

Couteron, P., Lejeune, O., 2001. Periodic spotted patterns in semi-arid vegetation explained by a propagation-inhibition model. J. Ecol. 89, 616–628. https://doi.org/10.1046/j.0022-0477.2001.00588.x

Dean, W.R.J., Hoffinan, M.T., Meadows, M.E., Milton, S.J., 1995. Desertification in the semi-arid Karoo, South Africa: review and reassessment. J. Arid Environ. 30, 247–264. https://doi.org/10.1016/S0140-1963(05)80001-1

Deblauwe, V., Barbier, N., Couteron, P., Lejeune, O., Bogaert, J., 2008. The global biogeography of semi-arid periodic vegetation patterns. Glob. Ecol. Biogeogr. 17, 715–723. https://doi.org/10.1111/j.1466-8238.2008.00413.x

Derner, J.D., Jin, V.L., 2012. Chapter 6 - Soil Carbon Dynamics and Rangeland Management, in: Liebig, M.A., Franzluebbers, A.J., Follett, R.F. (Eds.), Managing Agricultural Greenhouse Gases. Academic Press, San Diego, pp. 79–92. https://doi.org/10.1016/B978-0-12-386897-8.00006-1

Dickie, J.A., Parsons, A.J., 2012. Eco-geomorphological processes within grasslands, shrublands and badlans in the semi-arid Karro, South Africa. Land Degrad. Dev. 23, 534–547. https://doi.org/10.1002/ldr.2170

Doetterl, S., Berhe, A.A., Nadeu, E., Wang, Z., Sommer, M., Fiener, P., 2016. Erosion, deposition and soil carbon: A review of process-level controls, experimental tools and models to address C cycling in dynamic landscapes. Earth-Sci. Rev. 154, 102–122. https://doi.org/10.1016/j.earscirev.2015.12.005

d'Oleire-Oltmanns, S., Marzolff, I., Peter, K., Ries, J., 2012. Unmanned Aerial Vehicle (UAV) for Monitoring Soil Erosion in Morocco. Remote Sens. 4, 3390–3416. https://doi.org/10.3390/rs4113390

Dregne, H.E., 2002. Land Degradation in the Drylands. Arid Land Res. Manag. 16, 99–132. https://doi.org/10.1080/153249802317304422

Dregne, H.E., Chou, N.-T., 1992. Global desertification dimensions and costs. Degrad. Restor. Arid Lands 73–92.

du Preez, C.C., Kotzé, E., van Huyssteen, C.W., 2018. Southern African soils and their susceptibility to degradation, in: Holmes, P.J., Boardman, J. (Eds.), Southern African Landscapes and Environmental Change, Earthscan Studies in Natural Resource Management. Routledge, Taylor & Francis Group, London ; New York, NY, pp. 29–52.

Dube, T., Mutanga, O., Sibanda, M., Seutloali, K., Shoko, C., 2017. Use of Landsat series data to analyse the spatial and temporal variations of land degradation in a dispersive soil environment: A case of King Sabata Dalindyebo local municipality in the Eastern Cape Province, South Africa. Phys. Chem. Earth Parts ABC 100, 112–120. https://doi.org/10.1016/j.pce.2017.01.023

Dunkerley, D.L., Brown, K.J., 1999. Banded vegetation near Broken Hill, Australia: significance of surface roughness and soil physical properties. CATENA 37, 75–88. https://doi.org/10.1016/S0341-8162(98)00056-3

Eitel, J.U.H., Williams, C.J., Vierling, L.A., Al-Hamdan, O.Z., Pierson, F.B., 2011. Suitability of terrestrial laser scanning for studying surface roughness effects on concentrated flow erosion processes in rangelands. CATENA 87, 398–407. https://doi.org/10.1016/j.catena.2011.07.009

Eltner, A., Baumgart, P., Maas, H.-G., Faust, D., 2015. Multi-temporal UAV data for automatic measurement of rill and interrill erosion on loess soil. Earth Surf. Process. Landf. 40, 741–755. https://doi.org/10.1002/esp.3673

Esler, K.J., Archer, E., 2018. Southern African biomes, in: Holmes, P.J., Boardman, J. (Eds.), Southern African Landscapes and Environmental Change, Earthscan Studies in Natural Resource Management. Routledge, Taylor & Francis Group, London ; New York, NY, pp. 75–90.

Eswaran, H., Reich, P.F., Kimble, J.M., Beinroth, F.H., Padamnabhan, E., Moncharoen, P., 2000. Global carbon stocks, in: Lal, R., Kimble, J.M., Eswaran, H., Stewart, B.A. (Eds.), Global Climate Change and Pedogenic Carbonates. Lewis Publishers, Boca Raton, Florida, pp. 15–25.

Fang, C., Moncrieff, J.B., 2001. The dependence of soil CO2 efflux on temperature. Soil Biol. Biochem. 33, 155–165. https://doi.org/10.1016/S0038-0717(00)00125-5

FAO (Ed.), 2019. Degradation/Restoration | FAO SOILS PORTAL | [WWW Document]. URL http://www.fao.org/soils-portal/soil-degradation-restoration/en/ (accessed 24.04.19).

FAO (Ed.), 2011a. Manual for local level assessment of land degradation and sustainable land management, Part 1: Planning and methodological approach, analysis and reporting, Land Degradation Assessment in Drylands (LADA) Project. FAO, Rome.

FAO (Ed.), 2011b. Manual for local level assessment of land degradation and sustainable land management, Part 2: Field methodology and tools, Land Degradation Assessment in Drylands (LADA) Project. FAO, Rome.

FAO (Ed.), 2004. Carbon sequestration in dryland soils, World soil resources reports. FAO, Rome.

FAO, UNDP, UNEP (Eds.), 1994. Land degradation in South Asia: its severity, causes, and effects upon the people, World soil resources reports. Food and Agriculture Organization of the United Nations, Rome.

Foley, J.A., DeFries, R., Asner, G.P., Barford, C., Bonan, G., Carpenter, S.R., Chapin, F.S., Coe, M.T., Daily, G.C., Gibbs, H.K., Helkowski, J.H., Holloway, T., Howard, E.A., Kucharik, C.J., Monfreda, C., Patz, J.A., Prentice, I.C., Ramankutty, N., Snyder, P.K., 2005. Global Consequences of Land Use. Science 309, 570–574. https://doi.org/10.1126/science.1111772

Foster, I.D.L., Rowntree, K.M., Boardman, J., Mighall, T., 2012. Changing sediment yield and sediment dynamics in the Karoo uplands, South Africa; Post-European impacts. Land Degrad. Dev., 23 (6), 508-522.

Foster, I.D.L., Boardman, J., Gates, J.B., 2008. Reconstructing historical sediment yields from the infilling of farm reservoirs, Eastern Cape, South Africa, in: IAHS-AISH Publication. Presented at the International Commission on Continental Erosion (ICCE). Symposium, International Association of Hydrological Sciences, pp. 440–447.

Foster, I.D.L., Boardman, J., Keay-Bright, J., Meadows, M.E., 2005. Land degradation and sediment dynamics in the South African Karoo, in: Horowitz, A.J., Walling, D.E. (Eds.), Sediment Budgets 2 (Prooceedings of Symposium S1 Held during the Seventh IAHS Scientific Assembly at Foz Do Iguaçu, Brazil, April 2005), IAHS Publication. Int Assoc Hydrological Sciences, Wallingford, pp. 207–213.

Fox, R.C., Rowntree, K.M., 2013. Extreme weather events in the Sneeuberg, Karoo, South Africa: a case study of the floods of 9 and 12 February 2011. Hydrol Earth Syst Sci Discuss 10, 10809–10844.

Galle, S., Ehrmann, M., Peugeot, C., 1999. Water balance in a banded vegetation pattern: A case study of tiger bush in western Niger. CATENA 37, 197–216. https://doi.org/10.1016/S0341-8162(98)90060-1

Geerken, R., Ilaiwi, M., 2004. Assessment of rangeland degradation and development of a strategy for rehabilitation. Remote Sens. Environ. 90, 490–504. https://doi.org/10.1016/j.rse.2004.01.015

Geerken, R., Zaitchik, B., Evans, J.P., 2005. Classifying rangeland vegetation type and coverage from NDVI time series using Fourier Filtered Cycle Similarity. Int. J. Remote Sens. 26, 5535–5554. https://doi.org/10.1080/01431160500300297

Gibbs, H.K., Salmon, J.M., 2015. Mapping the world's degraded lands. Appl. Geogr. 57, 12–21. https://doi.org/10.1016/j.apgeog.2014.11.024

Govers, G., Quine, T.A., Desmet, P.J.J., Walling, D.E., 1996. The relative contribution of soil tillage and overland flow erosion to soil redistribution on agricultural land. Earth Surf. Process. Landf. 21, 929–946. https://doi.org/10.1002/(SICI)1096-9837(199610)21:10<929::AID-ESP631>3.0.CO;2-C

Gregorich, E.G., Greer, K.J., Anderson, D.W., Liang, B.C., 1998. Carbon distribution and losses: erosion and deposition effects. Soil Tillage Res. 47, 291–302. https://doi.org/10.1016/S0167-1987(98)00117-2

Griffiths, S., 2006. Remote Terrain Navigation for Unmanned Air Vehicles (Master's Thesis). Brigham Young University, Provo, Utah.

Gyde Lund, H., 2007. Accounting for the World's Rangelands. Rangelands, Rangelands 29, 3–10. https://doi.org/10.2111/1551-501X(2007)29[3:AFTWR]2.0.CO;2

Hoffman, M.T., Ashwell, A., 2001. Nature Divided: Land degradation in South Africa, 1st ed. University of Cape Town Press, Cape Town.

Hoffman, M.T., Cowling, R.M., 1990. Vegetation change in the semi-arid eastern Karoo over the last 200 years: an expanding Karoo - fact or fiction? S. Afr. J. Sci. 86, 286–294.

Hoffman, M.T., Todd, S., 2000. A National Review of Land Degradation in South Africa: The Influence of Biophysical and Socio-economic Factors. J. South. Afr. Stud. 26, 743–758. https://doi.org/10.1080/713683611

Hoffmann, T., Todd, S., Ntshona, Z., Turner, S., 1999. Land degradation in South Africa (Unpublished Final Report). National Botanical Institute and Programme for Land and Agrarian Studies, Cape Town.

Holmes, P., Boardman, J., Parsons, A., Marker, M., 2003. Geomorphological palaeoenvironments of the Sneeuberg Range, Great Karoo, South Africa. Journal of Quaternary Science, 18(8), 801-813.

Holmes, P.J., 2001. Central Great Karoo Headwater Catchments and Valley, Fills; an Overview of Short Term Change. South Afr. Geogr. J. 83, 274–282. https://doi.org/10.1080/03736245.2001.9713746

Holmes, P.J., 1998. Late quaternary palaeoenvironments of some central and marginal Great Karoo uplands. University of Cape Town, Cape Town, South Africa.

ISRIC, 2006. Soil and Terrain Database (SOTER) for South Africa [WWW Document]. ISRIC. URL http://data.isric.org/geonetwork/srv/eng/catalog.search#/metadata/c3f7cfd5-1f25-4da1-bce9-cdcdd8c1a9a9 (accessed 02.07.18).

Jamsranjav, C., Reid, R.S., Fernández-Giménez, M.E., Tsevlee, A., Yadamsuren, B., Heiner, M., 2018. Applying a dryland degradation framework for rangelands: the case of Mongolia. Ecol. Appl. 28, 622–642. https://doi.org/10.1002/eap.1684

Jong, R. de, Bruin, S. de, Schaepman, M., Dent, D., 2011. Quantitative mapping of global land degradation using Earth observations. Int. J. Remote Sens. 32, 6823–6853. https://doi.org/10.1080/01431161.2010.512946

Joshi, N., Baumann, M., Ehammer, A., Fensholt, R., Grogan, K., Hostert, P., Jepsen, M.R., Kuemmerle, T., Meyfroidt, P., Mitchard, E.T.A., Reiche, J., Ryan, C.M., Waske, B., 2016. A Review of the Application of Optical and Radar Remote Sensing Data Fusion to Land Use Mapping and Monitoring. Remote Sens. 8, 70. https://doi.org/10.3390/rs8010070

Kakembo, V., Rowntree, K.M., 2003. The relationship between land use and soil erosion in the communal lands near Peddie town, Eastern Cape, South Africa. Land Degrad. Dev. 14, 39–49. https://doi.org/10.1002/ldr.509

Kapalanga, T.S., 2008. A review of land degradation assessment methods. Land Restor. Train. Programme Keldnaholt 112, 17–68.

Keay-Bright, J., Boardman, J., 2009. Evidence from field-based studies of rates of soil erosion on degraded land in the central Karoo, South Africa. Geomorphology 103, 455–465. https://doi.org/10.1016/j.geomorph.2008.07.011

Keay-Bright, J., Boardman, J., 2007. The influence of land management on soil erosion in the Sneeuberg mountains, central Karoo, South Africa. Land Degrad. Dev. 18, 423–439. https://doi.org/10.1002/ldr.785

Keay-Bright, J., Boardman, J., 2006. Changes in the distribution of degraded land over time in the central Karoo, South Africa. Catena 67, 1–14. https://doi.org/10.1016/j.catena.2005.12.003

Knight, J., Holmes, P.J., 2018. Drylands and their unique challenges, in: Holmes, P.J., Boardman, J. (Eds.), Southern African Landscapes and Environmental Change, Earthscan Studies in Natural Resource Management. Routledge, Taylor & Francis Group, London ; New York, NY, pp. 136–152.

Lal, R., 2004. Carbon Sequestration in Dryland Ecosystems. Environ. Manage. 33. https://doi.org/10.1007/s00267-003-9110-9

Lal, R., 2002a. Soil carbon dynamics in cropland and rangeland. Environ. Pollut. 116, 353–362. https://doi.org/10.1016/S0269-7491(01)00211-1

Lal, R., 2002b. Carbon sequestration in dryland ecosystems of West Asia and North Africa. Land Degrad. Dev. 13, 45–59. https://doi.org/10.1002/ldr.477

Lal, R., 2001a. Fate of eroded soil carbon: emission or sequestration, in: Lal, R. (Ed.), Soil Carbon Sequestration and the Greenhouse Effect, SSSA Special Publication. Soil Science Society of America, Madison, Wisonsin, pp. 173–181.

Lal, R., 2001b. Soil degradation by erosion. Land Degrad. Dev. 12, 519–539. https://doi.org/10.1002/ldr.472

Lal, R., Stewart, B.A. (Eds.), 1990. Soil degradation, Advances in soil science. Springer, New York, NY Berlin.

Laliberte, A.S., Winters, C., Rango, A., 2011. UAS remote sensing missions for rangeland applications. Geocarto Int. 26, 141–156. https://doi.org/10.1080/10106049.2010.534557

Le Roux, J.J., Morgenthal, T.L., Malherbe, J., Pretorius, D.J., Sumner, P.D., 2008. Water erosion prediction at a national scale for South Africa. Water SA 34, 305–314.

Lobell, D.B., 2010. Remote Sensing of Soil Degradation: Introduction. J. Environ. Qual. 39, 1–4. https://doi.org/10.2134/jeq2009.0326

Luce, C.H., Black, T.A., 1999. Sediment production from forest roads in western Oregon. Water Resour. Res. 35, 2561–2570.

Ludwig, J.A., Wilcox, B.P., Breshears, D.D., Tongway, D.J., Imeson, A.C., 2005. Vegetation patches and runoff-erosion as interacting ecohydrological processes in semiarid landscapes. Ecology 86, 288–297. https://doi.org/10.1890/03-0569

Maestre, F.T., Cortina, J., 2002. Spatial patterns of surface soil properties and vegetation in a Mediterranean semi-arid steppe. Plant Soil 241, 279–291. https://doi.org/10.1023/A:1016172308462

Mararakanye, N., Roux, J.J.L., 2012. Gully location mapping at a national scale for South Africa. South Afr. Geogr. J. 94, 208–218. https://doi.org/10.1080/03736245.2012.742786

Marzolff, I., Poesen, J., 2009. The potential of 3D gully monitoring with GIS using high-resolution aerial photography and a digital photogrammetry system. Geomorphology, GIS and SDA applications in geomorphology 111, 48–60. https://doi.org/10.1016/j.geomorph.2008.05.047

Mason, S.J., Waylen, P.R., Mimmack, G.M., Rajaratnam, B., Harrison, J.M., 1999. Changes in Extreme Rainfall Events in South Africa. Clim. Change 41, 249–257. https://doi.org/10.1023/A:1005450924499

McCarty, G.W., Ritchie, J.C., 2002. Impact of soil movement on carbon sequestration in agricultural ecosystems. Environ. Pollut. 116, 423–430. https://doi.org/10.1016/S0269-7491(01)00219-6

Meadows, M.E., Hoffman, T.M., 2003. Land degradation and climate change in South Africa. Geogr. J. 169, 168–177. https://doi.org/10.1111/1475-4959.04982

Mighall, T.M., Foster, I.D.L., Rowntree, K.M., Boardman, J., 2012. Reconstructing recent land degradation in the semi-arid Karoo of South Africa: A palaeoecological study at Compassberg, Eastern Cape. Land Degrad. Dev., 23(6), 523-533.

Mondal, A., Khare, D., Kundu, S., 2017a. Uncertainty analysis of soil erosion modelling using different resolution of open-source DEMs. Geocarto Int. 32, 334–349. https://doi.org/10.1080/10106049.2016.1140822

Mondal, A., Khare, D., Kundu, S., Mukherjee, S., Mukhopadhyay, A., Mondal, S., 2017b. Uncertainty of soil erosion modelling using open source high resolution and aggregated DEMs. Geosci. Front. 8, 425–436. https://doi.org/10.1016/j.gsf.2016.03.004

Montanarella, L., Scholes, R., Brainich, E. (Eds.), 2018. The IPBES assessment report on Land Degradation and Restoration. Secretariat of the Intergovernmental Science-Policy Platform on Biodiversity and Ecosystem Services (IPBES), Bonn, Germany.

Mucina, L., Rutherford, M.C. (Eds.), 2006. The vegetation of South Africa, Lesoto and Swaziland, Strelitzia. South African National Biodiversity Institute, Pretoria.

Nachtergaele, F.O.F., Licona-Manzur, C., 2009. The Land Degradation Assessment in Drylands (LADA) Project: Reflections on Indicators for Land Degradation Assessment, in: Lee, C., Schaaf, T. (Eds.), The Future of Drylands. Springer Netherlands, Dordrecht, pp. 327–348. https://doi.org/10.1007/978-1-4020-6970-3_33

Neely, C., Bunning, S., Wilkes, A., 2009. Review of evidence on drylands pastoral systems and climate change: implications and opportunities for mitigation and adaptation., FAO Land and Water Discussion Paper, 8. FAO, Rome.

Neugirg, F., Stark, M., Kaiser, A., Vlacilova, M., Della Seta, M., Vergari, F., Schmidt, J., Becht, M., Haas, F., 2016. Erosion processes in calanchi in the Upper Orcia Valley, Southern Tuscany, Italy based on multitemporal high-resolution terrestrial LiDAR and UAV surveys. Geomorphology 269, 8–22. https://doi.org/10.1016/j.geomorph.2016.06.027

Nobajas, A., Waller, R.I., Robinson, Z.P., Sangonzalo, R., 2017. Too much of a good thing? the role of detailed UAV imagery in characterizing large-scale badland drainage

characteristics in South-Eastern Spain. Int. J. Remote Sens. 1–17. https://doi.org/10.1080/01431161.2016.1274450

Oldeman, L.R., Hakkeling, R.T.A., Sombroek, W.G., 1991. World map of the status of human-induced soil degradation: an explanatory note, 2nd ed. ISRIC; UNEP, Nairobi, Kenya : Wageningen, Netherlands.

Palmer, A.R., Novellie, P.A., Lloyd, J.W., 1999. Community patterns and dynamics, in: The Karoo: Ecological Patterns and Processes. University Press, Cambridge, pp. 208–223.

Pimentel, D., Harvey, C., Resosudarmo, P., Sinclair, K., Kurz, D., McNair, M., Crist, S., Shpritz, L., Fitton, L., Saffouri, R., 1995. Environmental and economic costs of soil erosion and conservation benefits. Sci.-AAAS-Wkly. Pap. Ed. 267, 1117–1122.

Ponce-Hernandez, R., Koohafkan, P., Antoine, J., 2004. Assessing carbon stocks and modelling win-win scenarios of carbon sequestration through land-use changes. Food and Agriculture Organization of the United Nations, Rome.

Powell, J.M., Fernandez-Rivera, S., Hiernaux, P., Turner, M., 1996. Nutrient cycling in integrated rangeland/cropland systems of the Sahel. Society for Range Management. Agricultural Systems, 52(2-3), 143-170.

Randerson, J.T., Chapin, F.S., Harden, J.W., Neff, J.C., Harmon, M.E., 2002. Net Ecosystem Production: A Comprehensive Measure of Net Carbon Accumulation by Ecosystems. Ecol. Appl. 12, 937–947. https://doi.org/10.1890/1051-0761(2002)012[0937:NEPACM]2.0.CO;2

Rango, A., Laliberte, A., Herrick, J.E., Winters, C., Havstad, K., Steele, C., Browning, D., 2009. Unmanned aerial vehicle-based remote sensing for rangeland assessment, monitoring, and management. J. Appl. Remote Sens. 3, 033542. https://doi.org/10.1117/1.3216822

Ravi, S., Breshears, D.D., Huxman, T.E., D'Odorico, P., 2010. Land degradation in drylands: Interactions among hydrologic–aeolian erosion and vegetation dynamics. Geomorphology 116, 236–245. https://doi.org/10.1016/j.geomorph.2009.11.023

Reinwarth, B., Petersen, R., Baade, J., 2019. Inferring mean rates of sediment yield and catchment erosion from reservoir siltation in the Kruger National Park, South Africa: An uncertainty assessment. Geomorphology 324, 1–13. https://doi.org/10.1016/j.geomorph.2018.09.007

Rietkerk, M., Boerlijst, M.C., van Langevelde, F., HilleRisLambers, R., de Koppel, J. van, Kumar, L., Prins, H.H.T., de Roos, A.M., 2002. Self-Organization of Vegetation in Arid Ecosystems. Am. Nat. 160, 524–530. https://doi.org/10.1086/342078

Rietkerk, M., Ketner, P., Burger, J., Hoorens, B., Olff, H., 2000. Multiscale soil and vegetation patchiness along a gradient of herbivore impact in a semi-arid grazing system in West Africa. Plant Ecol. 148, 207–224. https://doi.org/10.1023/A:1009828432690

Rodríguez-Caballero, E., Knerr, T., Weber, B., 2015. Importance of biocrusts in dryland monitoring using spectral indices. Remote Sens. Environ. 170, 32–39. https://doi.org/10.1016/j.rse.2015.08.034

Rogan, J., Chen, D., 2004. Remote sensing technology for mapping and monitoring land-cover and land-use change. Prog. Plan. 61, 301–325. https://doi.org/10.1016/S0305-9006(03)00066-7

Rowntree, K., Foster, I., 2012. A reconstruction of historical changes in sediment sources, sediment transfer and sediment yield in a small, semi-arid Karoo catchment, semi-arid South Africa. Z. für Geomorphol. Suppl. Issues 56, 87–100. https://doi.org/10.1127/0372-8854/2012/S-00074

Rowntree, K.M., 2014. Reprint of: The evil of sluits: A re-assessment of soil erosion in the Karoo of South Africa as portrayed in century-old sources. J. Environ. Manage. 138, 67–74. https://doi.org/10.1016/j.jenvman.2014.04.015

Saco, P.M., Willgoose, G.R., Hancock, G.R., 2007. Eco-geomorphology of banded vegetation patterns in arid and semi-arid regions. Hydrol. Earth Syst. Sci. 11, 1717–1730. https://doi.org/10.5194/hess-11-1717-2007

Safriel, U.N., Adeel, Z., 2005. Dryland Systems, in: Hassan, R., Scholes, R., Ash, N. (Eds.), Ecosystems and Human Well-Being: Current State and Trends. Washington, DC: Island Press, pp. 623–662.

Schlesinger, W.H., Raikes, J.A., Hartley, A.E., Cross, A.F., 1996. On the Spatial Pattern of Soil Nutrients in Desert Ecosystems. Ecology 77, 364–374. https://doi.org/10.2307/2265615

Schlesinger, W.H., Reynolds, J.F., Cunningham, G.L., Huenneke, L.F., Jarrell, W.M., Virginia, R.A., Whitford, W.G., 1990. Biological Feedbacks in Global Desertification. Science 247, 1043–1048. https://doi.org/10.1126/science.247.4946.1043

Schmidt, H., Karnieli, A., 2000. Remote sensing of the seasonal variability of vegetation in a semi-arid environment. J. Arid Environ. 45, 43–59. https://doi.org/10.1006/jare.1999.0607

Sonneveld, B.G.J.S., Dent, D.L., 2009. How good is GLASOD? J. Environ. Manage. 90, 274–283. https://doi.org/10.1016/j.jenvman.2007.09.008

Soriano, A., Sala, O.E., Perelman, S.B., 1994. Patch structure and dynamics in a Patagonian arid steppe. Vegetatio 111, 127–135. https://doi.org/10.1007/BF00040332

Stöcker, C., Eltner, A., Karrasch, P., 2015. Measuring gullies by synergetic application of UAV and close range photogrammetry—A case study from Andalusia, Spain. Catena 132, 1–11.

Sugden, J.M., 1989. Late quaternary palaeoecology of the central and marginal uplands of the Karoo, South Africa. University of Cape Town, Cape Town, South Africa.

Tucker, C.J., 1979. Red and photographic infrared linear combinations for monitoring vegetation. Remote Sens. Environ. 8, 127–150. https://doi.org/10.1016/0034-4257(79)90013-0

UN EMG (Ed.), 2011. Global drylands: a UN system-wide response. U. N. Environ. Manag. Group 131, 132.

UNCCD (Ed.), 1994. United Nations Convention to Combat Desertification in Those Countries Experiencing Serious Drought and/or Desertification Particularly in Africa. (No. A/AC.241/27), United Nations Environment Programme. United Nations, Geneva, Switzerland.

UNCCD (Ed.), 2015. Pivotal Soil Carbon, Science-Policy Brief 01. UN, Bonn.

US EPA (Ed.), 2016. Agriculture: Pasture, Rangeland and Grazing [WWW Document]. URL https://www.epa.gov/agriculture/agriculture-pasture-rangeland-and-grazing (accessed 1.4.17).

Valentin, C., d'Herbès, J.M., Poesen, J., 1999. Soil and water components of banded vegetation patterns. CATENA 37, 1–24. https://doi.org/10.1016/S0341-8162(99)00053-3

Van Oost, K., Govers, G., Quine, T.A., Heckrath, G., Olesen, J.E., De Gryze, S., Merckx, R., 2005. Landscape-scale modeling of carbon cycling under the impact of soil redistribution: The role of tillage erosion. Glob. Biogeochem. Cycles 19, n/a-n/a. https://doi.org/10.1029/2005GB002471

Van Oost, K., Quine, T.A., Govers, G., Gryze, S.D., Six, J., Harden, J.W., Ritchie, J.C., McCarty, G.W., Heckrath, G., Kosmas, C., Giraldez, J.V., Silva, J.R.M. da, Merckx, R., 2007. The Impact of Agricultural Soil Erosion on the Global Carbon Cycle. Science 318, 626–629. https://doi.org/10.1126/science.1145724

Viglietti, P.A., Rubidge, B.S., Smith, R.M.H., 2017. Revised lithostratigraphy of the Upper Permian Balfour and Teekloof formations of the main Karoo Basin, South Africa. South Afr. J. Geol. 120, 45–60. https://doi.org/10.25131/gssajg.120.1.45

Vinci, A., Brigante, R., Todisco, F., Mannocchi, F., Radicioni, F., 2015. Measuring rill erosion by laser scanning. CATENA 124, 97–108. https://doi.org/10.1016/j.catena.2014.09.003

Wang, R., Zhang, S., Pu, L., Yang, J., Yang, C., Chen, J., Guan, C., Wang, Q., Chen, D., Fu, B., Sang, X., 2016. Gully Erosion Mapping and Monitoring at Multiple Scales Based on Multi-Source Remote Sensing Data of the Sancha River Catchment, Northeast China. ISPRS Int. J. Geo-Inf. 5, 200. https://doi.org/10.3390/ijgi5110200

Wang, Z., Govers, G., Steegen, A., Clymans, W., Van den Putte, A., Langhans, C., Merckx, R., Van Oost, K., 2010. Catchment-scale carbon redistribution and delivery by water erosion in an intensively cultivated area. Geomorphology 124, 65–74. https://doi.org/10.1016/j.geomorph.2010.08.010

Watkeys, M.K., 1999. Soils of the arid south-western zone of Africa, in: The Karoo: Ecological Patterns and Processes. University Press, Cambridge, pp. 17–26.

Wessels, K.J., Prince, S.D., Frost, P.E., van Zyl, D., 2004. Assessing the effects of human-induced land degradation in the former homelands of northern South Africa with a 1 km AVHRR NDVI time-series. Remote Sens. Environ. 91, 47–67. https://doi.org/10.1016/j.rse.2004.02.005

Wessels, K.J., Prince, S.D., Malherbe, J., Small, J., Frost, P.E., VanZyl, D., 2007. Can human-induced land degradation be distinguished from the effects of rainfall variability? A case study in South Africa. J. Arid Environ. 68, 271–297. https://doi.org/10.1016/j.jaridenv.2006.05.015

Wessels, K.J., Prince, S.D., Reshef, I., 2008. Mapping land degradation by comparison of vegetation production to spatially derived estimates of potential production. J. Arid Environ. 72, 1940–1949. https://doi.org/10.1016/j.jaridenv.2008.05.011

Wiggs, G., Holmes, P., 2011. Dynamic controls on wind erosion and dust generation on west-central Free State agricultural land, South Africa. Earth Surf. Process. Landf. 36, 827–838. https://doi.org/10.1002/esp.2110

Wingate, V.R., Phinn, S., Kuhn, N., Bloemertz, L., Dhanjal-Adams, K., 2016. Mapping Decadal Land Cover Changes in the Woodlands of North Eastern Namibia from 1975 to 2014 Using the Landsat Satellite Archived Data. Remote Sens. 8, 681. https://doi.org/10.3390/rs8080681

Wingate, V.R., Phinn, S.R., Kuhn, N., Scarth, P., 2018. Estimating aboveground woody biomass change in Kalahari woodland: combining field, radar, and optical data sets. Int. J. Remote Sens. 39, 577–606. https://doi.org/10.1080/01431161.2017.1390271

Wynn, T., Mostaghimi, S., 2006. The Effects of Vegetation and Soil Type on Streambank Erosion, Southwestern Virginia, Usa1. JAWRA J. Am. Water Resour. Assoc. 42, 69–82. https://doi.org/10.1111/j.1752-1688.2006.tb03824.x

Zhang, J., Quine, T.A., Ni, S., Ge, F., 2006. Stocks and dynamics of SOC in relation to soil redistribution by water and tillage erosion. Glob. Change Biol. 12, 1834–1841. https://doi.org/10.1111/j.1365-2486.2006.01206.x

CHAPTER 2

Small-Scale Soil Heterogeneity on Degraded Rangelands in the South African Greater Karoo

Small-scale soil heterogeneity on degraded rangelands in the South African Greater Karoo

Juliane Krenz, Philip Greenwood and Nikolaus J. Kuhn
University of Basel, Klingelbergstrasse 27, 4056 Basel, Switzerland

Status: in preparation
Target journal: Journal of Arid Landscapes

2.1 ABSTRACT

Soil erosion in semi-arid drylands often leads to a redistribution of soil, thus creating patchworks of soils and vegetation that are different from their natural conditions. This spatial heterogeneity in soil parameters is highly dynamic and usually not depicted in conventional soil maps due to scalar impracticalities in their physical demarcation. Nevertheless, capturing patchiness is important for land management, soil restoration and soil-climate interaction. The study carries out a small-scale description of soil redistribution in a degraded rangeland with a silted-up reservoir in the Greater Karoo in South Africa to assess the relevance of soil heterogeneity within the catchment. Surface soil (N=32) and soil profile (N=24) samples were collected from areas of various degrees of degradation and analysed for particle size distribution, total nitrogen (TN), and total organic carbon (TOC). Although we found no significant difference in soil texture, the heterogeneous vegetation cover is reflected in a high level of soil heterogeneity. Average soil nutrient content was significantly greater in vegetated areas (grassland: TOC 1.10%, TN 0.10%, mixed vegetation: TOC 0.93%, TN 0.08%) than at degraded sites (TOC 0.47%, TN 0.4%). There is a strong potential for the formation of young anthropogenic soils on the numerous silted-up reservoirs in the Karoo. In the study area, sediments trapped behind dams differed in TOC (0.47%), TN (0.06%), and profile depth (up to 5m) significantly from natural soils. Consequently, they can be defined as a different soil type. Their different water and nutrient cycling may also affect biogeochemical fluxes. These specific properties of the soils forming on dam deposits should therefore be considered in land use management, but also studied in terms of their role in rangeland biogeochemical cycles.

Keywords
check dam, erosion, reservoir siltation, soil redistribution

2.2 INTRODUCTION

Soil erosion plays an important role in the global carbon (C) cycle (Berhe et al., 2005; Harden et al., 1999; Lal, 2005, 2003). However, there is an ongoing debate whether it acts as a net C source or sink (Chappell et al., 2016; Lal, 2019; Sanderman and Berhe, 2017; Van Oost et al., 2007, p. 200). Dryland ecosystems are vulnerable to soil erosion due to unevenly distributed or erratic rainfall and frequent droughts (FAO, 2004). Soil erosion in semi-arid drylands often leads to a redistribution of soil, thus creating patchworks of soils and, consequently, vegetation, that are different from their natural conditions (Cerdá, 2001; Ludwig et al., 2005; Rietkerk et al., 2002). Different soil characteristics, such as nutrient content (Rietkerk et al., 2002; Schlesinger et al., 1996) or soil erodibility (Cerdá, 1997; Dickie and Parsons, 2012) are associated with patches of bare soil and vegetation. This small-scale spatial heterogeneity in

soil parameters is highly dynamic and usually not depicted in conventional soil maps due to scalar impracticalities in their physical demarcation. Apart from impoverishment of soils by erosion, deposition of the eroded material contributes to the patchiness of soils (Bochet et al., 1999; Okin et al., 2006; Puigdefábregas, 2005). In the Karoo, one erosion measure are check dams, which were built to retain water or sediments (Boardman et al., 2003; Lü et al., 2012). Deposits formed both intentionally and unintentionally when reservoirs silted-up. In both cases, young and deep patches of substrate for soil formation have developed. These patches are regularly supplied with runoff and thus used as pasture for grazing after the water has subsided again. Hence, depositional areas behind dams often develop specific vegetation (Polyakov et al., 2014), which promotes livestock grazing and thus generates a particular ecological or even economical value.

Erosion and deposition in rangelands such as the Karoo generate a small-scale patchwork of soils. The lack of spatial information on these human-induced patchworks potentially affects the assessment of rangeland erosion on global C cycles. The Karoo rangelands are characterised by widespread erosion features of various shapes and degrees and silted-up reservoirs, which make them ideal for studying soil redistribution and soil patchiness. The purpose of this study is to undertake a small-scale description of soil redistribution in what we perceive to be a small, yet representative catchment in a degraded rangeland in the Greater Karoo in South Africa. The small-scale variability of soils in degraded Karoo rangelands is documented in order to assess the relevance of the human-induced patchiness for soil properties that are relevant for land management, soil restoration, and soil-climate interaction. The objectives of the study are (i) to document soil heterogeneity based on field observations and soil samples, (ii) to describe soil characteristics associated with the associated landscape, and (iii) to assess the relevance of soil heterogeneity in the catchment compared to conventionally available soil information.

2.3 STUDY AREA

The study area (Figure 2-1) is located in the Sneeuberg uplands in the Eastern Cape Province of South Africa which rise up to 2502 m at Kompassberg. Geologically, the area is composed of Upper Permian to Triassic mudstones and sandstones from the Beaufort Group, interspersed with Jurassic dolerite sills and dykes that outcrop on hilltops. With up to 500 mm annual precipitation, the region is wetter than surrounding lowlands due to orographic rainfall (Sugden, 1989). A summer rainfall regime is characteristic, where approximately 70% of the annual precipitation is received between October and March (Keay-Bright and Boardman, 2007). Vegetation is classified as False Upper Karoo in the valleys, and Karroid Merxmuellera Mountain veld on the hillslopes (Acocks, 1975). Vegetation consists of a mixture

of palatable and unpalatable grasses (e.g. *Merxmuellera disticha),* and shrubs (e.g. *Chrysocoma ciliata*, *Dicerothamnus rhinocerotis*, *Euryops annae,* and *Selago* spp.).

Soils are usually derived from the underlying doleritic material or silt, mud- and claystones (Council for Geoscience, 2008; ISRIC, 2006). Wide valleys have often been infilled with colluvial and alluvial material. Soil profiles are mostly shallow and often lack a distinct A horizon, presumably due to high erosion rates (Boardman et al., 2017, 2003). Soil maps of the study area have a resolution of 1:1,000,000 (ISRIC, 2006) and 1:5,000,000 (Soils Research Institute, 1965) and are classified as lithic leptosols (ISRIC, 2006), or semi-desert soils, and Lithosols with rock and rock debris (Soils Research Institute, 1965) Thus, spatial information on soils at the scale needed by farmers and land-managers is limited.

The Sneeuberg area shows typical features of land degradation, such as shrub encroachment and soil erosion, including rills, gullies and permanently crusted surfaces. Due to the intense grazing in the valley bottoms, they are mostly affected by erosion (Boardman et al., 2003; Foster et al., 2007). Another common feature are infilled reservoirs, which are now dry because dams have breached and in many instances are not economical to repair or maintain (Boardman et al., 2003). Boardman and Foster (2011) mapped 106 small farm dams in an area of about 100 km^2 in the Sneeuberg region, of which almost 50% are full of sediment with little or no remaining water storage capacity.

A silted-up reservoir (31.698558°S, 24.588183°E, Figure 2-1), labelled Dam 53 according to the reference system adopted by Boardman and Foster (2011), is located in an easily accessible small catchment (289 ha). It was chosen as the study site because, unlike other catchments, it was only used for grazing and thus represents a simple environment to assess cause and effect of land degradation on soil properties. There are some shallow, rain-fed pools in the upper part of the riverbed, but no perennial stream. The latest assessment of soil degradation, mapped based on high-resolution UAV imagery (Krenz et al., 2019), estimated an area of approximately 23 to 29% of the land within Dam 53 catchment as being affected by erosion. Historically, the area was used for sheep and cattle farming since the 18th century, but a permanent farm, Aandrus, was only established in the 1860s or 70s (Keay-Bright and Boardman, 2007). Grazing densities in the Sneeuberg region were about 10 large stock unit (LSU) per km^2 in the beginning of the 20th century (Keay-Bright and Boardman, 2006), but have now been reduced to about one LSU per 18 ha on the farm the study site belongs to (Jacobs, D., current manager of the farm, personal communication 2016). The study site is located at an altitude of approximately 1740 m a.s.l. Historic aerial imagery suggests that the 140 m long dam wall was probably constructed in the 1930s and anecdotal evidence suggests that it was breached during a prolonged storm in 1974 (Boardman et al., 2017). The reservoir water storage capacity was approximately 30490 m^3 when constructed. Since the breach, an ephemeral stream has incised more than 5 m into the dam deposits and to date has excavated approximately 2900 m^3 of dam sediment (Krenz and Kuhn, 2018).

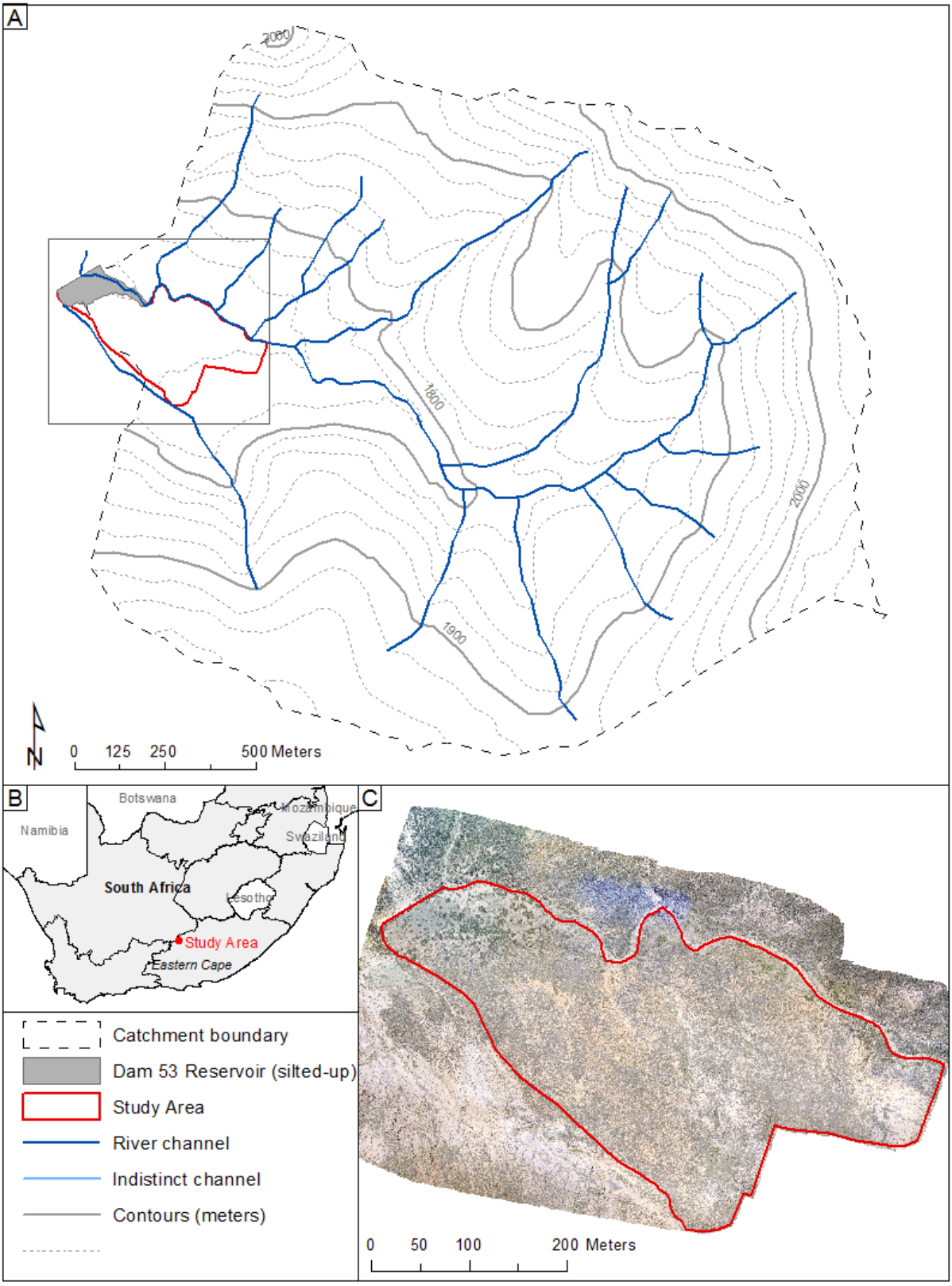

Figure 2-1 Overview of the studied catchment area (A), its location within South Africa (B) and an orthophoto (C) from the area. The study area is marked in red.

2.4 METHODOLOGY

2.4.1 SOIL SAMPLING

Soil samples were collected throughout the study site Figure 2-2, from areas of various degrees of soil and vegetation degradation, to identify differences in soil properties. Vegetation was used as an index for soil degradation because in rangelands it often reflects the different chemical, structural, and textural properties (Schlesinger et al., 1996, 1990). Soil samples assigned to the designated landscape units (LU) are described in Table 2-1.

In total, 32 surface soil samples (0-5 mm) were collected from degraded (N=14), grassland (N=5) and areas of mixed vegetation (N=13). In the area of the former reservoir (depositional LU) soil samples (N=18) were taken at a depth of 50 cm to avoid heterogeneities introduced at the surface, including trampling, burrowing, and droppings. In addition, soil pits were dug in the degraded LU (N=6), grassland LU (N=5), and mixed vegetation LU (N=13) to study potential differences in soil depth and the vertical distribution of texture and nutrients. Bulk soil samples were taken for each identified soil horizon. At some sizes in the degraded LU soil was so compact that it was impossible to take a complete set of surface and profile samples.

Table 2-1 Characteristics of different landscape units for soil sampling. The threshold value of at least 50% vegetation cover for the vegetated LU was chosen according to the Karoo Veld assessment form in (Esler et al., 2006), where an excellent veld condition is characterised among others by > 50% vegetation cover.

Landscape Unit (LU)	Description
Depositional	Former reservoir area, flat terrain behind the former dam wall
Degraded	Contiguous area of bare soil with little vegetation (individual shrubs or tussock grass) and large gaps between individual plants Vegetation cover < 50% Rill development Shrubs or tussocks often stand on pedestals
Grassland	Contiguous vegetation cover (> 50%), non-woody plants dominating
Mixed Vegetation	Contiguous vegetation cover interspersed with patches of bare soil or stones, at least 50% vegetation cover, neither woody nor non-woody plants dominating

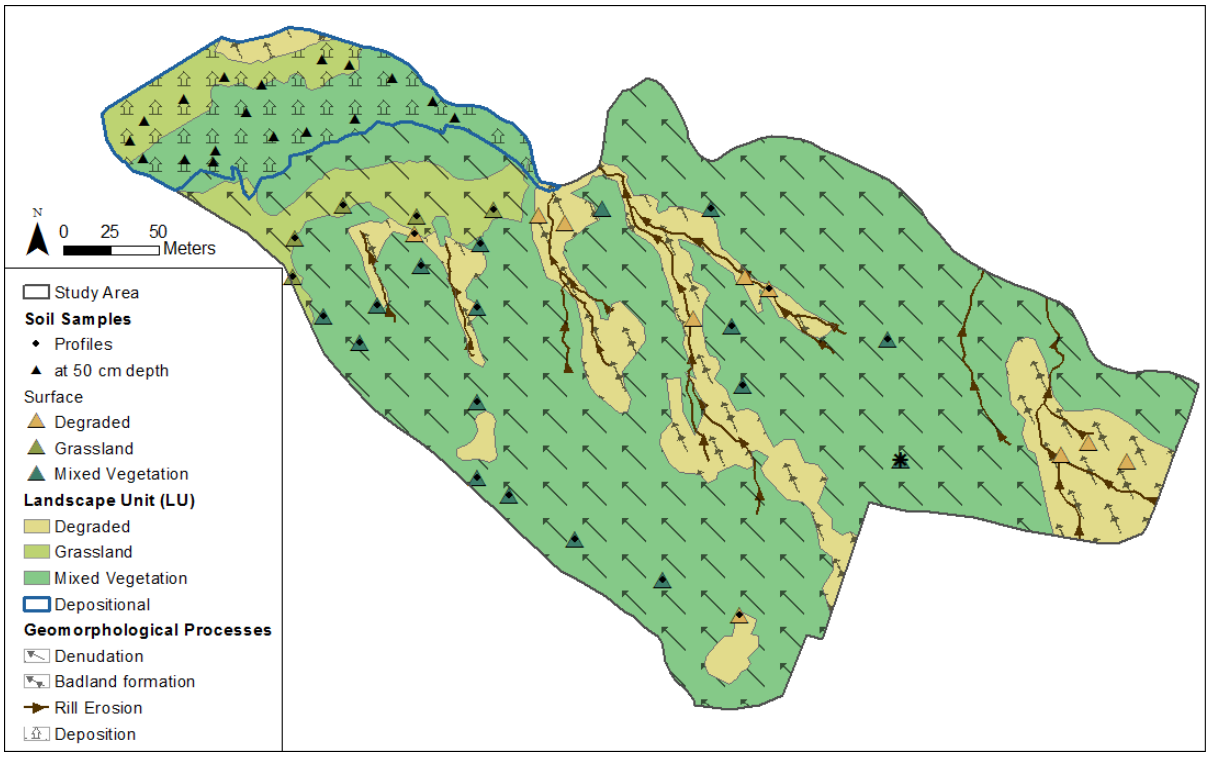

Figure 2-2 Map showing landscape units and locations of top soil samples. Samples marked with a dot inside the triangle are locations were soil profile samples were taken as well. The sampled marked with a black asterisk had an unusual deep soil profile.

2.4.2 LABORATORY ANALYSES

Colour, texture, C and nitrogen content were analysed to characterise soils from the different sampling sites, variations of which were interpreted as evidence of differences in soil quality and indicative of soil erosion and deposition processes. All soil samples were dried at 40°C before further soil analysis was conducted. A Munsell soil colour chart was used to determine the colour of dry soil samples. Particle size analysis (PSA) was performed using laser diffraction with three minutes ultrasound energy for more thorough aggregate dispersion (Malvern Mastersizer 2000). Prior to measurement, organic compounds were removed by heating 1 g of soil mixed with 10 ml of distilled water and 10 ml of 30% hydrogen peroxide in a water bath at 50°C until bubbling stopped and then slowly heated up till 90°C.

Both the total organic carbon (TOC) and total nitrogen (TN) content are one of the main indicators of soil quality in semi-arid soils (Muñoz-Rojas et al., 2016; Sharma et al., 2005). Total organic and inorganic carbon (TOC, TIC) were analysed from dry sieved samples using a LECO RC 612 Carbon Analyzer at 550 °C. Total nitrogen (TN) was analysed by dry combustion with a LECO CN628 Analyzer.

2.4.3 VERTICAL INTERPOLATION OF SOIL PARAMETERS

Only one soil sample was taken per horizon and analysed in the lab. The irregular depths of soil samples complicate the comparison and grouping of data from several profiles within the same LU. A depth-wise interpolation and visualisation of soil parameters was therefore conducted using the R software package "aqp" (Beaudette et al., 2013). Soil property data from each soil profile were normalised, aligned to a common depth and resampled at a regular depth-interval of 1 cm. Afterwards the soil property was summarised for each LU separately along depth intervals up to the maximum profile depth. The fraction of profiles contributing to the computation of the aggregated value is calculated at 10 cm intervals.

2.4.4 STATISTICAL ANALYSIS

Statistical analyses of soil data focussed on identifying potential differences within LUs and between LUs. Basic statistics included median, first and third quantiles for all soil parameters and all LUs (depositional, degraded, grassland and mixed vegetation). Additionally, non-parametric statistical tests were used to compare datasets from different LUs as normality could not be assumed. Normality of distributions was tested with the Shapiro-Wilk test individually for each variable. However, even for variables where normality was tested positively, we cannot assume normality because of our small sample sizes. We applied a Kruskal-Wallis test for our datasets with four groups (LUs) and a subsequent pair-wise comparison in RStudio (Version 1.0.143), based on R version 3.4.0. As a significance level $p < 0.05$ was used.

2.5 RESULTS

2.5.1 TOP SOIL CHARACTERISTICS

Top soil characteristics and results of the pairwise comparison are shown in Table 2-2 and Table 2-3 respectively. The major texture class according to the FAO soil classification (FAO, 2006) is sandy loam (21 out of 32 samples); eight samples are classified as loamy sand and three as loam. There was no significant difference in particle size distributions (Table 2-3). Average D10 and D50 sizes were finest for the mixed vegetation LU. The depositional LU, where samples were taken at 50 cm depth had the finest D90, but coarsest D10 and D50 compared to the other LUs. At a 95% confidence level, TOC, TIC, and TN content of the top soils showed significant differences between the four LUs. Comparing LUs pairwise, there is a significant difference for all TOC and TN distributions except between the depositional and degraded LU. The TOC content is generally low and varies for all top soil samples between 0.12% and 1.35%; with a mean of 0.47% for the degraded and the depositional LU, 0.93% for the mixed vegetation LU, and 0.99% for the grassland LU. TIC content was low and showed significant differences for most pairwise comparisons except depositional LU and degraded

LU, and depositional and grassland LU. TN was highest for the grassland LU (0.10%) and lowest for depositional and degraded LUs (both 0.06%).

Table 2-2 Top soil characteristics of landscape units. Samples from the depositional LU are not taken at the surface but at 50 cm depth.

		Landscape Unit			
Parameter		**Deposition**	**Degradation**	**Grassland**	**Mixed Vegetation**
Area [ha]		1.02	1.63	0.44	5.8
N		18	14	5	13
D10 [µm]	Mean	8.71 ± 8.20	3.84 ± 2.77	4.67 ± 2.29	3.49 ± 1.72
	Min	1.20	1.47	2.26	1.80
	Max	25.71	10.55	7.28	8.79
D50 [µm]	Mean	127.81 ± 120.53	95.45 ± 48.34	112.84 ± 40.92	84.68 ± 16.33
	Min	7.54	26.82	77.76	43.26
	Max	444.03	215.15	176.78	109.96
D90 [µm]	Mean	337.64 ± 274.44	407.87 ± 210.27	440.84 ± 201.22	346.97 ± 116.62
	Min	53.38	140.18	257.76	219.34
	Max	899.24	814.37	746.11	591.60
TOC [%]	Mean	0.47 ± 0.38	0.47 ± 0.20	1.10 ± 0.21	0.93 ± 0.21
	Min	0.13	0.12	0.85	0.69
	Max	1.4	0.78	1.31	1.35
TIC [%]	Mean	0.02 ± 0.001	0.01 ± 0.003	0.02 ± 0.003	0.02 ± 0.003
	Min	0.01	0.01	0.02	0.02
	Max	0.04	0.02	0.03	0.02
TN [%]	Mean	0.06 ± 0.03	0.06 ± 0.01	0.10 ± 0.03	0.08 ± 0.02
	Min	0.04	0.04	0.08	0.05
	Max	0.13	0.08	0.16	0.12

2.5.2 SOIL PROFILE PROPERTIES

Soil profile depth varied between 32 to 54 cm for the degraded LU, 34 to 70 cm for the grassland LU, and 39 to 62 cm for the mixed vegetation LU. One profile from the mixed vegetation LU had a depth of 110 cm. This profile was located in the South East of the catchment and is marked with a black asterisk in Figure 2-2. The deep soil depth can probably be attributed to the profiles' location at the toe of a hillslope. For all soil profiles, it should be noted that profiles were not dug down to bedrock, but were restricted by the hard compacted strata. Hence, it was only possible to sample six soil profiles for the degraded LU compared to 13 profiles for the vegetated LU.

For all profiles average D10, D50 and D90 sizes declined with increasing depth, with the strongest trend expressed by the grassland LU (Figure 2-3). While D10 and D50 decreased abruptly below 10 cm for the degraded and mixed vegetation LUs, it slightly increased for the grassland LU before it declined below 25 cm. The vertical nutrient distribution showed opposite patterns for the LUs. While TOC and TN steadily decreased with depth below approximately 12 cm for the degraded and mixed vegetation LU, both increased for the grassland LU.

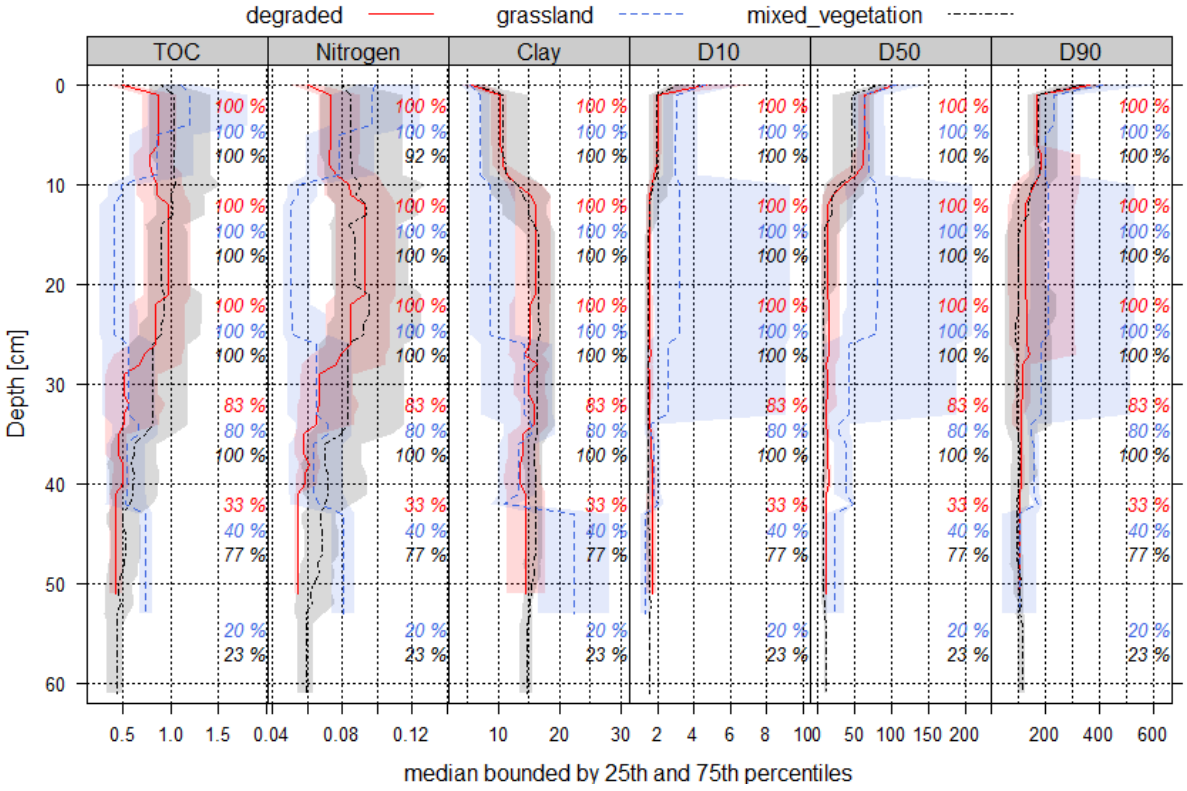

Figure 2-3 Physico-chemical soil parameters per depth for soil profiles of the different LUs (degraded LU N = 6, grassland LU N = 5, mixed vegetation LU, N = 13). Percentages on the right are percent of total profiles contributing values with depth per LU.

Table 2-3 Kruskal-Wallis (column 1) and pairwise comparison results (column 2-6) for differences between top soil samples from landscape units (LU). Significant results at the 0.95 level are presented in bold.

	All LUs	**Depositional and Degraded LU**	**Depositional and Grassland LU**	**Depositional and Mixed Vegetation LU**	**Degraded and Grassland LU**	**Degraded and Mixed Vegetation LU**	**Grassland and Mixed Vegetation LU**
D10	X2(3, 50) = 2.6591, p = 0.4472	0.2	0.68	0.29	0.33	0.54	0.43
D50	X2(3, 50) = 1.5802, p = 0.6639	0.86	0.74	0.65	0.61	0.27	0.2
D90	X2(3, 50) = 5.7519, p = 0.1243	0.065	0.15	0.17	0.89	0.18	0.28
TOC	X2(3, 50) = 23.449, p = 0.00003	0.53	**0.0081**	**0.0013**	**0.0014**	**0.00004**	0.17
TIC	X2(3, 50) = 16.444, p = 0.0009	0.63	0.057	**0.047**	**0.0026**	**0.00008**	0.24
Nitrogen	X2(3, 50) = 15.44, p = 0.0015	0.72	**0.019**	**0.036**	**0.0014**	**0.0028**	**0.038**

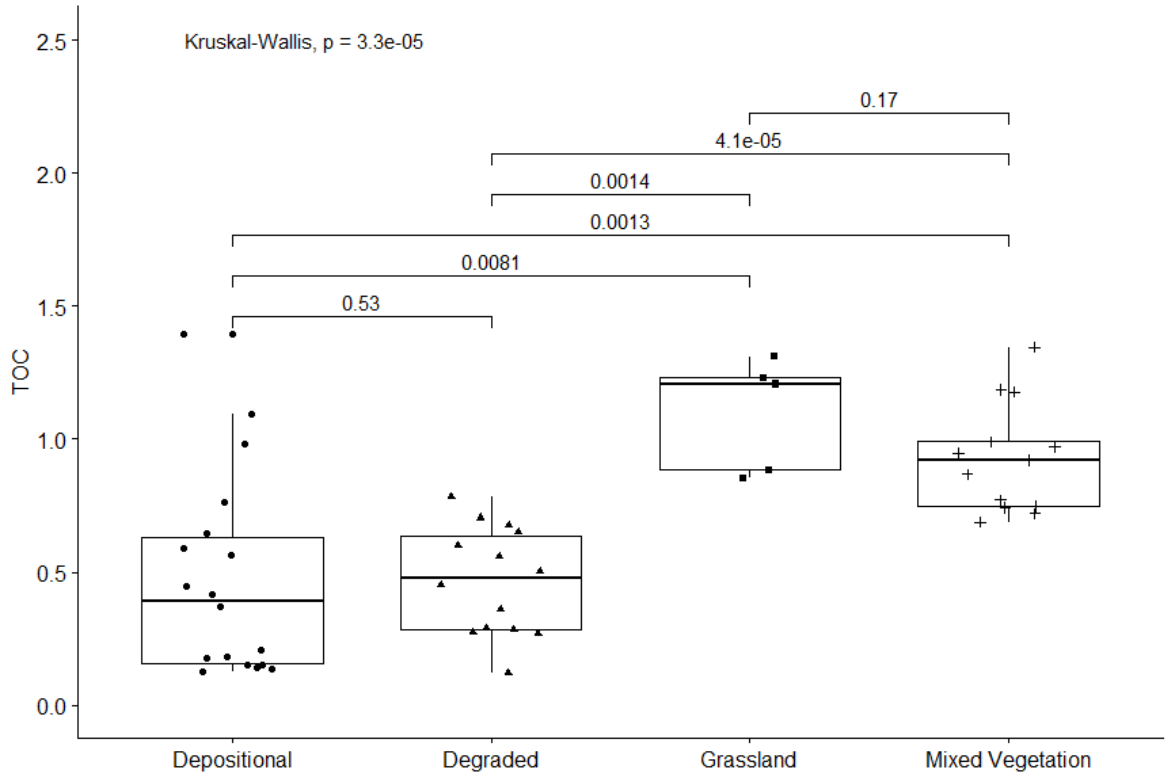

Figure 2-4 Distribution of TOC [%] content per landscape unit and accompanying significant levels.

2.6 DISCUSSION

2.6.1 SPATIAL HETEROGENEITY OF SOIL PROPERTIES

Textural differences between the LUs were not significant. Thus, it can be assumed that degradation and incision throughout the catchment are most likely not based on substrate differences, and degradation might have been induced after disturbance, by for instance, animal grazing or vegetation removal (Nouwakpo et al., 2016). Average D10 for the depositional area (8.71%) was about twice as high as for all other LUs (3.49-4.67%). Looking at the spatial distributions of texture of the depositional LU samples, this revealed that the finer samples were situated close to the former dam. Hence, a sorted distribution took place during sedimentation (McLaren and Bowles, 1985). The preferential deposition might have been masked by turbulence during runoff events or wind-induced waves over the reservoir surface (Greenwood et al., 2014). The depositional LU also had the largest range in texture, which could be an indicator that eroded material from various parts of the catchment was trapped behind the dam. This possible pathway of soil redistribution is supported by the wide range of TOC and TN as well (Table 2-2 Top soil characteristics of landscape units. Samples from the depositional LU are not taken at the surface but at 50 cm depth., Figure 2-4). Soil and C redistribution presumably followed topographic patterns as Ritchie and McCarty (2008) stated. Although they conducted research in cultivated systems, surface transport pathways

are probably similar in rangelands. For all soil profiles the clay proportion is increasing with depth. The low clay content and higher D10 sizes in the surface samples compared to the underlying layers presumable indicates erosion as fine particles have been washed away at the surface. The increase in the deeper layers, could possibly be explained by clay dislocation, a pedogenic process which happens under slightly acidic conditions.

The relative similarity of texture in the study area is not matched by the patterns of nutrient concentrations. Vegetated LUs had significantly higher TOC, TIC and TN contents than the degraded LU, while the depositional LU showed the same TOC and TN averages as the degraded LU. A possible explanation for this pattern is most likely vegetation cover and litter input in the vegetated LU (Bochet et al., 1999; Snyman, 2005). This also explains the low TOC content in the top 10 cm from the degraded profiles. Surprisingly, the vertical distribution of nutrients between 10 and 25 cm for the degraded and mixed vegetation LU was comparable and higher than for the grassland LU. This similarity could be attributed to randomness due to the small sample size of the degraded LU (N=6) and grassland LU (N=5) or differences in root depths. Soil analysis has shown that the heterogeneous vegetation cover is reflected in heterogeneous soil characteristics between areas affected by various degrees of erosion and degradation showing a disturbance of the natural soil catena, but also that the level of heterogeneity within the same landscape unit is high.

2.6.2 SPATIAL HETEROGENEITY OF THE LANDSCAPE

We found no regular type of vegetation pattern such as spotted, banded, tiger stripes (Rietkerk et al., 2002), or clumped, which is otherwise a common feature in Karoo shrublands (Blignaut and Milton, 2005). Rather than in a regular pattern, the soils appear to be organised into a source-sink system which is mainly shaped by runoff and characterised by eroding and depositional areas. This is especially evident looking at features at the degraded sites, such as shrubs and tussocks growing on earth mounds, or silted-up reservoirs that are partially covered with different vegetation types than the surrounding slopes. Not all erosion features in the landscape are still active. Rills and small gullies are presumably partially stable given the presence of established vegetation cover along their bases and sides.

2.6.3 ARE THE SNEEUBERG SOILS MORE HETEROGENEOUS THAN THE SOIL MAPS PREDICT?

According to the international FAO soil classification (ISRIC, 2006), soils in the Sneeuberg area are characterised as lithic Leptosols. Leptosols are generally defined as shallow soils with (i) either a “continuous rock or technic hard material starting 25 cm from the soil surface”, or a less than 20 vol% of “fine earth averaged over a depth of 75 cm from the soil surface or to continuous rock, whichever is shallower”, and (ii) “no calcic, chernic, duric, gypsic,

petrocalcic, petroduric, petrogypsic, petroplinthic or spodic horizon" (FAO, 2015). As a special case of Leptosols, the lithic Leptosols are even shallower and limited in depth by continuous hard rock at 10 cm. This might be true for hillslope soils of the Sneeuberg area, which were not sampled for this survey, but which were usually very shallow and had a large proportion of gravel or rock fragments (Boardman, 2015; Foster et al., 2007). However, soils of the footslopes did not meet the shallow depth criteria of the Leptosol. Even though footslope soils were very compacted and cemented and it was not possible to excavate all pits until bedrock was reached, any bedrock would have been situated deeper than 25 cm and soils showed a greater proportion of fine earth material than those defined for Leptosols by the FAO. The problem of not-capturing the soil type in the most intensely used and degraded part of study is exacerbated by the observed variability soil nutrient contents. They show a high spatial heterogeneity between degraded, vegetated, and depositional areas, which is not depicted in current soil maps, but of significant relevance for soil protection measures and adequate management strategies (Paterson et al., 2015).

2.6.4 A YOUNG SOIL TYPE IS FORMING

Besides the footslope soils that are mainly of a degraded nature, we suggest that there is a strong potential for the formation of young soils on the numerous silted-up reservoirs in the Karoo rangelands. These soils are characterised by a deep profile depth (up to 5 m) and nutrient contents significantly different from the natural soils. Since almost 50% of the mapped farm dams in this region are silted-up (Boardman and Foster, 2011), they should be properly managed by the farmers, but also not neglected in studies on local, regional and possibly global studies on biogeochemical cycles. Generally, these areas of accumulated fine sediments, support grasses which are more palatable than the rest of the valley floors. Consequently, they act as grazing sites and gathering points for domestic livestock and game and thus probably benefit from an increased manure input and thus nutrient supply. They also have a greater infiltration and water storage capacity compared to soils in surrounding areas, especially if these are degraded. Both factors improve seed germination and seedling survival, because water availability in soils is a major limiting factor for plant establishment in semi-arid environments (Bochet et al., 2009). Since root penetration depth is not limited by the underlying bedrock, deeper rooting bush species might establish and bush encroachment could be a consequence. Most of the silted-up reservoirs in the area are vegetated which increases the litter input and their nutrient content on the long-term. Hence, although they cover only a small proportion of area, in our case 10% of the study area, they presumably act differently in biogeochemical cycling than the surrounding shallow soils.

2.7 CONCLUSION

This study on soil patchiness in a degraded Karoo rangeland has illustrated the small-scale heterogeneity of soils. Soils in the study area are not classic Leptosols, unlike classified on soil maps. The main reason for this discrepancy is the various degree of soil erosion and degradation. Soil property patterns do not coincide with the vegetation cover, but show a high degree of variability within the same landscape units, especially for soil nutrients and TOC. Apart from soil degradation by erosion, sediments trapped behind dams can be identified as a depositional substrate where new and different soils can form. Their texture is finer and profiles deeper than both, the Leptosols and the degraded soils observed in the valley. The improved water supply and unimpeded root growth also offer more favourable conditions for vegetation and land use than naturally occurring soils in the Karoo. The large number of silted-up reservoirs in the Sneeuberg region, as well as in other semi-arid areas, potentially leads to the development of such anthropogenic soils on a significant proportion of rangelands. Their improved water and nutrient supply promotes plant growth and use for grazing. Water and nutrients potentially promote turnover rates in biogeochemical cycles, creating hotspots of soil-atmosphere interaction in drylands, similar to wetlands in more humid climatic conditions. Therefore, the biogeochemistry of these young anthropogenic soils forming behind dams should be explored.

2.8 ACKNOWLEDGEMENTS

We would like to thank Goswin Heckrath for his intensive field support, Lena Farré and Garbiel Weick for their help with sample collection, and Ruth Strunk for laboratory analysis. The authors are grateful to Shauna Westcott and Dirk Jacobs for access to the study site. Field work by Juliane Krenz was partially funded by the Tomscik Foundation and a Freiwillige Akademische Gesellschaft (University of Basel) grant.

2.9 REFERENCES

Acocks, J.P.H., 1975. Veld types of South Africa. Botanical survey memoir, No. 40, Pretoria.

Beaudette, D.E., Roudier, P., O'Geen, A.T., 2013. Algorithms for quantitative pedology: A toolkit for soil scientists. Comput. Geosci. 52, 258–268. https://doi.org/10.1016/j.cageo.2012.10.020

Berhe, A.A., Harden, J.W., Harte, J., Torn, M.S., 2005. Soil Degradation and Global Change: Role of Soil Erosion and Deposition in Carbon Sequestration.

Blignaut, A., Milton, S.J., 2005. Effects of Multispecies Clumping on Survival of Three Succulent Plant Species Translocated onto Mine Spoil in the Succulent Karoo Desert, South Africa. Restor. Ecol. 13, 15–19. https://doi.org/10.1111/j.1526-100X.2005.00003.x

Boardman, J., 2015. Rapid and selective clast weathering on an alluvial fan, eastern Karoo, South Africa. CATENA 126, 37–42. https://doi.org/10.1016/j.catena.2014.10.036

Boardman, J., Foster, I.D.L., 2011. The potential significance of the breaching of small farm dams in the Sneeuberg region, South Africa. J. Soils Sediments 11, 1456–1465. https://doi.org/10.1007/s11368-011-0425-5

Boardman, J., Foster, I.D.L., Rowntree, K.M., Favis-Mortlock, D.T., Mol, L., Suich, H., Gaynor, D., 2017. Long-term studies of land degradation in the Sneeuberg uplands, eastern Karoo, South Africa: A synthesis. Geomorphology 285, 106–120. https://doi.org/10.1016/j.geomorph.2017.01.024

Boardman, J., Parsons, A.J., Holland, R., Holmes, P.J., Washington, R., 2003. Development of badlands and gullies in the Sneeuberg, Great Karoo, South Africa. CATENA 50, 165–184. https://doi.org/10.1016/S0341-8162(02)00144-3

Bochet, E., García-Fayos, P., Poesen, J., 2009. Topographic thresholds for plant colonization on semi-arid eroded slopes. Earth Surf. Process. Landf. 34, 1758–1771. https://doi.org/10.1002/esp.1860

Bochet, E., Rubio, J.L., Poesen, J., 1999. Modified topsoil islands within patchy Mediterranean vegetation in SE Spain. CATENA 38, 23–44. https://doi.org/10.1016/S0341-8162(99)00056-9

Cerdá, A., 2001. Effects of rock fragment cover on soil infiltration, interrill runoff and erosion. Eur. J. Soil Sci. 52, 59–68. https://doi.org/10.1046/j.1365-2389.2001.00354.x

Cerdá, A., 1997. The effect of patchy distribution of Stipa tenacissima L. on runoff and erosion. J. Arid Environ. 36, 37–51. https://doi.org/10.1006/jare.1995.0198

Chappell, A., Baldock, J., Sanderman, J., 2016. The global significance of omitting soil erosion from soil organic carbon cycling schemes. Nat. Clim. Change 6, 187–191. https://doi.org/10.1038/nclimate2829

Council for Geoscience (Ed.), 2008. Simplified Geological Map of the Republic of South Africa and the Kingdoms of Lesotho and Swaziland. Pretoria.

Dickie, J.A., Parsons, A.J., 2012. Eco-geomorphological processes within grasslands, shrublands and badlans in the semi-arid Karro, South Africa. Land Degrad. Dev. 23, 534–547. https://doi.org/10.1002/ldr.2170

FAO (Ed.), 2015. World reference base for soil resources 2014: international soil classification system for naming soils and creating legends for soil maps. (Update 2015), World soil resources reports. FAO, Rome.

FAO (Ed.), 2006. Guidelines for soil description, 4th ed. ed. Food and Agriculture Organization of the United Nations, Rome.

FAO (Ed.), 2004. Carbon sequestration in dryland soils, World soil resources reports. FAO, Rome.

Foster, I.D.L., Boardman, J., Keay-Bright, J., 2007. Sediment tracing and environmental history for two small catchments, Karoo Uplands, South Africa. Geomorphology 90, 126–143. https://doi.org/10.1016/j.geomorph.2007.01.011

Greenwood, P., Walling, D.E., Quine, T.A., 2014. Using caesium-134 and cobalt-60 as tracers to assess the remobilization of recently-deposited overbank-derived sediment on river floodplains during subsequent inundation events. Earth Surf. Process. Landf. 39, 228–244.

Harden, J.W., Sharpe, J.M., Parton, W.J., Ojima, D.S., Fries, T.L., Huntington, T.G., Dabney, S.M., 1999. Dynamic replacement and loss of soil carbon on eroding cropland. Glob. Biogeochem. Cycles 13, 885–901. https://doi.org/10.1029/1999GB900061

ISRIC (Ed.), 2006. Soil and Terrain Database (SOTER) for South Africa [WWW Document]. ISRIC - World Soil Inf. URL http://data.isric.org/geonetwork/srv/eng/catalog.search#/metadata/c3f7cfd5-1f25-4da1-bce9-cdcdd8c1a9a9 (accessed 7.2.18).

Keay-Bright, J., Boardman, J., 2007. The influence of land management on soil erosion in the Sneeuberg mountains, central Karoo, South Africa. Land Degrad. Dev. 18, 423–439. https://doi.org/10.1002/ldr.785

Keay-Bright, J., Boardman, J., 2006. Changes in the distribution of degraded land over time in the central Karoo, South Africa. Catena 67, 1–14. https://doi.org/10.1016/j.catena.2005.12.003

Krenz, J., Greenwood, P., Kuhn, N.J., 2019. Soil Degradation Mapping in Drylands Using Unmanned Aerial Vehicle (UAV) Data. Soil Syst. 3, 33. https://doi.org/10.3390/soilsystems3020033

Krenz, J., Kuhn, N.J., 2018. Assessing Badland Sediment Sources Using Unmanned Aerial Vehicles, in: Nadal-Romero, E., Martínez-Murillo, J.F., Kuhn, N.J. (Eds.), Badlands Dynamics in a Context of Global Change. Elsevier, Amsterdam, pp. 255–276. https://doi.org/10.1016/B978-0-12-813054-4.00008-3

Lal, R., 2019. Accelerated Soil erosion as a source of atmospheric CO2. Soil Tillage Res. 188, 35–40. https://doi.org/10.1016/j.still.2018.02.001

Lal, R., 2005. Soil erosion and carbon dynamics. Soil Tillage Res. 81, 137–142. https://doi.org/10.1016/j.still.2004.09.002

Lal, R., 2003. Soil erosion and the global carbon budget. Environ. Int. 29, 437–450. https://doi.org/10.1016/S0160-4120(02)00192-7

Lü, Y., Sun, R., Fu, B., Wang, Y., 2012. Carbon retention by check dams: Regional scale estimation. Ecol. Eng. 44, 139–146. https://doi.org/10.1016/j.ecoleng.2012.03.020

Ludwig, J.A., Wilcox, B.P., Breshears, D.D., Tongway, D.J., Imeson, A.C., 2005. Vegetation patches and runoff-erosion as interacting ecohydrological processes in semiarid landscapes. Ecology 86, 288–297. https://doi.org/10.1890/03-0569

McLaren, P., Bowles, D., 1985. The effects of sediment transport on grain-size distributions. J. Sediment. Res. 55, 457–470. https://doi.org/10.1306/212F86FC-2B24-11D7-8648000102C1865D

Muñoz-Rojas, M., Erickson, T.E., Dixon, K.W., Merritt, D.J., 2016. Soil quality indicators to assess functionality of restored soils in degraded semiarid ecosystems. Restor. Ecol. 24, S43–S52. https://doi.org/10.1111/rec.12368

Nouwakpo, S.K., Williams, C.J., Al-Hamdan, O.Z., Weltz, M.A., Pierson, F., Nearing, M., 2016. A review of concentrated flow erosion processes on rangelands: Fundamental understanding and knowledge gaps. Int. Soil Water Conserv. Res. 4, 75–86. https://doi.org/10.1016/j.iswcr.2016.05.003

Okin, G.S., Gillette, D.A., Herrick, J.E., 2006. Multi-scale controls on and consequences of aeolian processes in landscape change in arid and semi-arid environments. J. Arid Environ., Special Issue Landscape linkages and cross scale interactions in arid and semiarid ecosystems 65, 253–275. https://doi.org/10.1016/j.jaridenv.2005.06.029

Paterson, G., Turner, D., Wiese, L., van Zijl, G., Clarke, C., van Tol, J., 2015. Spatial soil information in South Africa: Situational analysis, limitations and challenges. South Afr. J. Sci. 111, 1–7. https://doi.org/10.17159/sajs.2015/20140178

Polyakov, V.O., Nichols, M.H., McClaran, M.P., Nearing, M.A., 2014. Effect of check dams on runoff, sediment yield, and retention on small semiarid watersheds. J. Soil Water Conserv. 69, 414–421. https://doi.org/10.2489/jswc.69.5.414

Puigdefábregas, J., 2005. The role of vegetation patterns in structuring runoff and sediment fluxes in drylands: Vegetation and sediment fluxes. Earth Surf. Process. Landf. 30, 133–147. https://doi.org/10.1002/esp.1181

Rietkerk, M., Boerlijst, M.C., van Langevelde, F., HilleRisLambers, R., de Koppel, J. van, Kumar, L., Prins, H.H.T., de Roos, A.M., 2002. Self-Organization of Vegetation in Arid Ecosystems. Am. Nat. 160, 524–530. https://doi.org/10.1086/342078

Ritchie, J.C., McCarty, G.W., 2008. Redistribution of soil and soil organic carbon on agricultural landscapes. IAHS Publ. 325, 135–138.

Sanderman, J., Berhe, A.A., 2017. Biogeochemistry: The soil carbon erosion paradox. Nat. Clim. Change 7, 317–319. https://doi.org/10.1038/nclimate3281

Schlesinger, W.H., Raikes, J.A., Hartley, A.E., Cross, A.F., 1996. On the Spatial Pattern of Soil Nutrients in Desert Ecosystems. Ecology 77, 364–374. https://doi.org/10.2307/2265615

Schlesinger, W.H., Reynolds, J.F., Cunningham, G.L., Huenneke, L.F., Jarrell, W.M., Virginia, R.A., Whitford, W.G., 1990. Biological Feedbacks in Global Desertification. Science 247, 1043–1048. https://doi.org/10.1126/science.247.4946.1043

Sharma, K.L., Mandal, U.K., Srinivas, K., Vittal, K.P.R., Mandal, B., Grace, J.K., Ramesh, V., 2005. Long-term soil management effects on crop yields and soil quality in a dryland Alfisol. Soil Tillage Res. 83, 246–259. https://doi.org/10.1016/j.still.2004.08.002

Sharma, P., Abrol, V., Abrol, S., Kumar, R., 2012. Climate Change and Carbon Sequestration in Dryland Soils, in: Abrol, V. (Ed.), Resource Management for Sustainable Agriculture. InTech.

Snyman, H.A., 2005. Rangeland degradation in a semi-arid South Africa—I: influence on seasonal root distribution, root/shoot ratios and water-use efficiency. J. Arid Environ. 60, 457–481. https://doi.org/10.1016/j.jaridenv.2004.06.006

Soils Research Institute (Ed), 1965. Soil Map of South Africa.

Sugden, J.M., 1989. Late quaternary palaeoecology of the central and marginal uplands of the Karoo, South Africa. University of Cape Town, Cape Town, South Africa.

Van Oost, K., Quine, T.A., Govers, G., Gryze, S.D., Six, J., Harden, J.W., Ritchie, J.C., McCarty, G.W., Heckrath, G., Kosmas, C., Giraldez, J.V., Silva, J.R.M. da, Merckx, R., 2007. The Impact of Agricultural Soil Erosion on the Global Carbon Cycle. Science 318, 626–629. https://doi.org/10.1126/science.1145724

Xiang-zhou, X., Hong-wu, Z., Ouyang, Z., 2004. Development of check-dam systems in gullies on the Loess Plateau, China. Environ. Sci. Policy 7, 79–86. https://doi.org/10.1016/j.envsci.2003.12.002

Zhao, P., Shao, M., Melegy, A.A., 2010. Soil Water Distribution and Movement in Layered Soils of a Dam Farmland. Water Resour. Manag. 24, 3871–3883. https://doi.org/10.1007/s11269-010-9638-4

CHAPTER 3

Assessing Badland Sediment Sources Using Unmanned Aerial Vehicles

Assessing badland sediment surces using unmanned aerial vehicles

Juliane Krenz and Nikolaus J. Kuhn
University of Basel, Klingelbergstrasse 27, 4056 Basel, Switzerland

Status: Published
Krenz, J., Kuhn, N.J., 2018. Assessing Badland Sediment Sources Using Unmanned Aerial Vehicles, in: Nadal-Romero, E., Martínez-Murillo, J.F., Kuhn, N.J. (Eds.), Badlands Dynamics in a Context of Global Change. Elsevier, Amsterdam, pp. 255–276.
https://doi.org/10.1016/B978-0-12-813054-4.00008-3

3.1 ABSTRACT

Badland erosion is a major sediment source for river systems in drylands (Poesen et al., 2002). Identifying their relevance as sediment sources is critical for measures aimed at reducing reservoir siltation. However, the spatial resolution of commonly available data products on topography is usually not sufficient to calculate sediment losses accurately. Unmanned aerial vehicles (UAVs) can help to overcome the gap between traditional, expensive, time-consuming ground-based assessment and insufficient data availability or quality at aerial photography or satellite imagery scale levels. This study investigates the use of UAVs for generating high resolution DTMs of badlands in a remote catchment in the Karoo highveld in South Africa, which is affected by severe soil erosion and reservoir siltation, but where the relevance of badlands as sediment source is unclear. The chapter describes UAV hardware, image capture, DTM, and orthomosaic generation and a workflow for badland erosion estimation with the acquired imagery. The results show that erosion volumes in badlands accounted for only 17.2% of the reservoir storage capacity in the study area, which indicates that there are additional sediment sources within the catchment.

Keywords
badland assessment, DSM, DTM, orthomosaic, Pix4D, sediment source, soil erosion, UAV

3.2 MAPPING BADLANDS

Badlands are areas of intensive erosion, characterised by a strongly dissected and gullied landscape with sparse or absent vegetation unusable for agriculture (Bryan and Yair, 1982). They often develop on unconsolidated or poorly consolidated sedimentary deposits (silty clays, marls or shales) (Bryan and Yair, 1982) and frequently occur in arid and semi-arid areas where erosion is strongly correlated to rainfall (Clarke and Rendell, 2010). Currently, erosion of agricultural land leads to the expansion of many badlands in semi-arid regions, and soils characterised by slow formation and nutrient cycling are lost (Austin et al., 2004). Badland erosion is a major sediment source for river systems in drylands (Poesen et al., 2002). High erosion rates thus not only account for a loss of soil productivity (Lal, 1997), but ultimately can also lead to reservoir siltation (Pimentel et al., 1995).

Land degradation in South Africa is a significant environmental problem throughout the whole country (Meadows and Hoffman, 2002). Erosion frequently leads to the formation of badland features on overgrazed rangelands such as the Karoo highveld (Ainsle, 2002; Boardman et al., 2003; Hoffman and Ashwell, 2001). In the rangelands of the Karoo, erosion and gully development are occurring frequently and sedimentation of reservoirs is a widespread problem (Boardman and Foster, 2011; Rowntree and Foster, 2012). In the affected catchments, various types of badlands (Boardman and Foster, 2008; Rowntree, 2014) have

formed, most likely associated with the increase of agricultural activities in the beginning of the 20th century (Boardman et al., 2003). However, it remains unclear how much sediment the heavily eroded sites characterised by badland features contribute to watercourses and reservoirs because they are commonly associated with other erosion phenomena that are less incised, but more widespread. Identifying the relevance of the badlands as a sediment source in the Karoo is therefore critical for measures aimed at reducing reservoir siltation and ensuring the countries water supply (Nde, 2015; Oberholster and Ashton, 2008).

Estimating the volume of sediment supplied by badlands such as those on degraded rangeland in the Karoo could be done, in theory, by estimating the volume of material that has been eroded since their formation started several decades ago. Traditional field-based erosion monitoring and volume estimation via sediment traps, erosion pins or bridges is labor intensive and time consuming. Several studies also showed that point measurements, such as pins, only produce reasonable erosion rates for small areas (Boardman et al., 2015; Clarke and Rendell, 2010). A high density of erosion pins and several years of monitoring are therefore required for reliable large-scale extrapolation.

Detailed erosion mapping on catchment-scale could be achieved with terrestrial laser scanning (TLS) or total stations to generate high-precision terrain models. These methods are very time-consuming, labor-intensive and depend on the accessibility of the geomorphic features to be monitored. Their dissected character complicates ground-based terrain mapping and often requires positional changes to recover obstructions from the laser's field view (Brodu and Lague, 2012). Badlands are usually located in relatively remote areas with low population densities. Hence, remote sensing plays an important role in assessing and monitoring drylands. However, the spatial resolution of commonly available data products on topography such as open source SRTM DTMs from the US Geological Survey (30 x 30 m) is usually not sufficient to calculate sediment losses accurately (Laliberte et al., 2011; Mondal et al., 2017a, 2017b).

Unmanned Aerial Vehicles (UAVs) can help to overcome the gap between expensive, time-consuming ground-based measurements and the insufficient data availability or quality from coarse resolution imagery of satellite or airborne systems. In addition, UAV image acquisition is less influenced by obstructions because the camera's field of view is not stationary as for laser scanners (Brodu and Lague, 2012; Buckley et al., 2012). UAVs are also fairly inexpensive and allow a fast data acquisition and generation of user-specific data products, such as digital surface or terrain models (DSM/DTM), orthomosaics, or NDVI maps. Consequently, UAVs have an increasing popularity in remote sensing studies because they offer new opportunities for collecting spatial data of the environment at high-resolution, especially for study areas in rough and remote terrain. UAV imagery in combination with complementing terrestrial images can successfully fill data gaps, e.g. missing information as a result of overhanging gully walls (Stöcker et al., 2015). Several studies have recently

investigated the use of UAVs to monitor or assess the extent of gullies and badlands (Neugirg et al., 2016; Nobajas et al., 2017; Wang et al., 2016) and introduced workflows for UAV-based remote sensing (d'Oleire-Oltmanns et al., 2012; Laliberte et al., 2011). These studies focused largely on mapping gullies and badlands but disregarded the actual identification of badlands via a detailed 2D and 3D analysis.

The aims of this study are to investigate the use of UAVs for generating high resolution DTMs of badland features. The study was conducted in a catchment in the Karoo rangelands and included an assessment of the badland erosion as sediment source contributing to the siltation of a small reservoir at the lower end of the studied catchment. A comparison of available low resolution cartographic data of the catchment and the high resolution UAV-based DTM generated for this study, in combination with field visits, was used to assess the contribution of UAVs to badland erosion studies.

3.3 STUDY SITE, DATA ACQUISITION AND DTM GENERATION

3.3.1 STUDY SITE

The geomorphology and history of the region has been studied in detail by Boardman et al. (2003, 2017), Boardman and Foster (2008), Foster et al. (2012) and Keay-Bright and Boardman (2006, 2007). Based on their description of badlands and infilled reservoirs, a small catchment with severe badland erosion and a filled reservoir with a breached dam downstream of the badlands has been selected for this study. It is located in the Klein Seekoei river basin in the Great Karoo Region of South Africa, roughly 70 km north of Graaff-Reinet. Being part of the Sneeuberg Range the underlying geological material consists of horizontal Permian to Triassic sandstones, often with dolerite caps and intrusions. Less resistant mudstones, shales, and sandstones from the Balfour Formation cover the valley floors (Boardman et al., 2003). Overgrazing during the 20th century has probably led to land degradation and promoted the development of badlands on the footslopes and rill and gullies in valley. The catchment covers 3.2 km^2 and drains into the filled reservoir labelled as Dam 53 (31.698558°S, 24.588183°E) by Boardman and Foster (2011). The reservoir is located at appr. 1740 m a.s.l. and surrounded by hills up to 2080 m a.s.l. A main gully up to 6 meters deep and partly up to 10 m wide follows the thalweg of the catchment and forms the breach in the dam wall.

3.3.2 DATA ACQUISITION

For the assessment of badlands as sediment source in our study area, the volume of the material eroded from areas with badland-type of incision had to be compared to the volume of sediment in the reservoir. To conduct such an analysis, an orthomosaic showing potential sediment source regions and badlands, and a high-resolution digital terrain model (DTM) to

quantify the volume of soil displaced by erosion and current, as well as pre-dam topography were required. A digital contour map of the research area with 20 m contour lines was available from the National Geo-Spatial Information (NGO) Service of South Africa. This coarse resolution only enables the identification of major geomorphological features, but not small gullies in badlands. To calculate the volume of the material that was eroded from the badlands, the resolution, i.e. pixel size, of a DTM has to be an order of magnitude greater than the size of the eroded features. Badland incision in the Dam 53 watershed is typically 0.5 to 5 m deep and up to 10 m wide. The resolution of the DTM should therefore be on the order of centimeters. To create our own high-resolution orthomosaic, digital surface model (DSM), and digital terrain model (DTM), UAV imagery was acquired in February 2016. To compare the use of both DTMs for erosion volume estimation, we calculated a difference image, where we subtracted the interpolated DTM based on topographic data from the drone-acquired DTM on a cell by cell basis.

3.3.3 CAMERA AND UAV SETTINGS

The UAV used in our study was a Phantom 3 Professional quadrocopter with a gimbal manufactured by DJI (SZ DJI Technology Co., Ltd., Shenzhen, China) and equipped with a DJI FC300X camera (GoPro Inc., San Mateo, California, USA). Its low total weight (1.28 kg) and small size simplified the transport and allowed us to carry it easily around the uneven terrain. Images were taken at an altitude of 70 m above the ground with an angle of 90° and an average overlap of 90% to ensure sufficient overlap for photogrammetric processing. Compromising between a high resolution and the expenditure of time in the field and post-processing, resulted in a ground size resolution (GSD) of 3.1 cm. This required in total 19 flights to cover the study area at this level of detail. Images were taken with a resolution of 4000 x 3000 pixels at a focal length of 4, with an aperture of 1/2.8, and an exposure time automatically adjusted by the camera. The Phantom 3 is powered by electrical batteries and has a flight time of about 15 minutes per battery in average. Navigation was GPS-based using an image acquisition plan programmed in advance with Pix4D Capture App on an IPad mini A1550.

3.3.4 GROUND CONTROL

In order to produce high-resolution maps for measuring and mapping badlands, images have to be georeferenced and geometrically corrected. The Phantom 3 is equipped with GPS, but its horizontal accuracy is only about 1.5 m. This is not sufficient for a detailed badland volume assessment. For a higher accuracy, ground control points (GCPs) need to be measured to support the image processing and accuracy. These can be either distinctive geomorphic features or placed markers that can be identified on the aerial images. The positions of the GCPs were determined by a Trimble SPS851 with a horizontal accuracy of 0.25 m and recorded

with a GETAC PS336 data logger to increase the precision of the orthomosaic. Since we received an unknown error during post-processing the GPS positions, which resulted in horizontal offsets in various directions, we could not use the GCPs determined in the field. Thus, we obtained the geographic coordinates of three distinctive spots used as GCPs from Google Earth and identified these on the multiple photographs for higher accuracy.

3.3.5 IMAGE PROCESSING

The image processing workflow was photogrammetry-based and included orthorectification and 3D photo-reconstruction by bundle-block adjustment to create a Digital Surface and Terrain Model and an orthomosaic. We used the commercial photogrammetry software Pix4Dmapper Pro (Pix4D SA, Lausanne, Switzerland), version 4.1.10. The steps performed by Pix4Dmapper to create an orthomosaic, a DSM, and a DTM are illustrated in Figure 3-1 and Table 3-1 and can comprise the following steps. Firstly, during initial processing matching points have to be found automatically by the software by analyzing all imported images. Then, a bundle block adjustment is performed to reconstruct the exact camera position and orientation for every image. Knowing the orientation parameters of two images 3D object point coordinates can be determined and verified (Eltner et al., 2015b; Küng et al., 2011). To decrease the projection error, which represents the difference in location of a computed 3D point to the initial position on the image (2D keypoint) after re-projection it on the image, manual tie points (MTPs) can be added. A small projection error also improves the quality of the point cloud. Each of the MTPs is evaluated and marked on multiple images by the user. For accurate geolocation GCPs can be added similarly. In the second processing step all matching points are verified and their 3D coordinates are automatically calculated by the software. This results in a densified point cloud and a 3D textured mesh that reconstruct the camera orientation of all images. Finally, in the last processing step the 3D points are interpolated by the software to form a triangulated irregular network to obtain a DSM and DTM. Every image pixel is than projected on the DSM to obtain the georeferenced orthomosaic. All of the software outputs (DSM, DTM, orthomosaic) can be exported and used for further data analysis in ArcGIS.

Generating the data for the Karoo badlands required some further specific procedures. We added three manual tie points (MTPs). Each point was marked on 168, 87, and 100 and automatically verified on 166, 87, and 100 images respectively. For accurate geolocation three GCPs were marked and automatically verified on 9, 8, and 9 images.

3.3.6 IMAGE ANALYSIS

Land cover classification from UAV based aerial imagery equipped with a normal camera is challenging. Although the spatial resolution of the orthomosaic is very high compared to

satellite imagery, spectral information is low. The images recorded with an RGB-camera only contain information on the closely related red (R), green (G), and blue (B) spectral bands. Thus, image analysis was only based on information from the visual spectrum and groundthruthing was necessary to verify information obtained from the orthomosaic.

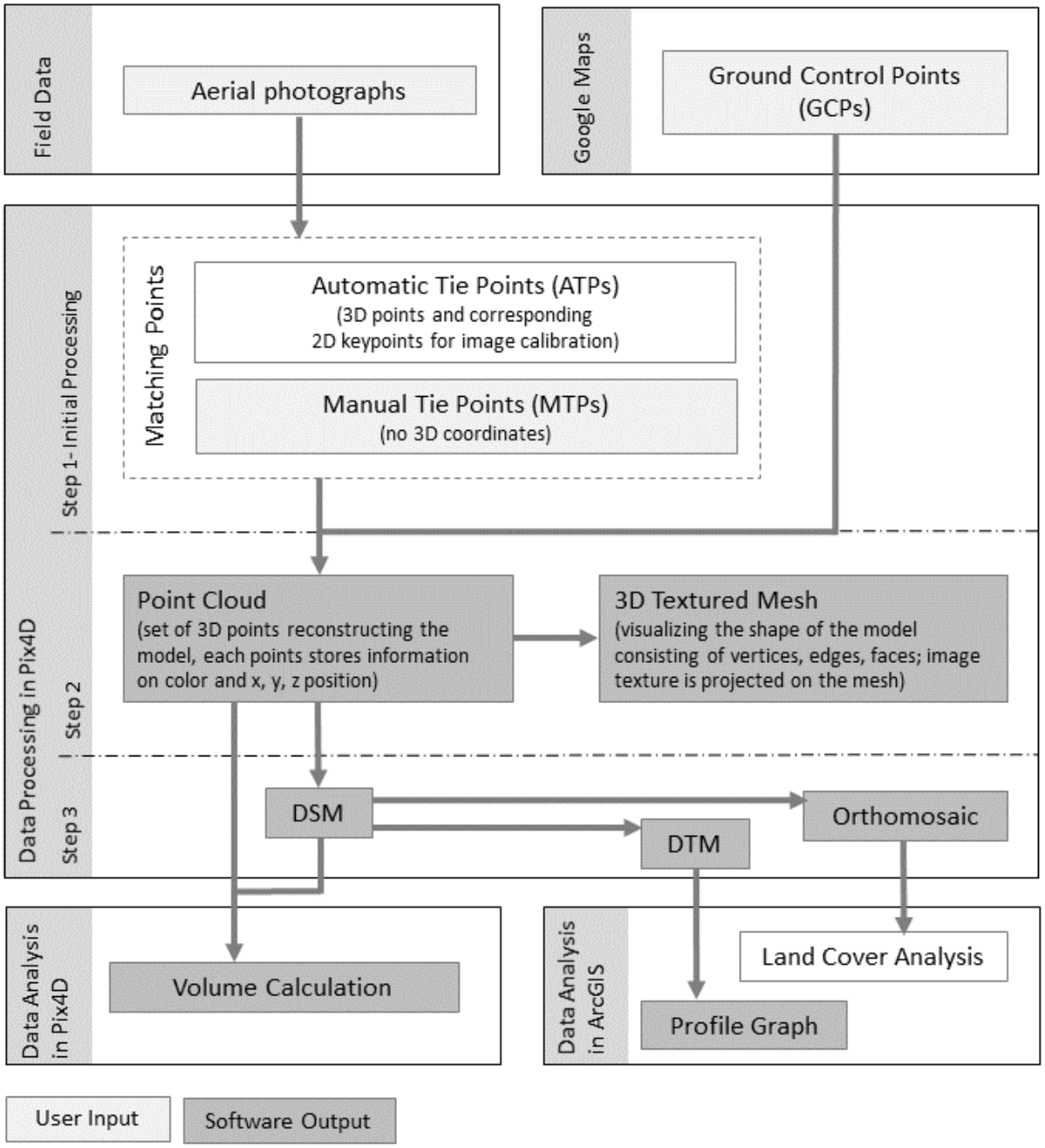

Figure 3-1 Schematic workflow of processing aerial imagery with Pix4D and ArcGIS. Light grey boxes represent inputs from the user, dark grey boxes output files from the respective software.

Table 3-1 Parameters used for the data processing in Pix4D.

Processing Option	Parameter	Impact
1. Initial Processing		
Keypoints Image Scale	Full, Image Scale: 1 (Original image size) (default)	more key points are extracted, increases the accuracy of the point cloud
2. Point Cloud and Mesh *(default settings were used as a trade-off of computational power, time and resulting file size)*		
Image Scale	Multiscale, ½ (Half image size, default)	additional 3D points are calculated
Point Density	Optimal (default)	one 3D point for 8 pixels of the original image is computed (4/ Image scale)
Minimum Number of Matches	3 (default)	correct re-projection of each 3D point in at least 3 images
3D Textured Mesh	High resolution, incl. color balancing	Maximises visualisation and creates homogenous texture
3. DSM, Orthophoto Mosaic and Index		
DSM	Noise Filtering, Sharp Surface Smoothing Resolution 1 x GSD	corrects erroneous points while preserving the orientation of surfaces, corners and edges
Orthomosaic	GeoTIFF, merged tiles (default) Resolution 1 x GSD	results into one single GeoTIFF file
Raster DTM Resolution	Merged tiles Resolution 5 x GSD (minimum possible)	results into one single GeoTIFF file with the highest resolution possible

3.3.7 IDENTIFICATION OF POTENTIAL SEDIMENT SOURCES AND SINKS

Eroding areas have to be identified to estimate the volume of potential sediment sources. The identification was based on a combination of on-site observations and differences mapped from the orthomosaic and DSM. In Pix4D the orthomosaic can be projected on the DSM via the point cloud. This enables a realistic view on the surface. Sediment sources in the context of this paper are any areas that show signs of erosion, such as areas of bare ground, especially if there is an elevation difference to the surrounding area. Cut banks in the dry river bed can also act as a sediment sources. Depositional areas, in our study the infilled reservoir behind the dam, are considered as potential sediment sink areas. A summary of characteristics of potential areas of erosion and deposition is shown in Table 3-2.

Table 3-2 Characteristics of potential source and sink areas within the catchment.

	Location	**Identification on orthomosaic**	**Identification on DSM**
Areas of erosion			
Badland	often connected to gullies	Bare soil, extensive extent	Elevation differences to surrounding, shrubs often on little soil mounds
Erosion rill	mostly directly connected to main channel	Bare soil, linear extent	Rill structure
Cut bank	within the main channel	channel bends, often with shadows	steep walls on channel bends
Areas of deposition			
Reservoir	SE-direction of former dam wall	Circumcised by a change in vegetation (shrub line), corresponds with water filled area on an old aerial photograph when dam was still intact	
Point bar	within the main channel	Vegetated areas	"sand banks"
Tussock grass	distributed in the catchment	bleached green-grey color	grassy structure, color

3.3.8 AREA AND VOLUME ESTIMATION

We estimated the volumes of the potential sediment sink and source areas to compare and investigate the relevance of badlands as sediment source areas in the catchment. We regarded the reservoir as the main sink area and neglected all minor sink areas like tussock grasses because their potential for trapping sediments is not assessable (Foster et al., 2008). The volume of cut banks and point bars was also excluded from the assessment because they probably only developed after the dam breached. We estimated the maximum storage capacity (RC) of the reservoir before it breached. The badlands were regarded as the potential main source of eroded sediment volume (V_s).

The maximum reservoir storage capacity (RC) was estimated based on (Foster et al., 2008). The equation 3.1 was slightly altered to represent natural conditions better based on trapezoidal instead of rectangular cross sectional areas

$$RC = \frac{h_x}{3} * \frac{A + A_h}{\sqrt{A - A_h}} \quad (3.1)$$

where h_x is the height of a layer x, A is the surface area of the reservoir, A_h the surface area for the corresponding layer x to the corresponding height h. The maximum surface area was based on an aerial photograph from 1945 that most likely showed the dam filled to capacity. The height of each sediment layer was based on the height of an outcrop of dam sediments in

the gully close to the breach. It was assumed that sediment depths is constant throughout the reservoir. For detailed cross sections further extensive field work would be needed. Current sediment volume was estimated using the RC and distracting the volume of sediment that was removed through incision of the stream after the dam breached and during ongoing erosional processes.

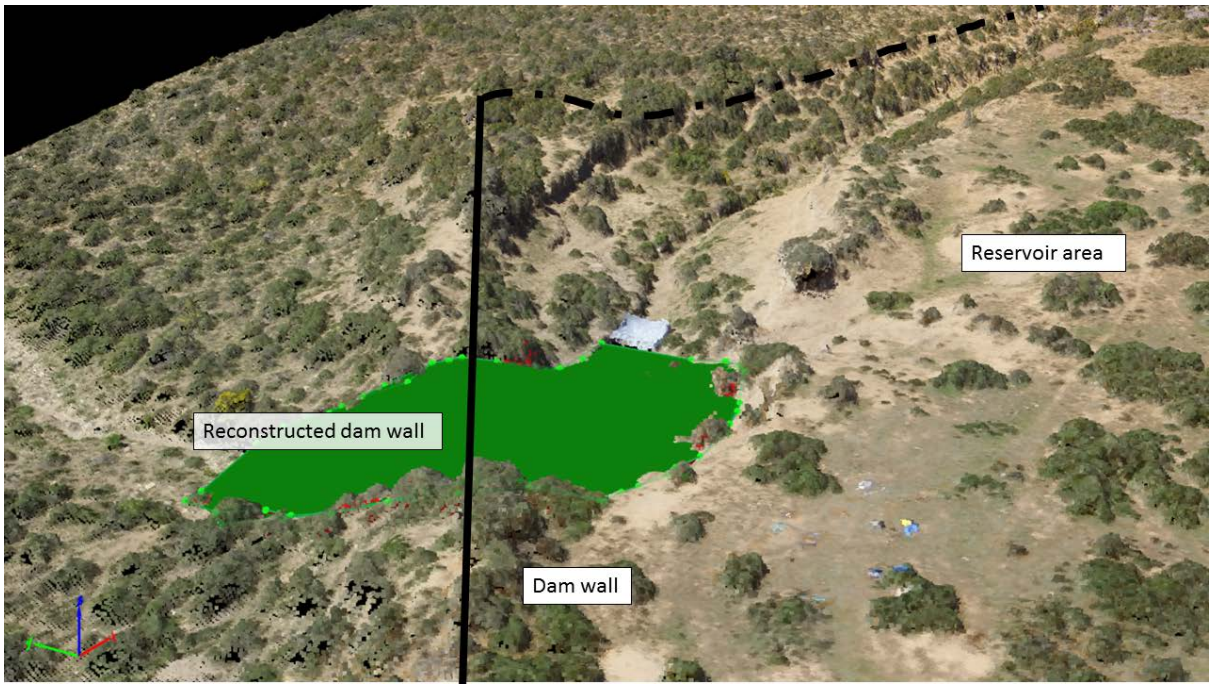

Figure 3-2 Reconstructed dam wall (green) of the reservoir with the software Pix4D. The breach of the dam wall released appr. 680 m^3 of material.

The volume of potentially eroded sediment from the badland (V_s) was estimated using the volume calculation tool in Pix4Dmapper. For the volume calculation the software needs the point cloud and the DSM. New volumes are added by marking vertices of the volume base surface on the DSM. The level of accuracy is proportional to the amount of vertices and increases the more vertices are set. Pix4Dmapper projects a grid on the volume base surface, where the width and length are equal to the ground sampling distance (GSD), and calculates the volume based on the height difference between terrain altitude (Z_{Ti}) and base altitude (Z_{Bi}) corresponding to the center of each cell (Figure 3-3).

$$V_i = GSD*GSD*(Z_{Ti} - Z_{Bi}) \quad (3.2)$$

We used the triangulated setting for the grid projection of the base surface that most likely represents an uneven soil surface best while connecting all vertices and triangulating the volume above (cut volume) and below (fill volume) the base surface. The cut volume represents the volume between the base and the 3D terrain, when the terrain is higher than the

base. The fill volume is the volume between the base and the terrain, when the terrain is lower than the base. Thus the fill volume represents our potentially eroded volume of soil from badland areas.

Volume errors are calculated by Pix4D itself solely based on the altitude difference because each cell has the same dimension in x and y direction (equal to the GSD). The difference in altitude is computed with an accuracy between 1 to 3 times the GSD. Thus an average error for the altitude of 1.5 times of the GSD is assumed for each cell volume and the error highly depends on the spatial resolution.

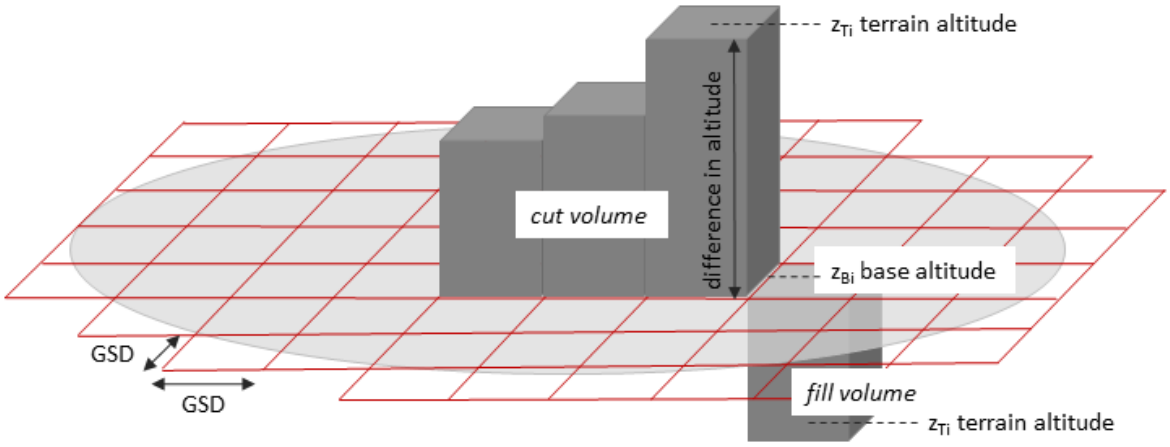

Figure 3-3 Schematic volume calculation for terrain (grey blocks) in Pix4D. The grey ellipse exemplifies the base surface of a drawn volume with the projected raster (red).

3.4 RESULTS

3.4.1 UAV IMAGERY AND QUALITY

3.4.1.1 HIGH-RESOLUTION ORTHOMOSAIC

The first set of analysis aimed to create an orthomosaic (Figure 3-4) and DTM from the UAV imagery. A total of 1113 JPEG photos were acquired, 1081 were used for calibration. The orthomosaic covered the 17.5 ha of highly eroded areas within our catchment and had a ground sampling distance (GSD) of 3.12 cm. Due to the high overlap, 97% of the images could be used for the calibration with a median of 29618.2 matching points per calibrated image. The mean reprojection error is 0.164 pixels. The root mean square error (RMSE) was 0.3 cm in x-direction, 0.2 cm in y-direction and 0.1 cm in z-direction. The perspective lense of our camera had a 2.74% relative difference between initial and optimised focal length, which is below the 5% threshold for a successful image optimisation. The projection error for the MTPs varied between 1.329 pixel (100 verified image marks out of 100 marked) to 2.283 pixel (166 verified image marks out of 168 marked). All parameters confirm that the orthomosaic is representing

the nature at a level of high accuracy. In Table 3-3 results of the image processing via Pix4Dmapper are summarised.

Table 3-3 Summary of result parameters after image processing in Pix4Dmapper.

Imagery and Resolution				**Bundle Block Adjustment**			**Geolocation**	
Images calibrated	Matching Points per calibrated images (Median)	Area covered [ha]	GSD [cm]	Number of 2D keypoints	Number of 3D points	Mean re-projection Error [pixel]	Number of GCPs	Mean RMSE (x/y/z) [cm]
1081	29618	17.50	3.12	31318717	7678458	0.164	3	0.3/0.2/0.1

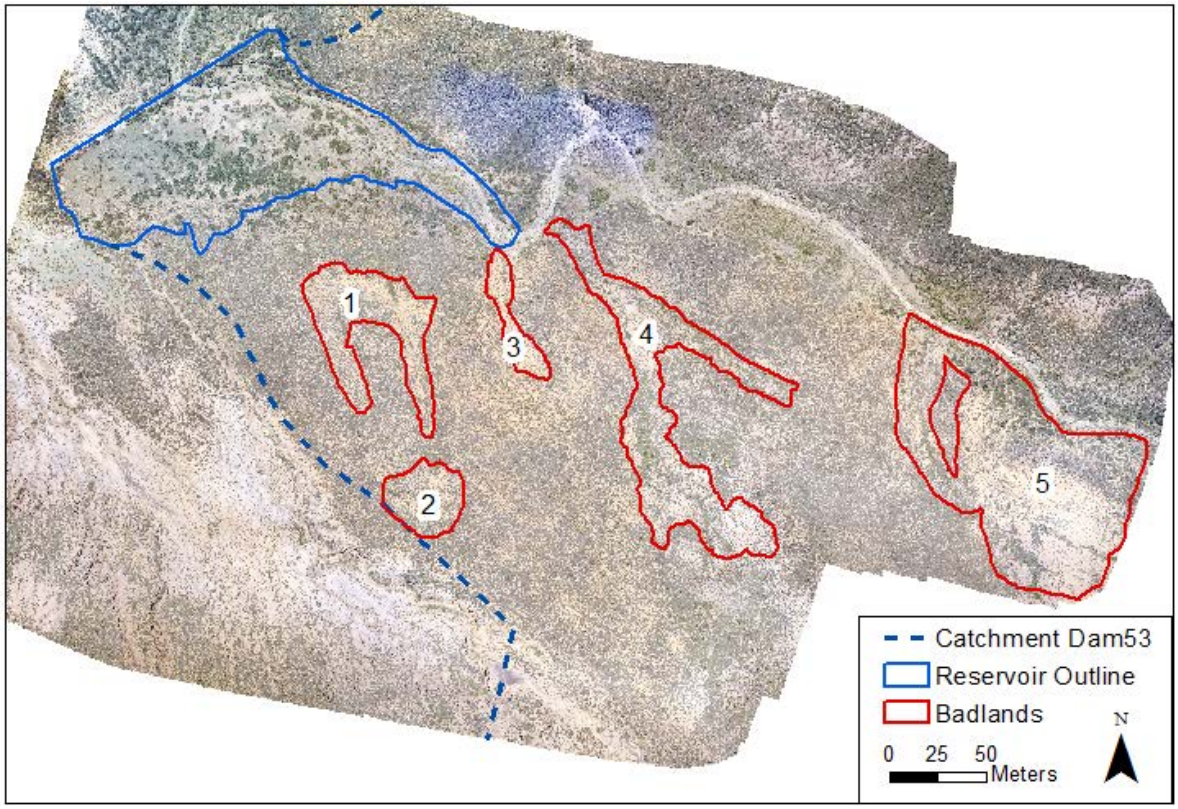

Figure 3-4 RGB-orthomosaic (resolution 3.12 x 3.12 cm/pixel) of the study area within the reservoir catchment. The area of the former reservoir is marked in blue, identified badland and gully systems in red.

The resulting orthomosaic enables a bird's-eye view on the study site. Bare soil and vegetated areas can be distinguished. In addition, we can even differentiate between shrubby or grassy vegetation. Hidden to the scientist in field, it shows that the borders of the former reservoir are still identifiable, mainly by a sharp line of vegetation change. Main geomorphic features such as the riverbed and ridges can also be recognised, as well as large badland areas.

3.4.1.2 HIGH-RESOLUTION DTMS

Two DTMs were created, one based on the 20 m contour lines from National Geo-Spatial Information (NGO) Service of South Africa (DTM A), and a second one based on the UAV imagery directly produced by the Pix4D software (DTM B, Figure 3-5). As presumed, they differ in their resolution and level of detail. DTM A (derived from the contour lines) has a resolution of 0.383 x 0.383 m per pixel. This is two and a half times the resolution of the DTM B (derived from the UAV imagery): 0.1562 x 0.1562 m per pixel. Due to internal algorithms the resolution of the generated DTM generalised to a cell size of at least five times the GSD (in our case: 5 x 3.12 cm/pixel). DTM A still allows to recognise main geomorphic features, such as the slope and river bed but it is unsuitable for our badland volume analysis. Due to the interpolation the land surface is very smooth and does show any geomorphic details such as the dam, its breach or the gully cut through the sediments. It is not possible to distinguish the badland areas that have been identified on the orthomosaic. DTM B has a higher resolution that enables recognition of much smaller geomorphic features, such as erosion rills, gully systems and some badlands that can be detected from the orthomosaic as well. A comparison of the absolute difference in altitude for both DTMs (Figure 3-7) shows that DTM A overpredicted the altitude especially in the main channel and badland areas due to a lack of resolution.

3.4.2 IMAGE ANALYSIS, AREA AND VOLUME ESTIMATION

3.4.2.1 RESERVOIR STORAGE CAPACITY (RC)

Based on an aerial picture from 1945, the maximum estimated surface area is 1.3 ha. Silted-up to the top, the reservoir had a RC of approximately 30490 m^3. After the breach 2908 m^3 ± 103 m^3 of sediment were removed from the silted-up material in the reservoir by headward gully erosion until the time the DTM was generated, which represents ~9.5% of the initial RC. Additionally, the breach released 680 m^3 of material from the dam wall that was transported downstream.

3.4.2.2 BADLAND VOLUMES AND SPATIAL EXTENT OF ERODING AREAS

Based on two profile graphs along the high-resolution DTM (Figure 3-5, Figure 3-6) we exclude eroding areas below the altitude of the dam crest (appr. 1740 m a.s.l.) as source areas for dam sediment because the steep increase within the profile at this altitude indicates headward erosion after the breaching. Five badland areas (Figure 3-4) of different scale and degree of erosion could be determined within the study area. The current extension of badlands is estimated to be 21060 m^2 (Table 3-4). The total volume of potentially eroded material from the badlands is 5265 m^3. This makes up only 17.3% of the RC, if we assume that all this material was transported to the reservoir and settled there.

Besides the badlands, areas which are characterised by no or low vegetation cover and forms such as erosion rills or gullies, and cut off slopes along the main channel where also identified as potential sediment sources. Their volume quantification was only possible as a rough estimate because their incision is not or only imprecisely recognizable on the DSM. Field observations on surface incision around vegetation mounds showed that on average 10 cm of A-horizon have been eroded. Assuming that this depth of top soil got eroded from the bare soil surface (2.6 ha) within the study area, sheet erosion would account for a volume of 2600 m^3.

Table 3-4 Overviews of the calculated volumes of eroded sediment from each identified badland within the study area according to two different approaches (triangulated, fit plane) and their spatial extent.

Badland	Area [m2]	Fill Volume [m3] Triangulated			Characteristics of the badland
		Vs [m^3]	Error [m^3]	Error [%]	
1	2928.87	274.55	± 97.11	35.37	shallow extensive erosion, sparsely vegetated
2	1275.46	72.29	± 35.23	48.73	shallow extensive erosion, sparsely vegetated
3	776.14	156.80	± 30.21	19.27	incised rill connected to the main channel, with almost no side rills yet
4	5844.33	1096.70	± 196.73	17.94	deeply incised main rill connected to the main channel, rill partly vegetated with shrubs
5	10235.70	3665.31	± 286.69	7.82	deeply incised rill with extensive fanlike network of smaller side rills
-	26000	2600	-	-	Estimated sheet erosion from bare soil surfaces over the study area
Total	47060.5	7865.65			

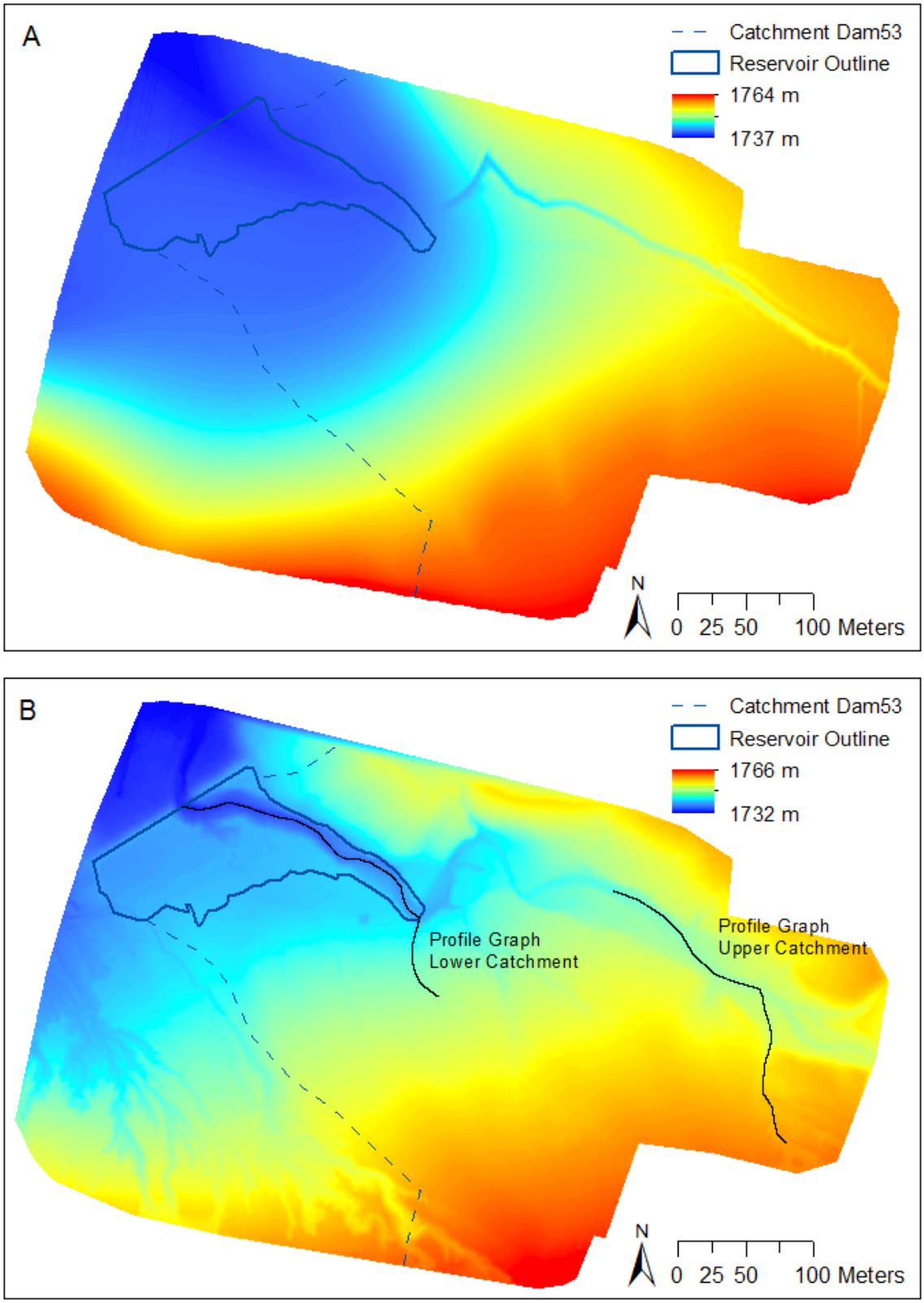

Figure 3-5 DTM derived from the 20 m contour lines (A) and the UAV imagery (B). Both have the same spatial extent but different resolutions. It can be clearly seen, that DTM A is based on an interpolation and thus looks smoother than the reality. Many features such as the badland in the southeast or the elevation difference behind the dam wall are lost due to the coarse input data.

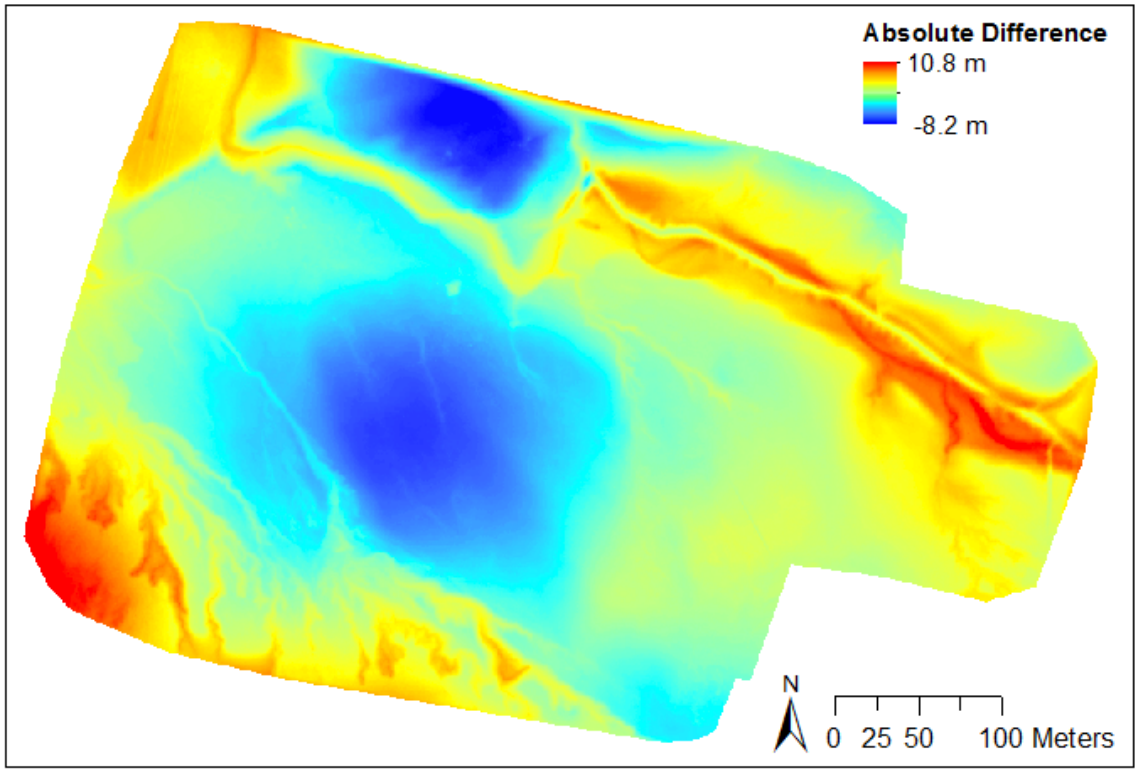

Figure 3-7 Absolute difference in altitude between the DTM interpolated from the
7 Absolute difference in altitude between the DTM interpolated from the contou
7 Absolute difference in altitude between the DTM interpolated from the contour lines
7 Absolute difference in altitude b

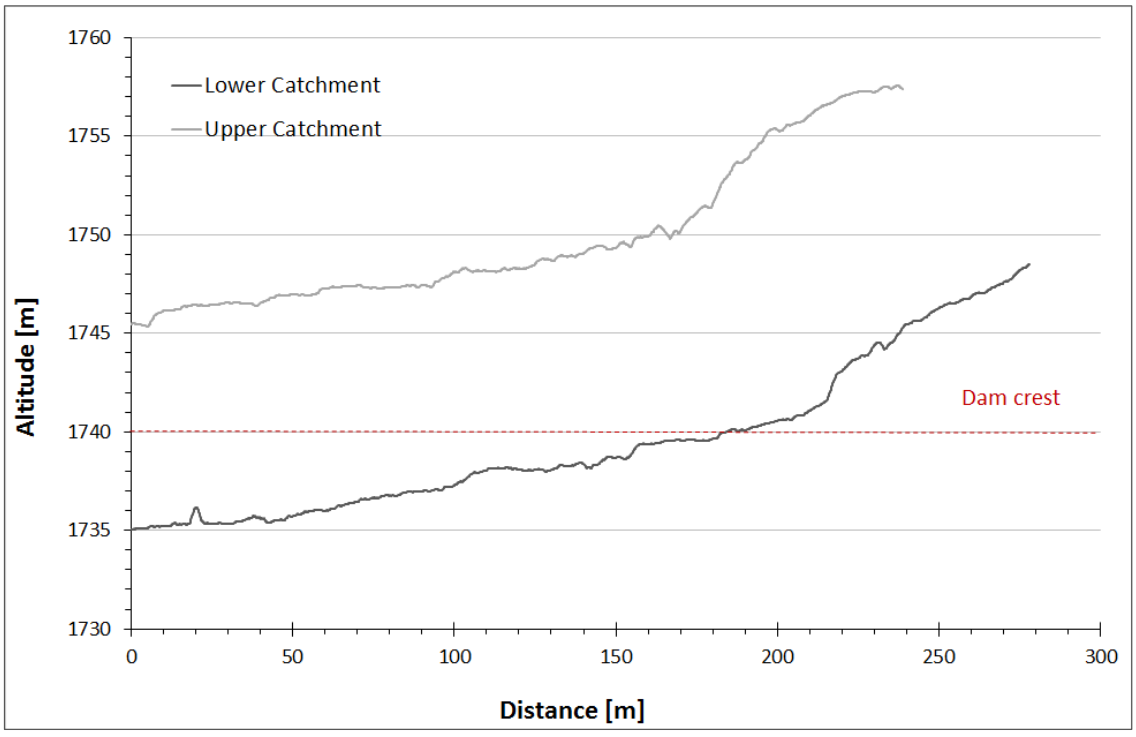

Figure 3-6 Profile graphs along the main channel for the lower and the upper catchment. The exact location of each profile graph is indicated in Figure 3-5. The red dashed line indicates the altitude of the dam crest at 1736 m.

3.5 DISCUSSION

3.5.1 COMPARISON OF INTERPOLATED AND UAV-ACQUIRED DTM

In this study we have described a workflow for the identification, mapping, and quantification of badlands using UAV imagery for a remote catchment where the availability of high resolution topographic data is limited. Even though the DTM interpolated from contour lines has a fine resolution (0.38 x 0-38 m), it does not allow for a detailed analysis of badlands compared with the UAV derived DTM. It is clearly visible that the interpolation from the 20 meter contour lines under sampled important information between the contours (Figure 3-5).The multi-resolution approach used by ArcGIS that starts with a coarser raster working towards finer resolution cannot compensate for the low-resolution input data. Additional point measurements on selected spots would increase the accuracy.

Another aim of this study was to estimate badland volumes which is not possible from our low-resolution interpolated DTM, whereas the UAV-acquired DTM represents badland and gully topography in high detail. A volume estimation using ArcGIS compared to Pix4D is time-consuming and requires many work steps. In addition, it relies on high-resolution input data that also enables the detection of shallow incised badlands. Thus, it is challenging too impossible to rely on topographic data from commonly available maps for detailed badland assessment using ArcGIS.

3.5.2 IMAGE QUALITY

The image quality of our final product is comparable to studies conducted by Neugirg et al. (2016) and Wang et al. (2016), both focusing on gully monitoring. Wang et al. (2016) mapped gullies on an agricultural site using a UAV and reached a GSD of 4.42 cm on a study site of 13.85 ha. Their study showed that the UAV images performed better in identifying the gullies than the high-resolution satellite image (Pleiades 1A, 0.7 m) regarding time-investment, but also accuracy. Higher resolution in the range of millimeters can be achieved with lower flight altitudes, but because of the greater cost in flying time and computing often only implemented on small study sites. Eltner et al. (2015) mapped erosion rills on a plot scale with a GSD of 0.2 to 0.4 cm from flight elevations between 8 and 11 meters. They compared Terrestrial Laser Scanning (TLS) and UAV data for erosion rill mapping and showed that the accuracy of all DSMs derived from UAV imagery was within the 1 cm accuracy of the TLS. These studies illustrate that UAV-based imagery is comparable to TLS, which is frequently used for measuring gully erosion due to its high accuracy. However, the data gathering by UAV allows a more rapid badland assessment (Neugirg et al., 2016) and processing time is steadily decreasing due to fast growing technological advancement. During the flight campaign we did not experience stability problems while acquiring the high resolution images as mentioned

disadvantageously in Milenković et al. (2016). However, we did not operate our UAV during strong winds or rain events.

3.5.3 CAN UAVS BE USED TO IDENTIFY BADLANDS AS SEDIMENT SOURCES?

The current study found that UAVs can be used to identify badlands and even smaller erosion features as sediment sources in small catchments. Combining an orthomosaic and a DSM generates a 3D photo reconstruction at a high resolution. It enabled us to remotely map badlands within the study area within several hours. In one case, it was even easier to detect the badland features from the orthomosaic than during the field visit because the agglomeration of bare soil areas was easier to distinguish. Transitions between different vegetation types or small changes in elevation are not easy to assess in the field and borders are often drawn subjectively. Aerial imagery can overcome this challenge. However, we noticed during the identification of potential sediment source areas using Pix4D that an identification relying just on bare soil patches using the orthomosaic is not sufficient. A detailed study of the 3D photo reconstruction illustrates that the eroding areas often have a greater extent than just the areas with bare soil because their edges are often still vegetated. For the actual area and volume estimation it was therefore important to look also at the DSM.

3.5.4 CAN UAVS BE USED TO QUANTIFY SEDIMENT SOURCES?

This study illustrates that UAV imagery in combination with photogrammetry software can be used to quantify badland volumes. Such estimates remain challenging for additional sediment source areas characterised by smaller erosion features, at least within relatively short data acquisition and processing times. Badlands are usually more dissected than gullies, which makes it more challenging to estimate their volume by the process we applied in this study. Vertices for the volume base surface have to be placed carefully to avoid missing an erosion feature. It is furthermore important that they are placed on the soil surface and not on bushes or tussocks because this would elevate the base surface and lead to an overestimation of the volume. It should be noted that volumes calculated for areas with shallow incision (e.g. badlands 1 and 2 in our study) have a higher degree of error than deeply incised areas.

Our additional estimations of the sediment volume loss from the reservoir after the dam breach is 36% lower than an estimate from Boardman and Foster (2011). They had attributed an amount of 4560 m^3 sediments removed by stream incision into the dam. It is unclear on which spatial extent they based their estimate. Thus, the difference is likely accountable due to dissimilar base surfaces for the volume calculations. However, we assume that a UAV based calculation results in a more representative estimation due to the higher-resolution of topographic data than field measurements.

We assume that cut banks and the main channel bottom also play a role in sediment input into the reservoir due to stream channel erosion (Evans, 1998; Trimble, 1997). Since the specific areas are mostly not vegetated, sediment is easily mobilised during storm events. However, their sediment share is probably low compared to densely grazed areas where cattle physically destroys gully banks and mobilise soil material (Evans, 1998). In addition, the construction of the dam raised the base level of erosion along the main channel, reducing its contribution to sediment load. Still, their volumes and sediment contribution cannot be determined by remote sensing applications without detailed knowledge of their shape before the construction of the reservoir. Since the available historical aerial photographs are of poor quality, all estimations would be just vague assumptions. Nevertheless, periodic future flight campaigns could determine the volume changes on an annual or event-based basis as successfully done in a gully monitoring study by d'Oleire-Oltmanns et al. (2012).

3.5.5 CAN UAVS BE USED TO IDENTIFY AND QUANTIFY SEDIMENT SINKS?

It is possible to identify sediment sink areas using a UAV, but it depends largely on the shape of the sink and might require additional information on topography if a simple shape does not represent the body of the sediment well. It is not possible to estimate the volume of the silted-up reservoir using the volume calculation tool in Pix4D because this would require a DTM of a mound or depression. Thus, our reservoir capacity relies on an assumed shape of the sediment body. The RC is 13% lower than an estimate for the same catchment from Boardman and Foster (2011), which can be explained by the difference in the underlying equations and a larger surface area used by Boardman and Foster (2011). It should be noted that both are only estimations that should be treated carefully, since we do not have information of the actual shape of the reservoir. A similar problem arises from the unknown channel morphology. The former reservoir can be distinguished from the surrounding, as well as stream banks within the main channel. The volume quantification of stream banks is technically feasible if an earlier orthomosaic was available for volume comparison, which was not the case for our study area. However, compared to the estimated volume of the sediment trapped behind the dam, this error is small because the banks have a volume of several tenths or hundreds of cubic meters only.

3.5.6 SEDIMENT VOLUME BALANCE

We have observed a significant difference between the estimated sediment storage and the badland volumes. 5265 m^3 of sediment from eroding badlands accounts for only 17.2% of the estimated reservoir storage capacity. This indicates that the badlands have not been the only sediment source of the reservoir. Even if our initial storage capacity is probably overestimated due to a lack of knowledge about the reservoir bottom shape, the difference still

remains large, leading to the same conclusion on badland sediment contribution. A conceivable possibility for an additional sediment source is the catchment itself, including the surrounding slopes. Assuming an additional 10 cm of top soil loss from non-vegetated areas throughout the catchment via sheet erosion accounts for another 2600 m^3 of sediment volume. Initially, we attributed only a minor importance to the slopes due to their very shallow soils, protected with stones and vegetation, and little evidence of overgrazing. However, it seems that their potential sediment contribution has been underestimated. This also raises the critical question on the actual contribution of sediment from accelerated erosion caused by overgrazing compared to the natural sediment delivery from the catchment.

3.6 CONCLUSION

The main aim of this research was to determine whether UAVs can be used to assess badlands as sediment sources. We have described a workflow for UAV-based badland assessment for a remote catchment in South Africa where the availability of fine resolution data is limited, but badland erosion and reservoir siltation are widespread problems. Combining ground-truthing and aerial photographs we obtained a high-resolution orthomosaic (GSD 3.12 cm) and DTM (GSD: 15.6 cm) that enabled us to identify, map, and quantify badlands. The high resolution and accuracy from the derived UAV imagery is closing the gap between satellite scale level and high resolution LIDAR point clouds that are not available for larger areas. It is a valuable tool if accurate data in the range of millimeters to centimeters are needed, especially where traditional erosion pin measurements or terrestrial laser scanning is too labour-intensive. In addition, the spatial and temporal resolution can be easily adjusted according to the scope of the project, data can be collected for individual events (e.g. before and after a rainstorm) or for routine badland monitoring aimed at gaining deeper understanding of their dynamics.

We showed that UAV-imagery is suitable for identifying, mapping, and quantifying badlands. However, it should be noted that the methodology is only as good as the underlying georeferencing. Therefore, GCPs should be placed cautiously in field or chosen carefully from online mapping products. Mapping and badland identification could also be improved with the use of spectral cameras that allow a better distinction of land cover than RGB-imagery. Regarding the volume assessment, best results were obtained for deeply incised badland systems that ideally would also have a low amount of vegetation cover. Quantifying sediment sinks is still challenging and often relies on former high-resolution or aerial imagery for a comparison. The presented volumes should therefore be considered as good estimates rather than precise absolute amounts. Still the data can help to evaluate the relevance of badlands as sediment sources.

As UAV technologies and capabilities are constantly improving, UAV-based badland mapping is becoming a valuable tool and offers a high flexibility regarding spatial and temporal resolution, in particular for producing high-resolution images in remote areas. There is potentially a wide range of UAV-derived data products for research and land management requiring information on badland morphologies and dynamics. Improving our understanding of badlands by collecting detailed information with UAVs enables upscaling and thus to address regional environmental issues, e.g. sediment management in the Orange river basin (Boardman et al., 2003) or the global development of badland areas as a consequence of environmental change (Feng and Fu, 2013; Parry et al., 2007).

3.7 ACKNOWLEDGEMENTS

We thank Shauna Westcott and Dirk Jacobs for access to the site. We are grateful to Philipp Greenwood, Goswin Heckrath, and Ruth Strunk for intensive field support. In addition, we like to thank Brigitte Kuhn for UAV piloting and for help with the post-processing. The data has been processed with Pix4Dmapper Pro by Pix4D and ArcGIS 10.5 by ESRI. Fieldwork by JK was partially funded by the Tomscik Foundation and a Freiwillige Akademische Gesellschaft (University of Basel) grant.

3.8 REFERENCES

Ainsle, A. (Ed.), 2002. Cattle ownership and production in the communal areas of the Eastern Cape, South Africa, Programm for Land and Agrarian Studies Research Report No. 10. Programme for Land and Agrarian Studies, Cape Town.

Austin, A.T., Yahdjian, L., Stark, J.M., Belnap, J., Porporato, A., Norton, U., Ravetta, D.A., Schaeffer, S.M., 2004. Water pulses and biogeochemical cycles in arid and semiarid ecosystems. Oecologia 141, 221–235. https://doi.org/10.1007/s00442-004-1519-1

Boardman, J., Favis-Mortlock, D., Foster, I.D.L., 2015. A 13-year record of erosion on badland sites in the Karoo, South Africa: A 13-Year Record of Erosion on Badland Sites in the Karoo. Earth Surf. Process. Landf. 40, 1964–1981. https://doi.org/10.1002/esp.3775

Boardman, J., Foster, I.D.L., 2008. Badland and gully erosion in the Karoo, South Africa. J. Soil Water Conserv. 63, 121A–125A. https://doi.org/10.2489/jswc.63.4.121A

Boardman, J., Foster, I.D.L., 2011. The potential significance of the breaching of small farm dams in the Sneeuberg region, South Africa. J. Soils Sediments 11, 1456–1465. https://doi.org/10.1007/s11368-011-0425-5

Boardman, J., Parsons, A.J., Holland, R., Holmes, P.J., Washington, R., 2003. Development of badlands and gullies in the Sneeuberg, Great Karoo, South Africa. CATENA, Gully Erosion and Global Change 50, 165–184. https://doi.org/10.1016/S0341-8162(02)00144-3

Brodu, N., Lague, D., 2012. 3D terrestrial lidar data classification of complex natural scenes using a multi-scale dimensionality criterion: Applications in geomorphology. ISPRS J. Photogramm. Remote Sens. 68, 121–134. https://doi.org/10.1016/j.isprsjprs.2012.01.006

Bryan, R., Yair, A., 1982. Badland: geomorphology and piping. Norwich: Geo Books.

Buckley, S.J., Kurz, T.H., Schneider, D., 2012. The benefits of terrestrial laser scanning and hyperspectral data fusion products. ISPRS - Int. Arch. Photogramm. Remote Sens. Spat. Inf. Sci. XXXIX-B7, 541–546. https://doi.org/10.5194/isprsarchives-XXXIX-B7-541-2012

Clarke, M.L., Rendell, H.M., 2010. Climate-driven decrease in erosion in extant Mediterranean badlands. Earth Surf. Process. Landf. 35, 1281–1288. https://doi.org/10.1002/esp.1967

d'Oleire-Oltmanns, S., Marzolff, I., Peter, K., Ries, J., 2012. Unmanned Aerial Vehicle (UAV) for Monitoring Soil Erosion in Morocco. Remote Sens. 4, 3390–3416. https://doi.org/10.3390/rs4113390

Eltner, A., Baumgart, P., Maas, H.-G., Faust, D., 2015. Multi-temporal UAV data for automatic measurement of rill and interrill erosion on loess soil. Earth Surf. Process. Landf. 40, 741–755.

Evans, R., 1998. The erosional impacts of grazing animals. Prog. Phys. Geogr. 22, 251–268. https://doi.org/10.1177/030913339802200206

Feng, S., Fu, Q., 2013. Expansion of global drylands under a warming climate. Atmos Chem Phys 13, 081-10.

Foster, I.D.L., Rowntree, K.M., Boardman, J., Mighall, T., 2012. Changing sediment yield and sediment dynamics in the Karoo uplands, South Africa; Post-European impacts.

Foster, I.D.L., Boardman, J., Gates, J.B., 2008. Reconstructing historical sediment yields from the infilling of farm reservoirs, Eastern Cape, South Africa, in: IAHS-AISH Publication. Presented at the International Commission on Continental Erosion (ICCE). Symposium, International Association of Hydrological Sciences, pp. 440–447.

Hoffman, M.T., Ashwell, A., 2001. Nature Divided: Land degradation in South Africa, 1st ed. University of Cape Town Press, Cape Town.

IPCC, 2007. Climate Change 2007: Impacts, Adaptation and Vulnerability. Contribution of Working Group II to the Fourth Assessment Report of the Intergovernmental Panel on Climate Change. Cambridge University Press, Cambridge, UK.

Keay-Bright, J., Boardman, J., 2007. The influence of land management on soil erosion in the sneeuberg mountains, central Karoo, south Africa. Land Degrad. Dev. 18, 423–439. https://doi.org/10.1002/ldr.785

Keay-Bright, J., Boardman, J., 2006. Changes in the distribution of degraded land over time in the central Karoo, South Africa. Catena 67, 1–14. https://doi.org/10.1016/j.catena.2005.12.003

Küng, O., Strecha, C., Beyeler, A., Zufferey, J.-C., Floreano, D., Fua, P., Gervaix, F., 2011. The accuracy of automatic photogrammetric techniques on ultra-light UAV imagery, in: UAV-g 2011-Unmanned Aerial Vehicle in Geomatics. Presented at the UAV-g 2011 - Unmanned Aerial Vehicle Geomatics, Zürich, Switzerland.

Lal, R., 1997. Degradation and resilience of soils. Philos. Trans. R. Soc. Lond. B Biol. Sci. 352, 997–1010.

Laliberte, A.S., Winters, C., Rango, A., 2011. UAS remote sensing missions for rangeland applications. Geocarto Int. 26, 141–156. https://doi.org/10.1080/10106049.2010.534557

Meadows, M.E., Hoffman, M.T., 2002. The nature, extent and causes of land degradation in South Africa: legacy of the past, lessons for the future? Area 34, 428–437. https://doi.org/10.1111/1475-4762.00100

Milenković, M., Karel, W., Ressl, C., Pfeifer, N., 2016. A COMPARISON OF UAV AND TLS DATA FOR SOIL ROUGHNESS ASSESSMENT. ISPRS Ann. Photogramm. Remote Sens. Spat. Inf. Sci. III-5, 145–152. https://doi.org/10.5194/isprsannals-III-5-145-2016

Mondal, A., Khare, D., Kundu, S., 2017a. Uncertainty analysis of soil erosion modelling using different resolution of open-source DEMs. Geocarto Int. 32, 334–349. https://doi.org/10.1080/10106049.2016.1140822

Mondal, A., Khare, D., Kundu, S., Mukherjee, S., Mukhopadhyay, A., Mondal, S., 2017b. Uncertainty of soil erosion modelling using open source high resolution and aggregated DEMs. Geosci. Front. 8, 425–436. https://doi.org/10.1016/j.gsf.2016.03.004

Nde, S.C., 2015. Farm dam siltation, sediment management and sediment source tracing in the Zeerust-Swartruggens Area, North West Province. North-West University, Potchefstroom, South Africa.

Neugirg, F., Stark, M., Kaiser, A., Vlacilova, M., Della Seta, M., Vergari, F., Schmidt, J., Becht, M., Haas, F., 2016. Erosion processes in calanchi in the Upper Orcia Valley, Southern Tuscany, Italy based on multitemporal high-resolution terrestrial LiDAR and UAV surveys. Geomorphology 269, 8–22. https://doi.org/10.1016/j.geomorph.2016.06.027

Nobajas, A., Waller, R.I., Robinson, Z.P., Sangonzalo, R., 2017. Too much of a good thing? the role of detailed UAV imagery in characterizing large-scale badland drainage characteristics in South-Eastern Spain. Int. J. Remote Sens. 1–17. https://doi.org/10.1080/01431161.2016.1274450

Oberholster, P.J., Ashton, P.J., 2008. State of the nation report: An overview of the current status of water quality and eutrophication in South African rivers and reservoirs. Parliam. Grant Deliv. Pretoria Counc. Sci. Ind. Res. CSIR.

Pimentel, D., Harvey, C., Resosudarmo, P., Sinclair, K., Kurz, D., McNair, M., Crist, S., Shpritz, L., Fitton, L., Saffouri, R., 1995. Environmental and economic costs of soil erosion and conservation benefits. Sci.-AAAS-Wkly. Pap. Ed. 267, 1117–1122.

Poesen, J., Vandekerckhove, L., Nachtergaele, J., Oostwoud Wijdenes, D., Verstraeten, G., van Wesemael, B., 2002. Gully erosion in dryland environments. Bull LJ Kirkby MJ Eds Dryland Rivers Hydrol. Geomorphol. Semi-Arid Channels Wiley Chichester UK 229–262.

Rowntree, K., Foster, I.D.L., 2012. A reconstruction of historical changes in sediment sources, sediment transfer and sediment yield in a small, semi-arid Karoo catchment, semi-arid South Africa. Z. für Geomorphol. Suppl. Issues 56, 87–100. https://doi.org/10.1127/0372-8854/2012/S-00074

Rowntree, K.M., 2014. Reprint of: The evil of sluits: A re-assessment of soil erosion in the Karoo of South Africa as portrayed in century-old sources. J. Environ. Manage. 138, 67–74. https://doi.org/10.1016/j.jenvman.2014.04.015

Stöcker, C., Eltner, A., Karrasch, P., 2015. Measuring gullies by synergetic application of UAV and close range photogrammetry—A case study from Andalusia, Spain. Catena 132, 1–11.

Trimble, S.W., 1997. Contribution of Stream Channel Erosion to Sediment Yield from an Urbanizing Watershed. Science 278, 1442–1444. https://doi.org/10.1126/science.278.5342.1442

Wang, R., Zhang, S., Pu, L., Yang, J., Yang, C., Chen, J., Guan, C., Wang, Q., Chen, D., Fu, B., Sang, X., 2016. Gully Erosion Mapping and Monitoring at Multiple Scales Based on Multi-Source Remote Sensing Data of the Sancha River Catchment, Northeast China. ISPRS Int. J. Geo-Inf. 5, 200. https://doi.org/10.3390/ijgi5110200

CHAPTER 4

Soil degradation mapping in drylands using unmanned aerial vehicle data

Soil degradation mapping in drylands using unmanned aerial vehicle data

Juliane Krenz, Philip Greenwood and Nikolaus J. Kuhn
University of Basel, Klingelbergstrasse 27, 4056 Basel, Switzerland

Status: Published
Krenz, J., Greenwood, P., Kuhn, N.J., 2019. Soil Degradation Mapping in Drylands Using Unmanned Aerial Vehicle (UAV) Data. Soil Syst. 3, 33.
https://doi.org/10.3390/soilsystems3020033

Status: Published
Krenz, J., Greenwood, P., Kuhn, N.J., 2020. Correction: Krenz, J., et al. Soil Degradation Mapping in Drylands Using Unmanned Aerial Vehicle (UAV) Data. Soil Syst. 2019, 3, 33. Soil Syst. 4, 33. https://doi.org/10.3390/soilsystems4020033

The version printed in this thesis is the original research article (Krenz et al., 2019) updated with the correct figures of the corrected research article (Krenz et al., 2020).

4.1 ABSTRACT

Arid and semi-arid landscapes often show a patchwork of bare and vegetated spaces. Their heterogeneous patterns can be of natural origin, but may also indicate soil degradation. This study investigates the use of unmanned aerial vehicle (UAV) imagery to identify the degradation status of soils, based on the hypothesis that vegetation cover can be used as a proxy for estimating the soils' health status. To assess the quality of the UAV-derived products, we compare a conventional field-derived map (FM) with two modelled maps based on (i) vegetation cover (RGB map), and (ii) vegetation cover, topographic information, and a flow accumulation analysis (RGB+DEM map). All methods were able to identify areas of soil degradation but differed in the extent of classified soil degradation, with the RGB map classifying the least amount as degraded. The RGB+DEM map classified 12% more as degraded than the FM, due to the wider perspective of the UAV compared to conventional field mapping. Overall, conventional UAVs provide a valuable tool for soil mapping in heterogeneous landscapes where manual field sampling is very time consuming. Additionally, the UAVs' planform view from a bird's-eye perspective can overcome the limited view from the surveyors' (ground-based) vantage point.

Keywords
erosion; landscape mapping; soil degradation; soil mapping; unmanned aerial vehicle (UAV)

4.2 Introduction

Arid and semi-arid landscapes often show a heterogeneous pattern of bare and vegetated spaces. Most common vegetation patterns are banded (Saco et al., 2007; Valentin et al., 1999) or spotted (Couteron and Lejeune, 2001; Deblauwe et al., 2008). This patchwork of vegetation is also reflected in heterogeneous chemical, structural, and textural soil properties (Schlesinger et al., 1996, 1990), which introduce spatial variations in factors such as infiltration capacity (Bochet et al., 2000; Cammeraat and Imeson, 1999; Cerdá, 1997), soil nutrient content (Rietkerk et al., 2000; Schlesinger et al., 1996) and soil erodibility (Castillo et al., 1997; Cerdá, 1997; Wynn and Mostaghimi, 2006). The vegetation patterns can be of natural origin (HilleRisLambers et al., 2001; Rietkerk et al., 2002), but may also indicate soil degradation, i.e., the decline of soil functions and productivity caused by erosion, nutrient depletion, salinization, or loss of soil structure (Cammeraat and Imeson, 1999).

The spatial heterogeneity of dryland landscapes indicates that underlying soil types are inherently variable. This variability is often not depicted on soil maps. Most common soil maps for South Africa are large scale, varying between 1:1 and 1:5 million and including the Soil and Terrain (SOTER) database (FAO et al., 2003) and the "Soil Atlas of Africa" (Dewitte et al., 2013), and are not able to represent the variety of the natural soil types. Ref. (Hengl et

al., 2015) used random forest models to predict common soil properties, such as organic carbon, pH, and soil texture, at a 250 m × 250 m resolution to bridge the gap in soil information in Africa. Although a large amount of soil investigations has been carried out in South Africa, information access is restricted. Local or provincial soil information is often archived and not freely available to the public due to a lack of a central repository (Paterson et al., 2015). Long-term erosion monitoring in the Karoo by (Boardman et al., 2017) showed evidence of considerable soil degradation and badlands formation but information on the soils' degradation status and the loss of soil functions and productivity is usually not included in soil maps. In addition to this limited access, national or regional maps seldom reflect this degree of heterogeneity, mainly due to the high labor, financial, and time-investment costs associated with manual land cover mapping, soil sampling, and analysis. However, high resolution soil maps are of growing importance for environmental planning at regional or local scales (Behrens et al., 2005) and for farmers to facilitate decision-making on best agricultural practices (Sanchez et al., 2009), such as precision farming or grazing practices aimed at land restoration (Hengl et al., 2015), as well as for conservationists to implement protection measures in the form of erosion prevention (Hengl et al., 2015; Sanchez et al., 2009). Digital soil mapping using mathematical models therefore represents an alternative to the typically resource-intensive conventional methods of soil mapping (Nussbaum et al., 2011). Soil characteristics or soil types are usually predicted based on factors about the terrain or climate (Behrens et al., 2010), using classical machine learning methods such as classification and regression tree analyses (Behrens et al., 2010; Illés et al., 2011), neural networks (Behrens et al., 2005), or geostatistical approaches (Hengl, 2009). But since vegetation cover is closely related to soil properties (Schlesinger et al., 1996), land cover maps can provide useful information to identify differences in soil development (Dube et al., 2017).

The quality of the prediction produced by any soil mapping model strongly depends on the spatial scale of the input data. The spatial resolution of commonly available global or continental data products on land cover, such as open source Global Land Survey (GLS) data from NASA and the US Geological Survey (30 m × 30 m), MODIS-based Global Land Cover Climatology (500 m × 500 m) (Broxton et al., 2014), or soil types such as the African Soil Atlas (Jones et al., 2013), is usually too coarse to reflect landscape heterogeneity in semi-arid areas. Unmanned aerial vehicles (UAVs) can help to overcome the gap between expensive, time-consuming ground-based assessment and insufficient data quality from coarse resolution imagery derived from satellite systems. Capturing high resolution terrain or land cover information enables the generation of user-specific data products, such as 2D or 3D terrain models, orthomosaics, and normalised difference vegetation index (NDVI)-maps. Consequently, UAVs have recently gained popularity in remote sensing studies and have been used in a variety of high resolution topographic studies, e.g., for gully mapping

(Wang et al., 2016) and quantifying gully volumes (d'Oleire-Oltmanns et al., 2012; Neugirg et al., 2016; Nobajas et al., 2017). Compared to field mapping, which produces rather inflexible maps once compiled and the results committed to paper, or a similarly static digital data products due to the intense labor involved in their creation, UAV mapping can be conducted more frequently at lower cost and with a finer resolution, which allows rapid monitoring of changes in natural soil states such as displacement of soil after landslides (Lucieer et al., 2014) or monitoring the evolution of an active volcano (Nakano et al., 2014). UAV imagery does provide limited information on the soils themselves but can be used to infer, for example, the state of soil degradation through density and patterns of vegetation or through capturing fine-scaled features of topography such as rills and gullies.

Based on the relationship between the state of a soil and its vegetation cover (Bartley et al., 2006; Ludwig et al., 2007), this study investigates the use of UAV imagery to identify soil degradation. In addition, intense destruction of soil by erosion can be associated with erosion features, such as rills or badlands, visible in digital terrain models (Puigdefábregas, 2005; Rogers and Schumm, 1991). Data generated by inexpensive and commercially available UAVs were chosen on purpose because they offer the greatest potential for wide application in soil and land management. To assess the quality of these UAV-derived products on vegetation and topography, we compare a conventionally derived field map with two modelled maps. One is exclusively based on vegetation cover, assuming vegetation is indicative of low soil degradation by erosion (Puigdefábregas, 2005; Rogers and Schumm, 1991). The second map is based on vegetation cover combined with terrain information, assuming that visualisation of features such as rills, gullies, and sediment deposits contribute to assessing soil degradation and redistribution.

4.3 MATERIALS AND METHODS

4.3.1 STUDY SITE

The chosen study area is located in the Klein Seekoei River basin in the Great Karoo Region of South Africa and is situated approximately 70 km north of Graaff-Reinet. It is part of the Sneeuberg uplands, a landscape of flat valley bottoms and gently sloping lower valley sides interspersed with hills and mountain ranges extending from 1650 up to 2502 m above sea level (a.s.l) at the Compassberg. According to (Esler et al., 2006), in areas of the Karoo with seasonally distributed precipitation of almost 500 mm per year, such as the Sneeuberg uplands, in the absence of human intervention a vegetation cover of 50–70% could be expected. Land degradation is a common problem in the area and is reflected by frequent rill and gully erosion in the valley bottoms, as well as badland development on the footslopes of many hills (Boardman et al., 2017; Foster et al., 2005; Keay-Bright and Boardman, 2007; Mighall et al., 2012). The study catchment covers 3.2 km^2 and drains into

the in-filled reservoir labelled Dam 53 (31.698558° S, 24.588183° E) by (Boardman and Foster, 2011). The reservoir is located at approximately 1740 m a.s.l. and is surrounded by hills up to 2080 m a.s.l. Aerial photos indicate that it was constructed in the late 1920s and almost completely filled with sediment by the mid-1970s. A main gully up to 6 m deep and partly up to 10 m wide follows the thalweg of the catchment, forming a breach in the dam wall and incising backwards into the sediment. We focused on the lower part of the catchment, just behind the former dam wall, which shows various grades of land degradation and covers roughly 289 ha. The catchment was chosen because it shows many typical features of vegetation degradation, erosion and deposition of soil. The relatively small size meant that detailed mapping was feasible, both on the ground as well as with the UAV.

4.3.2 FIELD MAPPING

In an on-site assessment throughout the complete study area, differences in vegetation cover or vegetation type, as well as prominent erosion features (i.e., rills, gullies, and extended absence of A-horizon), were visually assessed and their positions were recorded with a handheld Garmin GPSMap60. The GPS data of the recorded land cover types and erosion features was transferred to a GIS and transformed into the Field Map (FM). Six different types of vegetation cover and erosion could be distinguished: shrubs, thorny shrubs, grasses, mixed vegetation, bare soil, and erosion rills. Detailed descriptions of selection criteria and distinguished vegetation and erosion types are presented in Table 4-1.

4.3.3 LAND COVER MAPPING

To create a high resolution map of soil degradation in our study area, a land cover classification was carried out using UAV imagery acquired in February 2016 using a Phantom III Professional quadrocopter (SZ DJI Technology Co., Ltd., Shenzhen, China) equipped with a DJI FC300X camera (GoPro Inc., San Mateo, CA, USA) for RBG-images according to (Krenz and Kuhn, 2018). Images were taken at an altitude of 70 m above the ground with an average overlap of 90% to ensure sufficient overlap for photogrammetric processing. Compromising between a high resolution and the expenditure of image acquisition and post-processing resulted in a ground size resolution of 3.1 cm of the orthomosaic. Image processing, including orthorectification and production of a high-resolution orthophoto and a digital elevation model (DEM), was done with the photogrammetry software Pix4Dmapper Pro (Pix4D SA, Lausanne, Switzerland). The land cover classification map generated by the supervised classification of the orthomosaic is referred to as the Land Cover (LC). In our study, land cover only refers to the actual surface cover, such as grasses, shrubs, stones or bare soil, and disregards any additional information

on the relief. Even though we mapped six different classes on site for the FM, we combined those classes as shown in Table 4-1 to simplify the land cover classification.

The LC was classified using a supervised support vector machine (SVM) classification with the help of ArcGIS Pro 2.2.3. This classification was chosen over the very popular maximum likelihood classification (MLC) approach because it has shown more accurate results in other studies (Huang et al., 2002; Mondal et al., 2012; Szuster et al., 2011). The pixel-based MLC approach assigns a pixel to the corresponding class with the maximum likelihood. It is a parametric classification that is limited by assuming a normal distribution of class signatures which requires the users to determine the classification scheme. Unlike the MLC, the non-parametric SVM classification employs optimisation algorithms to locate optimal boundaries between classes (Huang et al., 2002). While its strength lies in a binary classification system, the SVM has recently also been shown to reflect accurate land cover categories in multiclass approaches (Foody and Mathur, 2004; Szuster et al., 2011). An image analysis pre-study was conducted to identify the segmentation parameters that yielded in the most accurate segmentation of the orthophoto. Forty training samples per LC class (bare soil, shrubs, and grasses) were used for the LC classification and each segmented image was tested for accuracy as described in 2.4. We found the parameters producing the most accurate segmented image to be 20 (spectral detail), 15 (spatial detail), and 5 (minimum segment size in pixels) and used the resulting image for the SVM analysis.

4.3.4 ACCURACY ASSESSMENT

To assess the LC map accuracy, and thus compare the LC classes expressed in the UAV-derived map to reference data collected, 150 randomly stratified points per LC class were generated on the classified LC map. These were then validated visually point by point using the orthophoto and field knowledge to create a classified point dataset, which was used for further accuracy analysis. A confusion matrix representing the overall accuracy, producer's and user's accuracy, and the kappa index (Congalton, 2001; Jensen, 1996) was calculated using ArcGIS. The kappa index is a measure for the accuracy of the classified map compared to the reference map. It is computed as follows

$$K = \frac{N \sum_{i=1}^{n} m_{i,i} - \sum_{i=1}^{n} (R_i C_i)}{N^2 - \sum_{i=1}^{n} (R_i C_i)} \tag{4-1}$$

Definitions for the variables used in Equation 4-1 may be given as:

i	class number
N	total number of classified values compared to reference values
mi,i	number of values belonging to reference class I that have been classified as class i
Ci	total number of predicted (classified) values belonging to class i
R	total number of reference values belonging to class i

Table 4-1 Description of the identified land cover types. The vegetation cover (first column) describes classes visually assessed in the field, while the LC class describes the classification used for the image analysis of the orthophoto. The arrows indicate how individual vegetation cover classes were combined to give LC classifications. Descriptions were based on those given in Thompson (1996) and have been modified according to site-characteristics.

Vegetation Cover	Description	Implication	Land Cover (LC)	Identification from the Orthophoto
Bare soil	Areas (>1 m²) of exposed sand, soil, or rock with no or very little vegetation	Threatened by erosion due to lack of protecting vegetation cover	→ Bare Soil	Higher overall reflectance (whiter appearance) → areas of mostly white to sandy colors (often slightly yellow or orange) with no apparent line structure that could indicate grasses; stones often very white and characterised through their angular shape
Rills	Rill structure of bare soil, no or little shrub vegetation	Threatened by intensive erosion due to concentrated runoff		
Shrubs	Woody-plants dominating, typically broad-leaved, branching at or near the ground, up to 1 m in height	Threatened by erosion if roots are exposed or shrubs grow on pedestals	→ Shrubs	In this area characterised by a light bright green to dark green or blueish green color
Thorny Shrubs	Woody-plants with thorns dominating, up to 1 m in height, mostly Lycium horridum	Threatened by erosion if roots are exposed or shrubs grow on pedestals		
Mixed Vegetation	Areas where neither grasses nor shrubs are dominant	Threatened by erosion if vegetation cover < 50%	→ Grasses	Color appearance is more faded (beige to light grey green) than the color of the shrubs; in a high resolution image grasses can be distinguished from shrubs by their long, narrow, and sometimes curled leaves
Grasses	Non-woody, grass-like, herbaceous plants dominating, grass-like plants often grow as tussocks	Threatened by erosion if vegetation cover < 50% or tussock grasses grow on pedestals		

Producer's accuracy refers to the probability that land cover on the ground is classified as is given on the map. It is calculated by dividing the number of correctly classified reference points by the total number of reference points for a land cover class. User's accuracy, on the other hand, indicates how often a class on the map will actually be present on the ground. For user's accuracy the total amount of correct classifications for a particular class is divided by the total number of sampling points of the referring LC class, which in our case was 150.

4.3.5 LANDSCAPE UNIT (LU) MAPPING

The second map generated from the UAV data is referred to as the Landscape Unit (LU) map because it also contains information on topography. The rationale for distinguishing landscape units is the relationship of soil, soil erosion, and deposition to terrain. Areas of interest were, in particular, bare soil areas with visible erosion features such as rills and areas with exposed shrub roots, since these are indicators of erosion and soil degradation (Morgan, 2005). Vegetation cover greater than 50% was used as an index for healthy soil (Esler et al., 2006). A transformation of the Land Cover (LC) raster to a LC density map to assess the percentage of bare soil cover was needed. Therefore, the LC raster was converted to a point dataset, where each raster cell represented a point with its specific land cover (bare soil, shrub, or grass). Using a Kernel density function the density of bare soil points in the neighbourhood was calculated. Two bare soil threshold maps were generated from the Kernel density map: (i) bare soil larger than 50% representing moderately degraded areas and (ii) bare soil larger than 70% representing severely degraded areas. Areas smaller than 10 m^2 and fully enclosed by an area of different degradation status were appointed to the surrounding area. We assumed that the different classification of these tiny patches was mainly attributed to uncertainties in a distinct LC class allocation of transitional areas and therefore allocated these areas to the surrounding LU. For the final LU maps we used two approaches (Figure 4-1, Figure 4-2). For the RGB map, which is based on land cover, the orthophoto (Figure 4-4A), the LC map (Figure 4-4B), and the derived bare soil density map were exclusively used. For simplification and because the map is based on a true colour image (the orthophoto), we named it RGB map based on the additive primary colours red, green and blue that are typically used for the display of images in digital cameras. For the RGB+DEM map, LUs were categorised based on visual and elevation differences combining information from the orthophoto, the LC map, the density map, the high-resolution DEM (Figure 4-4C), and the DEM derivatives, such as slope and flow direction. The extent of the different LUs was then mapped using an overlay analysis in ArcGIS. The depositional area was in both approaches mapped based on field observations and historical aerial imagery that showed the spatial extent of the former reservoir.

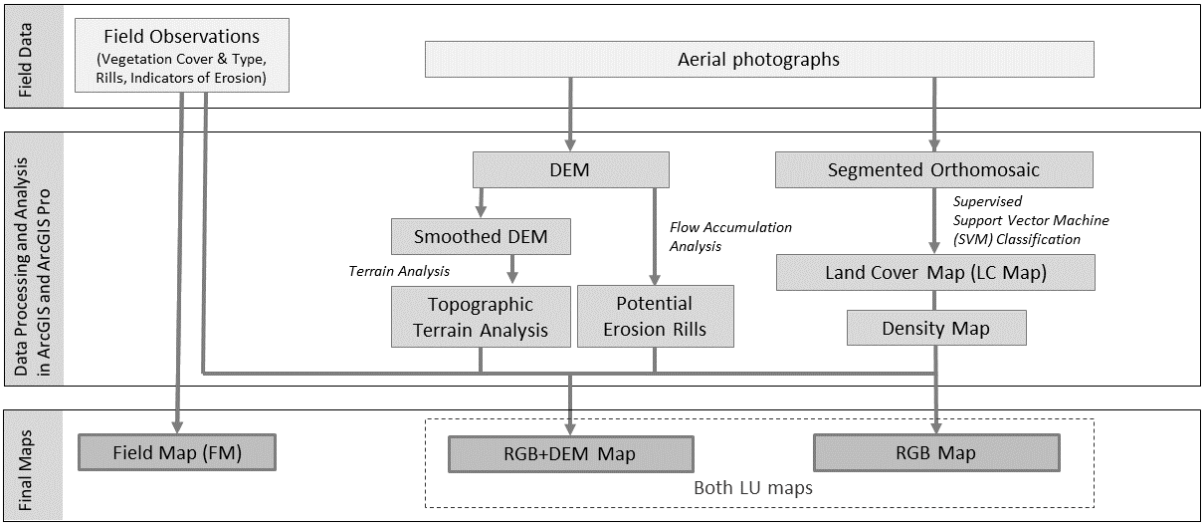

Figure 4-1 Workflow for image classification and landscape unit mapping.

4.3.6 INCORPORATING TERRAIN ATTRIBUTES IN LU MAPPING

Soils and landscapes co-evolve and are inherently related to each other (Jenny, 1941; Moore et al., 1993). Therefore, we used the DEM and DEM derivatives to identify areas of similar states of soil degradation. The most frequent terrain attributes used for digital soil mapping are elevation, slope, aspect, and curvature, often combined with hydrological features, such as flow accumulation (Behrens et al., 2005). Aspect was found to have a low predictive value for estimating soil attributes by (Dobos and Hengl, 2009). Since our study area is fairly small and differences in aspect or curvature of the foot slope are small, we decided to focus on flow direction, flow accumulation, and the topographic position index (TPI).

Flow accumulation analysis of DEMs can be used to identify rills which are indicative of erosion and/or transport of sediment from an eroding upslope area (Schwanghart et al., 2013). To test the quality of this analysis, the result was compared to actual rills mapped in the field. An unweighted (accumulation with equal cell weights) single-flow path model was used in ArcGIS to identify flow accumulation paths in the study area (Figure 4-2). Identified paths were then compared with on-site observations of erosion rills. A single-flow path model was chosen because it identifies parallel and converging water and sediment fluxes, which is ideal to study connected rill systems and mass fluxes that are trapped and stored behind dams (Schäuble et al., 2008). The resulting image from the initial flow accumulation analyses was reclassified using a threshold value to highlight the pathways of high flow and to create a stream network raster, in which all streams are represented by the value 1 and background data by NoData values. The reclassification was done iteratively until a sufficient amount of flow accumulation pathways were eliminated and first artefacts occurred.

The TPI, introduced by (Weiss, 2001), can be used to determine the ruggedness of the terrain. Rough surfaces concentrate flow, promote rill formation, and consequently lead to

higher sediment yields (Römkens et al., 2002). TPI is usually used for landform classifications such as hilltops, upper/mid/lower slopes, flat areas, or valleys. Its calculation as the difference between a cell value and the average cell value of the neighborhood around the cell also enables micro topographic analysis on high-resolution DEMs, and, thus, an identification of badland areas or rill systems. We calculated TPI from a smoothed DEM to reduce the noise of micro topography, such as surface morphological changes caused by stones, or small hollows detected by high-resolution DEM.

For the final RGB+DEM map the areas classified as moderately or severely degraded based on the bare soil density were further analysed and combined with the terrain attributes. Vegetated areas with more than 50% of the area having a negative TPI and fully enclosed by a degraded LU where attributed to the corresponding degraded LU. Vegetated or moderately degraded areas where more than 50% of the area had a negative TPI were attributed to the moderately degraded LU or the severely degraded LU, respectively.

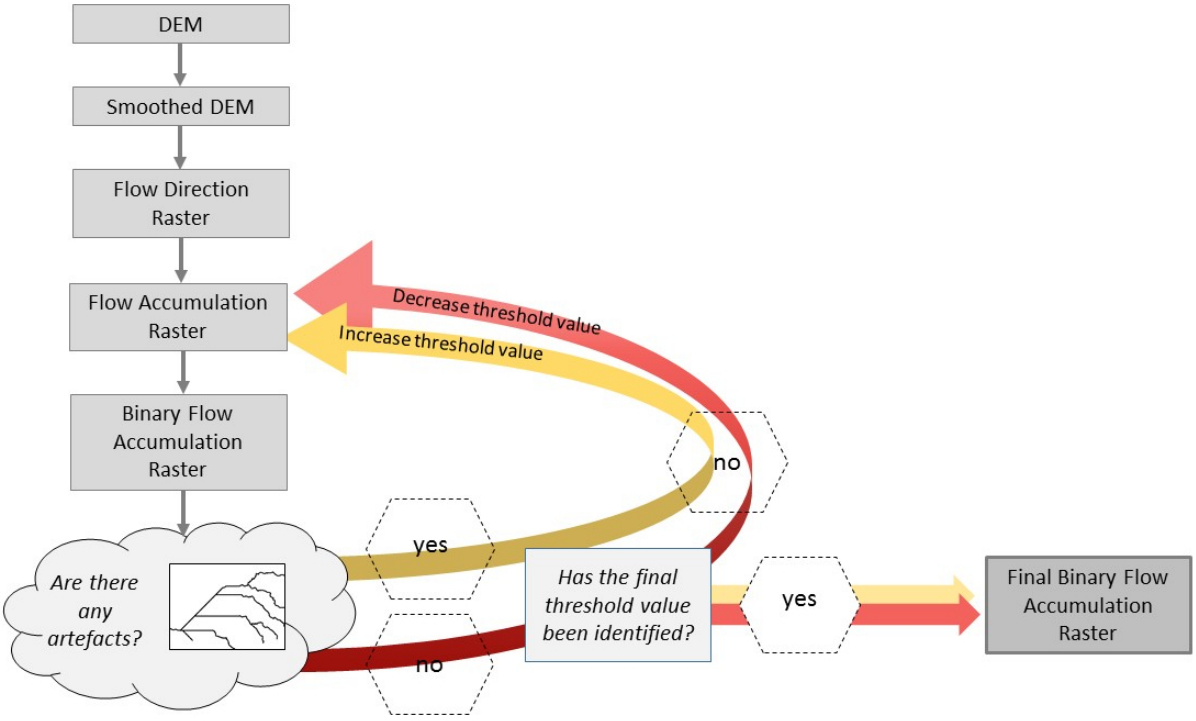

Figure 4-2 Workflow of the flow accumulation analysis for the identification of potential erosion rills.

4.4 RESULTS

4.4.1 FIELD MAPPING

A Field Map showing the results of the conventional land cover mapping is shown in Figure 4-3. The composition of shrub species differs throughout the studied area. The thorny

shrub *Lycium horridum* was only found close to the former reservoir, whereas in the catchment area a mix of different shrub species occurred, these being mainly *Chrysocoma ciliata*, *Dicerothamnus rhinocerotis*, *Felicia* spp., *Helichrysum* spp., and *Selago* spp. Grasses are found throughout the whole study area, mostly interspersed with shrubs. Most of the catchment was covered with tussock grass, while short grass dominated the former reservoir area. Seven, partly bifurcated, erosion rills covering a length of 1.08 km were also identified.

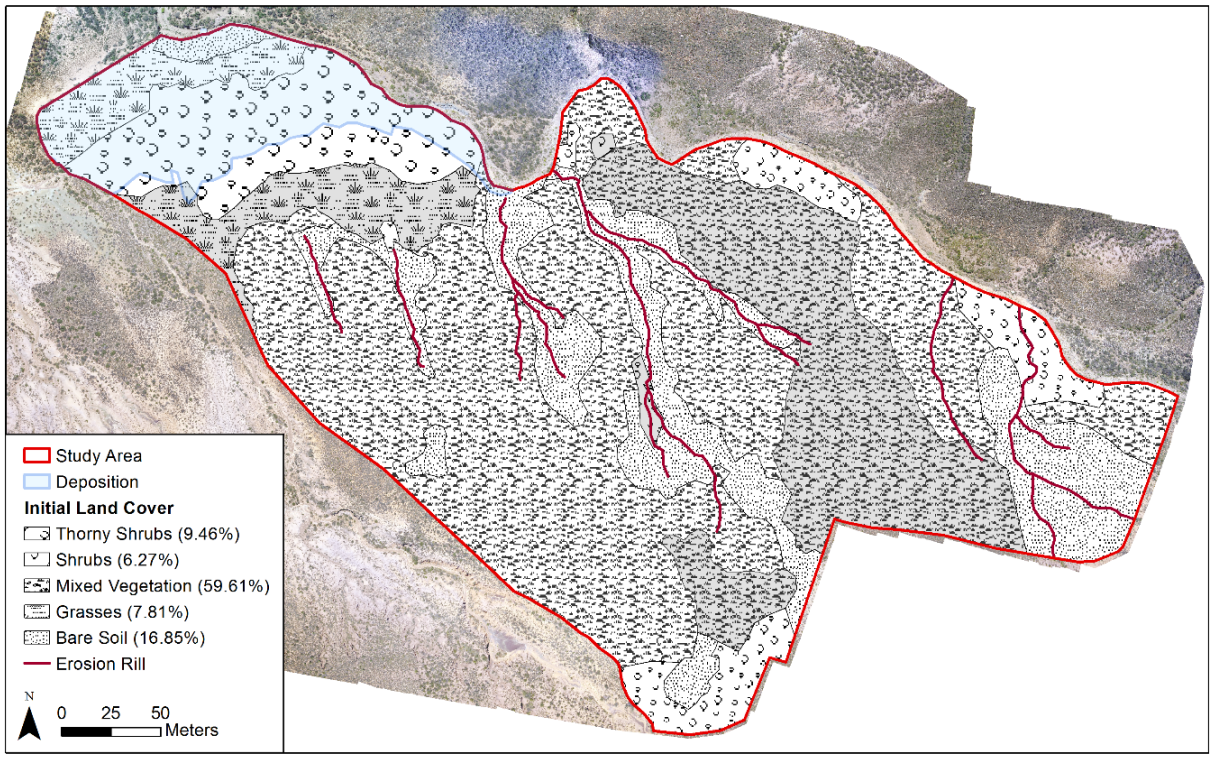

Figure 4-3 Field map (FM) derived from on-site land cover assessment. Percentages in parentheses reflect the share of the total study area. Areas highlighted in grey had a vegetation cover > 75%.

4.4.2 LAND COVER CLASSIFICATION AND ACCURACY

The LC classification (Figure 4-4B) identified 37.5% (3.64 ha) of the study area as not vegetated (bare soil or stones), 53.9% (5.25 ha) as grasses, and 8.6% (0.83 ha) as shrubs. As the FM and LC map shows, shrubs occur mainly in the northern part of the study area along the main gully and close to the former edges of the reservoir that is now fully silted-up. Additionally, they grow in higher densities alongside or within the bed of larger erosion rills. Differences in grass species, as in the field assessment, were not detected by the LC map. Non-vegetated (bare soil and stone cover) areas show some rills that were also observed on-site.

The overall accuracy of the LC classification, representing the proportion of reference sites that were mapped correctly according to the orthophoto, is 78% (Table 4-2). User's accuracy

was highest for the bare soil (85%) and lowest for the shrubs (74%). Producer's accuracy was lowest for the grasses (66%)

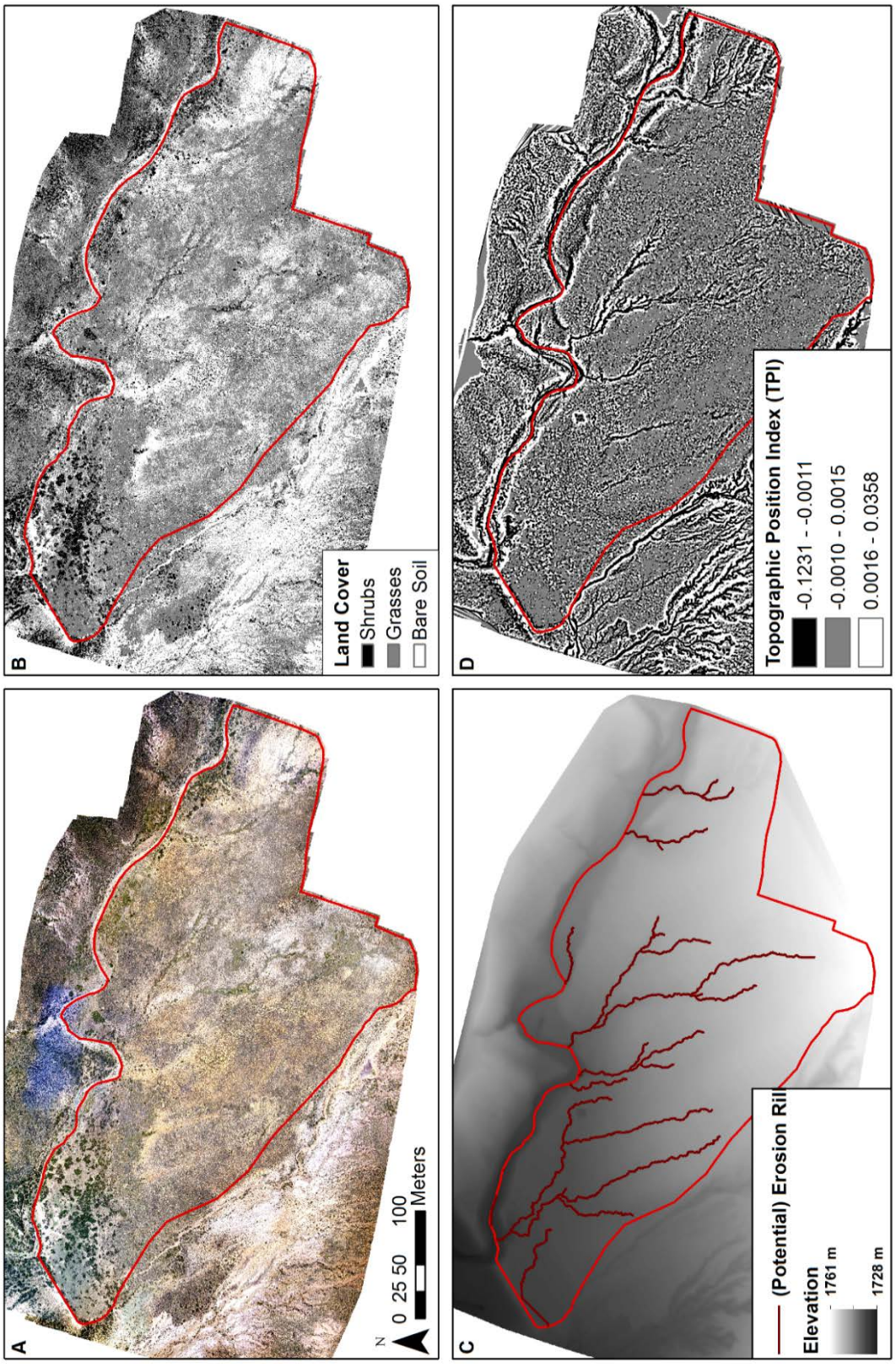

Figure 4-4 The orthophoto (A) was used for supervised land cover classification (B) (LC map). The DEM (C) was used for flow accumulation analysis to identify potential erosion rills and for the TPI (D) as a basis for landscape unit classification. The study area is marked in red. All maps are at the same scale.

Table 4-2 Confusion matrix representing accuracy assessment results for the supervised land cover classification using the SVM algorithm. Accuracy assessment was performed using 150 randomly selected sample points per LC class.

		Reference Data				
	LC Class	**Shrubs**	**Grasses**	**Bare Soil**	**Total**	**User's Accuracy**
Classified	Shrubs	111	37	2	150	74%
	Grasses	20	114	16	150	76%
	Bare Soil	2	21	127	150	85%
	Total	133	172	145	450	
	Producer's Accuracy	83%	66%	88%		78%
	Kappa	0.67				

4.4.3 MAPPING LANDSCAPE UNITS

The high level of patchiness in this landscape is shown in the orthophoto (Figure 4-4A). Five different LUs could be identified and are described in Table 4-3. Visual impressions of LUs in the field and on the orthophoto are shown in Figure 4-5. The RGB classification (Figure 4-6, Table 4-3) attributes 0.72 ha to the severely degraded LU, 1.6 ha to the moderately degraded LU, and 6.47 ha to the vegetated LU; the RGB+DEM (Figure 4-7) classification accounted for 1.23 ha, 1.55 ha, and 6.15 ha, respectively. Two states of degradation could be identified: moderately and severely degraded. The latter of the two consisted of lower vegetation cover (< 30%) and shrubs or grasses were smaller and sparsely distributed throughout, whereas moderately degraded areas, by contrast, were either characterised by a low vegetation cover or negative TPI. The RGB map attributed a lower amount of area to the moderately and severely degraded area (both combined made up 24%) than the RGB+DEM map (29%), and it identified fewer erosion rills (Table 4-3). Both the RGB and RGB+DEM maps identified all degraded areas that were mapped on the FM

The lowest negative TPI characterises rills or gully bottoms, which in our case can be regarded as equal to rill bottoms. Hence, erosion rills are mostly overlapping with either of the degraded LUs, or they link different areas of degradation. Most erosion rills are connected to the main gully or, as for the most rills in the west of the study area, directly to the reservoir. The area of deposition, which is characterised by the flat area behind the former dam wall, has an extent of 1.02 ha. This includes the former depositional area of the reservoir within the study area and an area severely affected by erosion located just behind the dam breach.

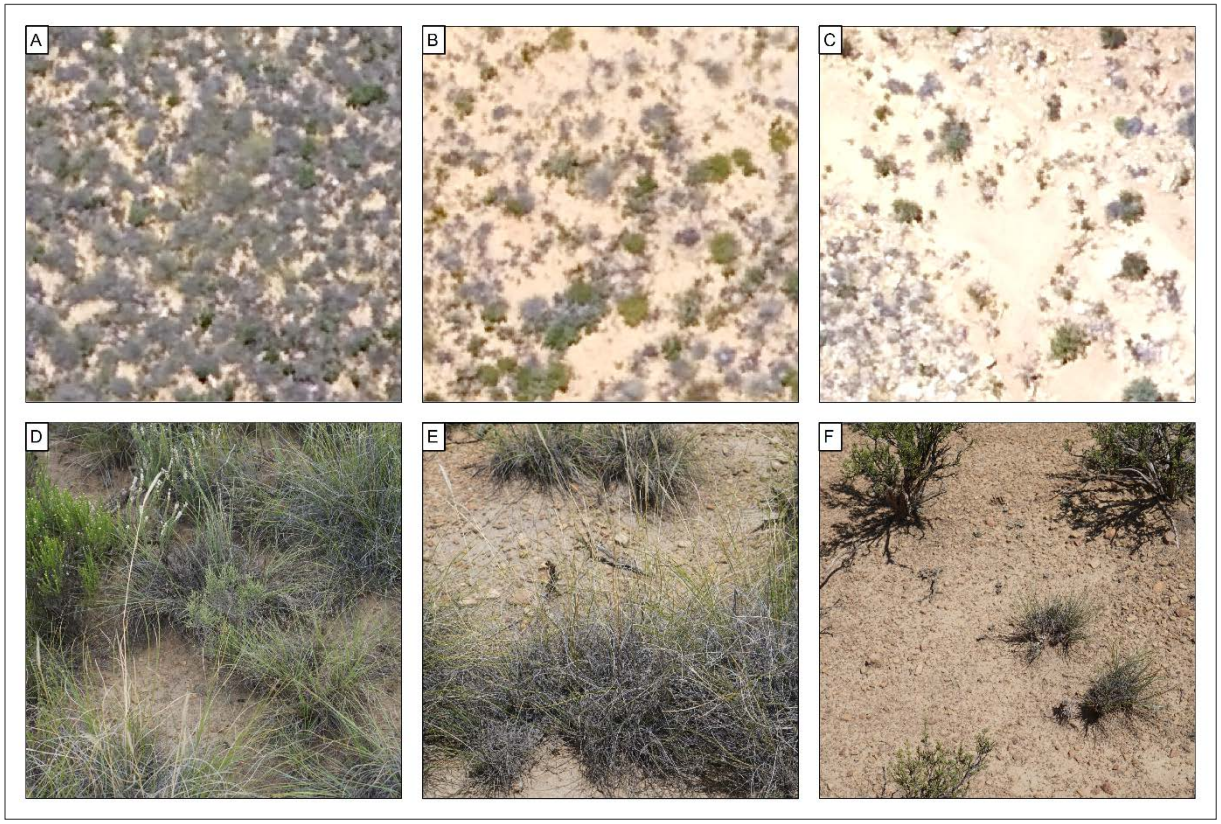

Figure 4-5 Visual appearance of different landscape units: vegetated (A,D), moderately degraded (B,E), and severely degraded (C,F). The top row (A–C) shows a 10 × 10 m cutout from the orthophoto used for classification. The bottom row (D–F) shows typical impressions from the field.

Table 4-3 Characteristics of landscape units for their identification in the field and on the orthophoto and their area on the classified maps. A threshold value of at least 50% vegetation cover for the vegetated LU was chosen according to the Karoo Veld assessment form in (Esler et al., 2006), where an excellent veld condition was characterised by, among other things, > 50% vegetation cover. Total length of all erosion rills is given in km and marked with *.

Landscape Unit (LU)	**Identification**		**Area (ha)**	
	In Field	**On UAV Imagery/DEM/Derivative**	**RGB Map**	**RGB+DEM Map**
Depositional	Flat terrain behind the former dam wall	Former reservoir area on historical aerial images, sharp elevation change at the dam wall	1.02	1.02
Severely degraded	Crusted soils Contiguous area of bare soil with little vegetation (individual shrubs or tussock grass) and large gaps between individual plants, vegetation cover < 30% Clearly developed rills		0.72	1.23
Moderately degraded	Very low TPI Contiguous area of bare soil more regularly interspersed with vegetation but vegetation cover <50% Some rills		1.6	1.55
Erosion rill	Rill structure	Line structure of bare soil, possibly flow accumulation paths on DEM Very low TPI	0.95 *	2.12 *
Vegetated	Contiguous vegetation cover interspersed with patches of bare soil or stones, at least 50% covered with vegetation		6.47	6.15

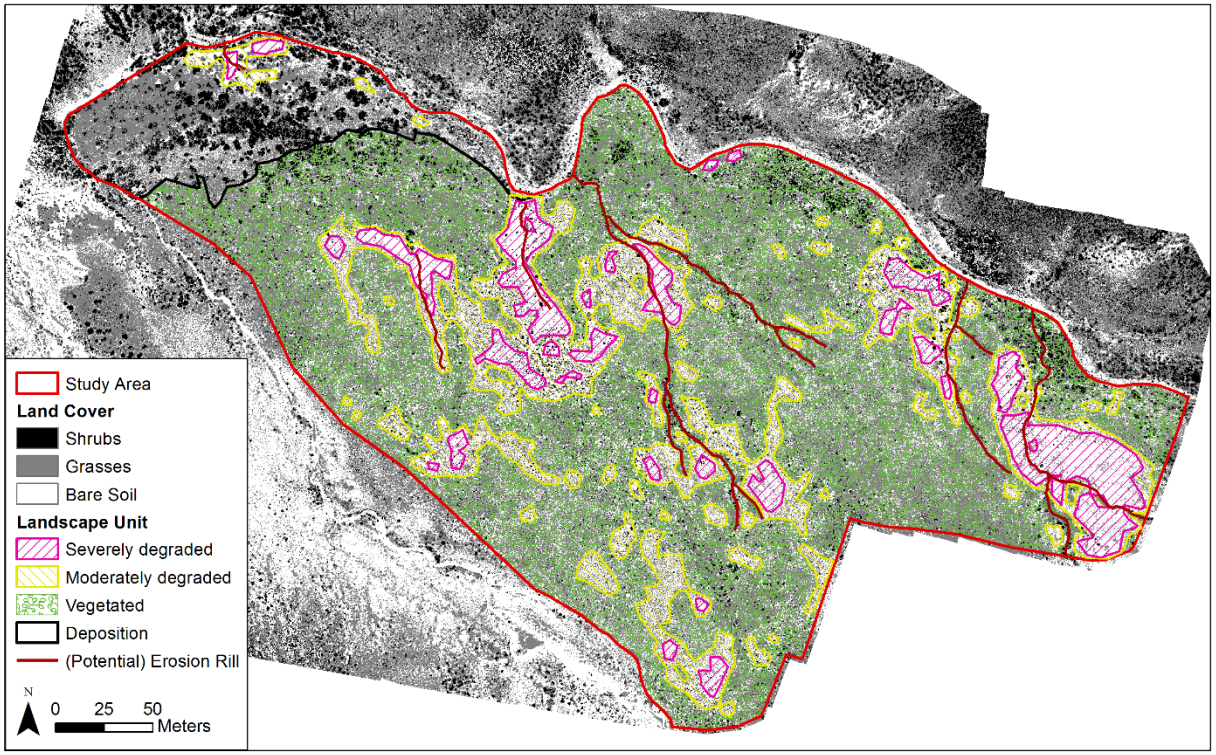

Figure 4-6 RGB map showing identified landscape units based on classified land cover.

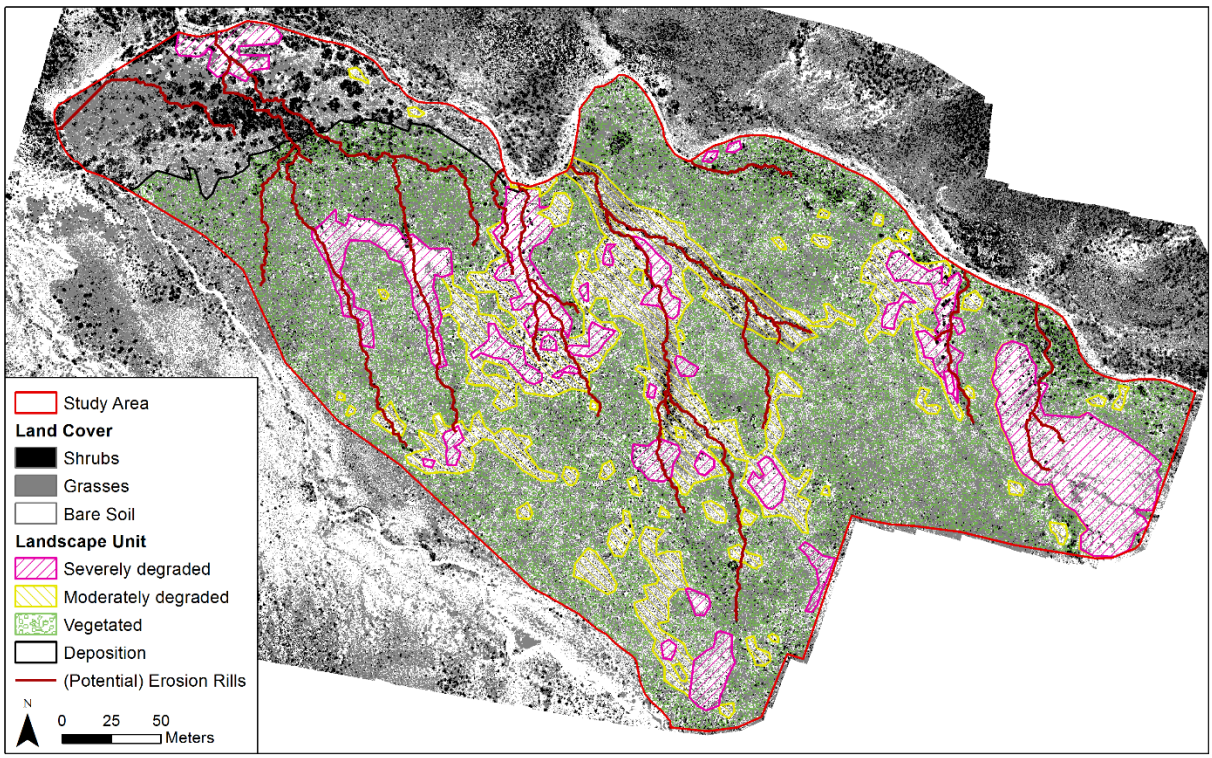

Figure 4-7 RGB+DEM map showing identified landscape units, classified land cover and DEM derivatives.

4.4.4 WHICH INFORMATION FROM REMOTE SENSING PRODUCTS IS NEEDED IN ORDER TO IMPROVE TRADITIONAL FIELD MAPPING IN HETEROGENEOUS LANDSCAPES?

The studies carried out for this PhD have shown that remote sensing products can deliver valuable information for mapping heterogeneous landscapes. The question that follows is how these data products can be used to complement and reduce the effort of field mapping and increase the information content of soil maps. The major limitations of conventional field mapping are the high time and analytical investments, which usually lead to an interpolation across the few sampling points. Hence, interrelationships between remote sensing imagery and local key landscape properties linked to degradation such as vegetation cover, soil surface roughness, soil moisture, SOC, soil clay content and soil texture need to be understood to compensate for time consuming and costly field mapping and sampling. Vegetation cover as a proxy for soil health is already widely used in remote sensing studies (Bai et al., 2008a, 2008b; Krenz et al., 2019; Pickup and Chewings, 1994) and is therefore a first step into reducing field sampling. In semi-arid dryland areas, where vegetation is usually sparse and of fading colours, it can be difficult to distinguish plants from the surrounding bare ground only using an orthophoto (Chapter 4). Therefore, additional spectral information from beyond the visible light spectrum is needed to reduce uncertainties. Normalised difference vegetation index (NDVI) and vegetation optical depth (VOD) are helpful indices for degradation mapping, as they provide relevant information on vegetation cover (Andela et al., 2013; Tian et al., 2016; Wessels et al., 2008), either being sensitive to the chlorophyll concentrations (NDVI) or to water content in both leafy and woody vegetation components (VOD). The use of multispectral data can further deliver information on relevant soil characteristics influencing the susceptibility to soil erosion, as visible near-infrared (vis-NIR) airborne spectroscopy has shown for estimating soil parameters, such as texture and SOC (Gomez et al., 2008; Guo et al., 2019). However, especially using multispectral data with vegetation cover as a proxy for degradation is limited by different sensitivity and phenological cycles of herbaceous and woody vegetation (Andela et al., 2013). Hence, best results are obtained shortly after the rainy season (Schmidt and Karnieli, 2000).

As soil characteristics and topography are interrelated (Gerrard, 1981; Jenny, 1941), topographic parameters derived from DEMs combined with mathematical models have been widely used for the prediction of soil properties related to soil degradation. Some examples are the prediction of SOC (Mora-Vallejo et al., 2008; Terra et al., 2004), texture (Sumfleth and Duttmann, 2008), clay content (Minasny and McBratney, 2007; Mora-Vallejo et al., 2008), and horizon thickness (Gessler et al., 2000; Hengl et al., 2004; Herbst et al., 2006; Sumfleth and Duttmann, 2008). However, most of the previous studies relied on satellite data for their research, which is not of sufficient resolution to identify degradation features in heterogeneous landscapes. High-resolution aerial images and DEMs as delivered by UAVs can bridge this

gap (Chapter 3, 4) and even detect small-scale patterns and topographic changes, such as erosion rills (Chapter 4). Identifying vegetated areas with denudation still remains a problem. In this case a field visit is vital for estimating the affected areas until covariance between small-scale topography, vegetation and denudation are perceived. For all issues, UAV imagery should ideally be captured first to identify presumptive areas of degradation, followed by field sampling in the prioritised areas to confirm the assumptions.

Another asset of using aerial imagery in heterogeneous landscapes is its objectivity. Field mapping can include a high level of uncertainty due to subjective evaluation. Even though a range of guidelines and assessment forms exists (Esler et al., 2006; FAO, 2011; Oldeman, 1988; Petri et al., 2019; Stocking and Murnaghan, 2013), different surveyors might interpret the same level of degradation differently. Largely automated digital mapping techniques can overcome this challenge, but threshold values for degradation classification need to be defined and evaluated regarding their applicability in different landscapes and ecosystems. While the relationship between vegetation cover, spatial vegetation patterns, runoff, and sediment yield has been investigated thoroughly (Bautista et al., 2007; Cammeraat and Imeson, 1999; Ludwig and Tongway, 1995; Puigdefábregas, 2005) and estimates for threshold values of vegetation cover for the reduction of erosional processes in semi-arid regions are given (Esler et al., 2006; Sauer and Ries, 2008), similar thresholds have, to the knowledge of the author, not been developed for remote sensing of soil degradation. To develop such tools, accessible soil databases on soil properties for thorough model calibrations, including upscaling of the small-scale degradation assessments to regional scales or larger, are required. Despite data upscaling procedures being complex, and the amount of local information needed for validating satellite imagery probably differing between landscapes, field scale information is necessary to verify relationships between spatial distributions of soil characteristics for upscaling the soil prediction. The studies conducted for this PhD highlight that the combination of field mapping and UAVs offers an approach to generate the required data in a feasible manner, including a digital bridge between the scales captured by UAVs and satellites.

4.5 DISCUSSION

4.5.1 COMPARISON OF FIELD MAPPING AND RGB MAP

Both methods were able to identify areas of soil degradation. However, their spatial extent differed slightly (Figure 4-8). Assuming that all bare soil areas of the FM are indicative of soil degradation in the UAV-derived digital RGB map, the extent of degradation mapped in the field was 5% lower than that mapped using UAV imagery. Severely degraded areas could be clearly distinguished from their surrounding by their lower vegetation cover and were identified using both approaches. However, two problems occurred. Firstly, digital mapping based on the orthophoto did not identify areas of soil degradation that had a vegetation cover

larger than 50%, such as vegetated erosion rills or rills surrounded by vegetation. This lower percentage of correct identification is attributed to the vegetation cover of the rills, which leaves them partially invisible on the UAV imagery. Secondly, the UAV-based mapping revealed areas of degradation which were not identified in the field. This was probably due to a difficult delineation of cover types in the field due to (i) smooth transitions between increasing/decreasing vegetation cover or type, (ii) the spatial heterogeneity, and (iii) a limited straight down view by the surveyor as opposed to the planform overview from the UAVs' perspective. Consequently, such visual delineation of LUs in the field depends on their spatial heterogeneity and can be influenced by subjectively introducing a random mapping error, as is mentioned by (Behrens et al., 2005). In addition, smaller degraded areas that are surrounded by vegetated areas might be invisible from the surveyors' vantage point and might be missed due to time constraints during field mapping. Degraded areas that were not identified on the FM but during digital mapping are marked in white in Figure 4-8.

4.5.2 COMPARISON OF FIELD MAPPING AND RGB+DEM MAP

Similarly to the digital RGB mapping, the RGB+DEM mapping also identified areas of soil degradation. The RGB+DEM map identified areas of medium vegetation cover with disturbed soil surfaces much better than the field mapping approach, leading to an additional 12% of soil assessed as moderately or severely degraded. The moderately degraded areas were largely identified with the help of the DEM and the TPI. As (Moore et al., 1993) stated in 1993, including terrain attributes and thereby increasing the information input can enhance spatial modelling. The small-scale topographic information of the roughness index (TPI) enabled the identification of areas with disturbed soil surface structure in our study area. Accordingly, small erosion rills that were not connected to larger rills were readily identifiable on the digital map. In heterogeneous landscapes, small features are more difficult to depict than large features and afford more time-investment. They can be missed by conventional mapping, illustrating a benefit of using UAVs which enable complete spatial coverage.

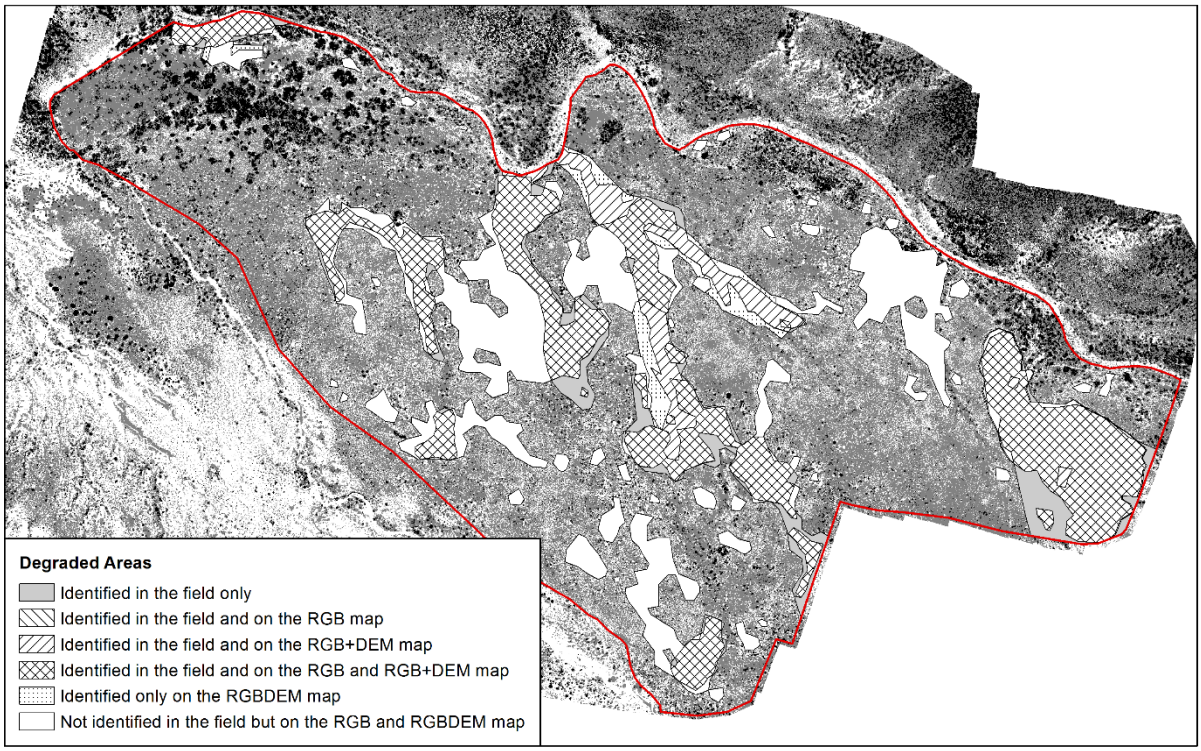

Figure 4-8 A map indicating areas that were identified as degraded with either method: manual field mapping or digital mapping.

4.5.3 COMPARISON OF RGB AND RGB+DEM MAP

Degraded, vegetated, and depositional LUs could be detected from the aerial image. However, we identified two key differences between the RGB and RGB+DEM classifications. Firstly, the RGB+DEM classification classified a larger proportion of the area as degraded, which we attribute to incorporating topography data and DEM derivates. Incorporating DEM derivates enabled the identification of moderately degraded areas that still had a high vegetation cover but already showed a high terrain roughness, which can lead to concentrated flow and rill formation if connectivity is high.

A second key difference is the greater number of rills that were identified on the RGB+DEM map than on the RGB map. In our study area, approximately 40% of the rills were covered with vegetation and thus not identified when land cover was the only parameter for identification. In particular, deeply incised rills showed some vegetation cover (Figure 4-9), attributed to probably a higher water availability through runoff accumulation in the rills. Vegetation in the rills also indicates that they primarily act as transport pathways for water and sediment and are not eroding actively anymore. Such erosion related features are ignored when just using RGB data. These results show that vegetation cover on aerial pictures cannot exclusively be used as a soil health indicator but emphasises that topographic information should also be incorporated.

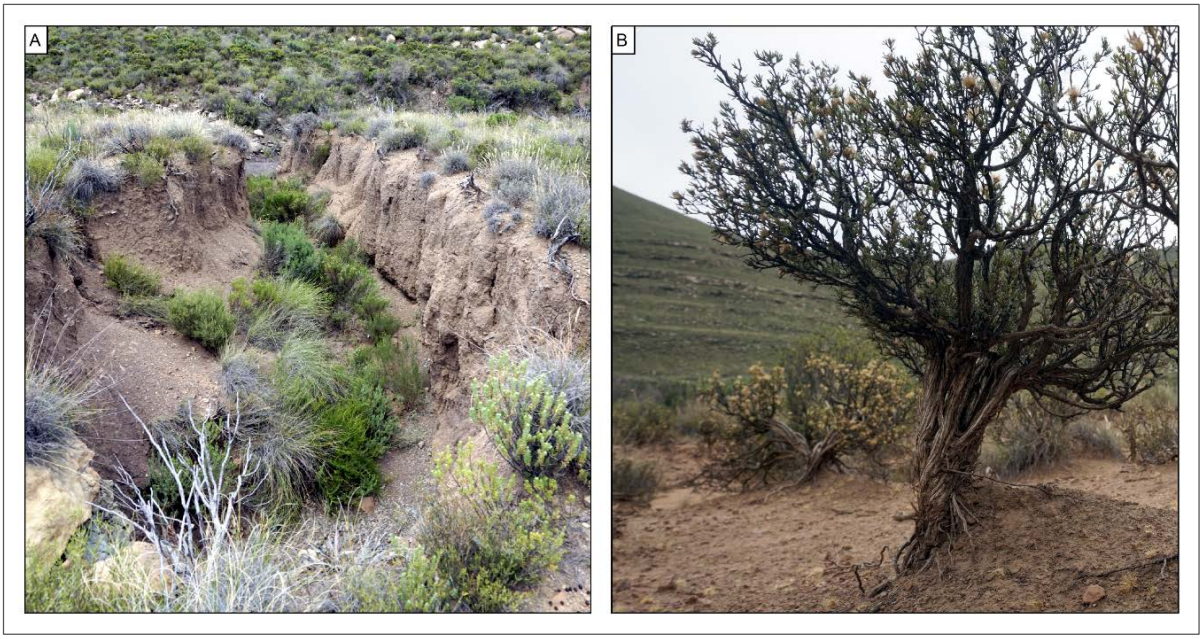

Figure 4-9 (A) An overgrown gully, the bottom is covered in shrubs. This will not be detected as degraded on the RGB map if vegetation cover is used only as a proxy for digital mapping. (B) Typical earth mound around stem/roots of shrubs in eroding areas indicate the "original" height of the soil surface. The difference between the ground to the left and right of the shrub is approximately 4 cm.

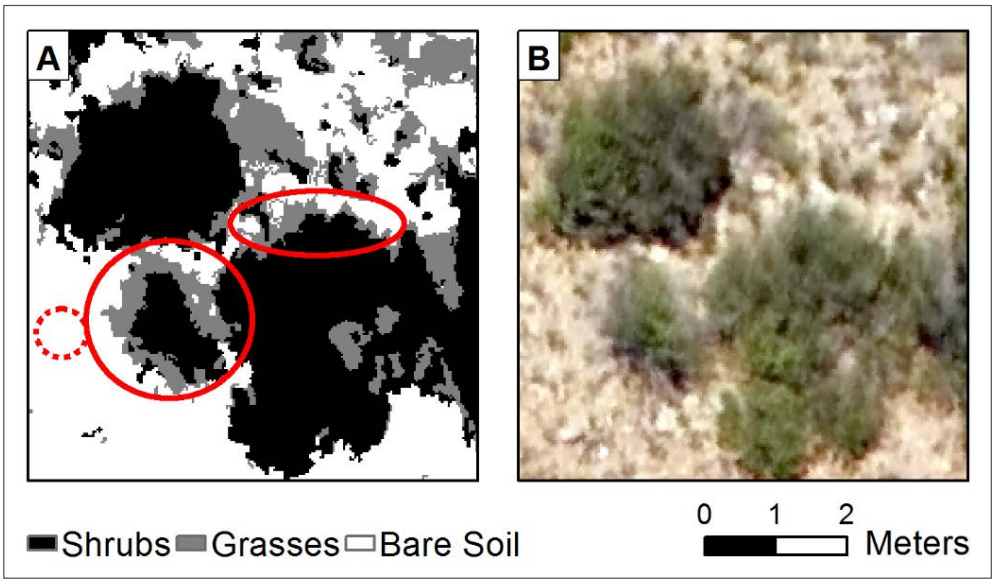

Figure 4-10 Examples of misclassification on the LC map (A) compared to the orthophoto (B): edges of shrubs were often misclassified as grasses (solid line). Small patches of grasses were incorrectly classified as bare soil (dashed line).

4.5.4 POTENTIAL AND LIMITATIONS OF USING UAV IMAGERY FOR ASSESSING SOIL DEGRADATION

UAV imagery served as a base for mapping landscape units. An exact classification of bare soil and vegetated areas was therefore crucial for further landscape analysis (Figure 4-4B) and degradation mapping. The kappa coefficient of 0.67 (Table 4-2) indicates that the classified map moderately agrees with the associated reference data (Jensen, 1996). It is important to emphasise that the accuracy of the classification strongly depends on the resolution of the input data used for the image analyses (Nussbaum et al., 2011) and the selection of training data. Our training dataset used for the SVM classification was chosen very carefully. Training polygons were only assigned to a certain class if there was no doubt on the class affiliation. As a result, transitional areas between shrubs and grasses or grasses and bare soil are probably underrepresented in the training data introducing uncertainties in the distinction of boundaries between these classes. For the accuracy assessment, all randomly stratified points for the accuracy assessment could be attributed to a distinct land cover class. However, this required some ground knowledge of the differences in shapes and colours of shrubs and grasses in the study area.

Additionally, heterogeneous landscapes or land cover classes complicate a successful classification, because the landscape is composed of a mosaic of different land covers, such as shrubs, grasses, and bare soil that do not always show distinct boundaries (Smith et al., 2003). The moderate overall accuracy of 78%, resulting in an inaccuracy of 22%, can be largely attributed to misclassified vegetation. Grass had the lowest producer's accuracy (Table 4-2) with two thirds of the accuracy assessment points incorrectly assigned to shrubs or bare soil. Taking a closer look at the misclassified pixels and aligning them with the field observations revealed that the edges of bushes were often misclassified as grasses (Figure 4-10). Additionally, misclassified shrub pixels were often accounted as Dicerothamnus rhinocerotis. This shrub has a dull greyish green color which was often incorrectly classified as grass. Grasses, which cover a variety of different shades of green, including very low brightness, were also misinterpreted as shrubs or bare soil (Figure 4-10). Using a density map to identify healthy landscape areas with a vegetation cover larger 50%, revealed many lower vegetated patches smaller 20 m^2 that were not detected during the field mapping. These patches could be the first indicator of arising degraded areas. However, their extent should be treated with caution due to uncertainties in boundary regions.

Due to missing near-infrared spectra, which contain much information on vegetation, a separation between different shrub types and areas with mixed vegetation, as in the FM, was not successful. If more detailed information on vegetation cover and types of vegetation is needed, or a distinct separation between grasses and shrubs is necessary, multispectral data should be used (Bannari et al., 1995; Geerken et al., 2005; Su et al., 2007; Xie et al., 2008). Since the aim of our study was the mapping of soil degradation, we condensed shrub-dominated

and grass-dominated areas into one LU (vegetated) and dispensed with the detailed classes as for the field mapping. Condensing these two LUs into one showed that roughly 60% of the study area is covered with vegetation. This agreed with our initial expectation based on (Esler et al., 2006) of 50–70% vegetation cover in these climatic conditions.

4.5.5 CAN FIELD MAPPING DELIVER THE STATUS QUO?

Both digitally-derived maps classified a larger area as degraded than the field mapping. However, fewer rills were visible in the RGB map than in the FM. The RGB+DEM map, using the UAV imagery and topographic data, revealed the highest percentage of degraded areas. We attribute the improved quality of the map to the identification of features such as rills which were otherwise masked by even sparse shrub cover.

The final question of our study is whether field mapping can be considered as a benchmark. Depending on the homogeneity of the landscapes, field maps can deliver a precise standard map of a study area. However, with increased heterogeneity, the time required for data collection will increase, as well as the transfer time to a geographic information system and map creation. Comparing UAV-based maps and our field map revealed that conventional mapping has further shortcomings: (i) vegetation acts as a cover and inhibits the detection of smaller patches without vegetation and soil degradation from the surveyors' position; (ii) smaller topographic features such as rills, especially if they are not connected to larger systems, might be missed because they are hidden from view by overhanging branches of shrubs; and (iii) the smooth transition between moderately degraded and non-degraded areas makes a delineation difficult in the field and introduces a subjective individual error source.

A final argument for the use of conventional UAV mapping, particularly for land management, is the fast acquisition and processing of the data compared to conventional field mapping. Even if some misclassification occurs, land cover, and implicitly soil quality changes, can be detected more regularly, which over time leads to a quality similar to or better than an out-of-date conventionally produced map. Furthermore, the spatial resolution of UAV-derived products is higher, though their level of detail of the classification depends on input data (Nussbaum et al., 2011) and on the spatial prediction method used (Illés et al., 2011). However, if the vegetation type is of research interest, then a complimentary field survey is necessary, ideally also being amended with the use of multispectral data.

4.6 CONCLUSION

In this study, the suitability of UAV data to map soil degradation was investigated and compared to conventional field mapping. The results show that UAV imagery and data products generated with them can contribute to identifying soil degradation with similar accuracy to conventional field mapping. Most notably, UAV-based degradation mapping

enabled the most severely degraded areas to be identified in a feasible manner based on their limited vegetation cover. The LC classification performed well for bare soil areas (producer's accuracy: 92%, user's accuracy: 85%), illustrating that UAV imagery delivers sufficient information for soil degradation mapping on a catchment scale. However, our results indicate that digital mapping still potentially underestimates the area of soil degradation. This may be mainly attributed to small-scale heterogeneity of land cover, a difficult distinction between bare soil ground cover and fading green tussock grasses, and shrubs inhibiting a clear view of the ground and its actual condition. Tussocks growing on pedestals or exposed shrub roots cannot be detected with UAV imagery at the catchment scale in a time-efficient way. In this case, ground-truthing would add valuable information.

Major improvements to RGB-based and vegetation density-based mapping were able to be achieved when fine-scaled topographic information derived from DEM generated from UAV data was used to identify different landscape units. Therefore, we recommend combining an orthophoto at least with a DEM and a flow accumulation model to gain information on erosion rills and moderately degraded areas.

The results of our study demonstrate that UAVs provide a valuable tool for rapid assessment of soil degradation, in particular in heterogeneous landscapes where manual field sampling is very time consuming and subject to subjective assessments by the surveyor. When exact information on vegetation cover is required and for land cover analysis in savanna-like landscapes, where RGB colors represent different shades of beige to light greyish green, multispectral cameras should be used.

4.7 ACKNOWLEDGEMENTS

We would like to thank Goswin Heckrath and Ruth Strunk for their assistance with fieldwork, Brigitte Kuhn for UAV piloting and helping with the post-processing, and Lena Farré for graphical advice, as well as the anonymous reviewers for their constructive review comments. The authors are grateful to Shauna Westcott and Dirk Jacobs for access to the study site.

4.8 REFERENCES

Bannari, A., Morin, D., Bonn, F., Huete, A.R., 1995. A review of vegetation indices. Remote Sens. Rev. 13, 95–120. https://doi.org/10.1080/02757259509532298

Bartley, R., Roth, C.H., Ludwig, J., McJannet, D., Liedloff, A., Corfield, J., Hawdon, A., Abbott, B., 2006. Runoff and erosion from Australia's tropical semi-arid rangelands: influence of ground cover for differing space and time scales. Hydrol. Process. 20, 3317–3333. https://doi.org/10.1002/hyp.6334

Behrens, T., Förster, H., Scholten, T., Steinrücken, U., Spies, E.-D., Goldschmitt, M., 2005. Digital soil mapping using artificial neural networks. J. Plant Nutr. Soil Sci. 168, 21–33. https://doi.org/10.1002/jpln.200421414

Behrens, T., Zhu, A.-X., Schmidt, K., Scholten, T., 2010. Multi-scale digital terrain analysis and feature selection for digital soil mapping. Geoderma 155, 175–185. https://doi.org/10.1016/j.geoderma.2009.07.010

Boardman, J., Foster, I.D.L., 2011. The potential significance of the breaching of small farm dams in the Sneeuberg region, South Africa. J. Soils Sediments 11, 1456–1465. https://doi.org/10.1007/s11368-011-0425-5

Boardman, J., Foster, I.D.L., Rowntree, K.M., Favis-Mortlock, D.T., Mol, L., Suich, H., Gaynor, D., 2017. Long-term studies of land degradation in the Sneeuberg uplands, eastern Karoo, South Africa: A synthesis. Geomorphology. https://doi.org/10.1016/j.geomorph.2017.01.024

Bochet, E., Poesen, J., Rubio, J.L., 2000. Mound development as an interaction of individual plants with soil, water erosion and sedimentation processes on slopes. Earth Surf. Process. Landf. 25, 847–867. https://doi.org/10.1002/1096-9837(200008)25:8<847::AID-ESP103>3.0.CO;2-Q

Broxton, P.D., Zeng, X., Sulla-Menashe, D., Troch, P.A., 2014. A Global Land Cover Climatology Using MODIS Data. J. Appl. Meteorol. Climatol. 53, 1593–1605. https://doi.org/10.1175/JAMC-D-13-0270.1

Cammeraat, L.H., Imeson, A.C., 1999. The evolution and significance of soil–vegetation patterns following land abandonment and fire in Spain. CATENA 37, 107–127. https://doi.org/10.1016/S0341-8162(98)00072-1

Castillo, V.M., Martinez-Mena, M., Albaladejo, J., 1997. Runoff and Soil Loss Response to Vegetation Removal in a Semiarid Environment. Soil Sci. Soc. Am. J. 61, 1116–1121. https://doi.org/10.2136/sssaj1997.03615995006100040018x

Cerdá, A., 1997. The effect of patchy distribution of Stipa tenacissima L. on runoff and erosion. J. Arid Environ. 36, 37–51. https://doi.org/10.1006/jare.1995.0198

Congalton, R.G., 2001. Accuracy assessment and validation of remotely sensed and other spatial information. Int. J. Wildland Fire 10, 321–328. https://doi.org/10.1071/wf01031

Couteron, P., Lejeune, O., 2001. Periodic spotted patterns in semi-arid vegetation explained by a propagation-inhibition model. J. Ecol. 89, 616–628. https://doi.org/10.1046/j.0022-0477.2001.00588.x

Deblauwe, V., Barbier, N., Couteron, P., Lejeune, O., Bogaert, J., 2008. The global biogeography of semi-arid periodic vegetation patterns. Glob. Ecol. Biogeogr. 17, 715–723. https://doi.org/10.1111/j.1466-8238.2008.00413.x

Dewitte, O., Jones, A., Spaargaren, O., Breuning-Madsen, H., Brossard, M., Dampha, A., Deckers, J., Gallali, T., Hallett, S., Jones, R., Kilasara, M., Le Roux, P., Michéli, E., Montanarella, L., Thiombiano, L., Van Ranst, E., Yemefack, M., Zougmore, R., 2013. Harmonisation of the soil map of Africa at the continental scale. Geoderma 211–212, 138–153. https://doi.org/10.1016/j.geoderma.2013.07.007

Dobos, E., Hengl, T., 2009. Chapter 20 Soil Mapping Applications, in: Hengl, Tomislav, Reuter, H.I. (Eds.), Developments in Soil Science, Geomorphometry. Elsevier, pp. 461–479.

d'Oleire-Oltmanns, S., Marzolff, I., Peter, K., Ries, J., 2012. Unmanned Aerial Vehicle (UAV) for Monitoring Soil Erosion in Morocco. Remote Sens. 4, 3390–3416. https://doi.org/10.3390/rs4113390

Dube, T., Mutanga, O., Sibanda, M., Seutloali, K., Shoko, C., 2017. Use of Landsat series data to analyse the spatial and temporal variations of land degradation in a dispersive soil environment: A case of King Sabata Dalindyebo local municipality in the Eastern Cape Province, South Africa. Phys. Chem. Earth Parts ABC 100, 112–120. https://doi.org/10.1016/j.pce.2017.01.023

Esler, K.J., Milton, S.J., Dean, W.R.J. (Eds.), 2006. Karoo veld ecology and management, 1st ed. ed. Briza, Pretoria, South Africa.

FAO, ISRIC, UNEP, 2003. Soil and Terrain Database for Southern Africa, 1:2 M scale. FAO, Rome [WWW Document]. Soil Terrain SOTER Database Programme. URL https://www.isric.org/projects/soil-and-terrain-soter-database-programme (accessed 2.15.19).

Foody, G.M., Mathur, A., 2004. A relative evaluation of multiclass image classification by support vector machines. IEEE Trans. Geosci. Remote Sens. 42, 1335–1343. https://doi.org/10.1109/TGRS.2004.827257

Foster, I.D.L., Boardman, J., Keay-Bright, J., Meadows, M.E., 2005. Land degradation and sediment dynamics in the South African Karoo, in: Horowitz, A.J., Walling, D.E. (Eds.), Sediment Budgets 2 (Prooceedings of Symposium S1 Held during the Seventh IAHS Scientific Assembly at Foz Do Iguaçu, Brazil, April 2005), IAHS Publication. Int Assoc Hydrological Sciences, Wallingford, pp. 207–213.

Geerken, R., Zaitchik, B., Evans, J.P., 2005. Classifying rangeland vegetation type and coverage from NDVI time series using Fourier Filtered Cycle Similarity. Int. J. Remote Sens. 26, 5535–5554. https://doi.org/10.1080/01431160500300297

Hengl, T., 2009. A practical guide to geostatistical mapping, 2nd extended ed. ed. Office for Official Publications of the European Communities, Amsterdam.

Hengl, T., Heuvelink, G.B.M., Kempen, B., Leenaars, J.G.B., Walsh, M.G., Shepherd, K.D., Sila, A., MacMillan, R.A., Mendes de Jesus, J., Tamene, L., Tondoh, J.E., 2015. Mapping Soil Properties of Africa at 250 m Resolution: Random Forests Significantly Improve Current Predictions. PLoS ONE 10. https://doi.org/10.1371/journal.pone.0125814

HilleRisLambers, R., Rietkerk, M., Bosch, F. van den, Prins, H.H.T., Kroon, H. de, 2001. Vegetation Pattern Formation in Semi-Arid Grazing Systems. Ecology 82, 50–61. https://doi.org/10.1890/0012-9658(2001)082[0050:VPFISA]2.0.CO;2

Huang, C., Davis, L.S., Townshend, J.R.G., 2002. An assessment of support vector machines for land cover classification. Int. J. Remote Sens. 23, 725–749. https://doi.org/10.1080/01431160110040323

Illés, G., Kovács, G., Heil, B., 2011. Comparing and evaluating digital soil mapping methods in a Hungarian forest reserve. Can. J. Soil Sci. 91, 615–626. https://doi.org/10.4141/cjss2010-007

Jenny, H., 1941. Factors of soil formation: a system of quantitative pedology. McGraw Hill, New York.

Jensen, J.R., 1996. Introductory digital image processing®: a remote sensing perspective, 2nd edition. ed, Prentice Hall series in geographic information science. Prentice Hall, Upper Saddle River, NJ.

Jones, A., Breuning-Madsen, H., Brossard, M., Dampha, A., Deckers, J., Dewitte, O., Gallali, T., Hallett, S., Jones, R., Kilasara, M., Le Roux, P., Micheli, E., Montanarella, L., Spaargaren, O., Thiombiano, L., Van Ranst, E., M, M., Zougmoré, R.B. (Eds.), 2013. Soil Atlas of Africa. European Commission, Luxembourg. https://dx.doi.org/10.2788/52319

Keay-Bright, J., Boardman, J., 2007. The influence of land management on soil erosion in the Sneeuberg mountains, central Karoo, South Africa. Land Degrad. Dev. 18, 423–439. https://doi.org/10.1002/ldr.785

Krenz, J., Kuhn, N.J., 2018. Assessing Badland Sediment Sources Using Unmanned Aerial Vehicles, in: Badlands Dynamics in a Context of Global Change. Elsevier, pp. 255–276. https://doi.org/10.1016/B978-0-12-813054-4.00008-3

Krenz, J., Greenwood, P., Kuhn, N.J., 2020. Correction: Krenz, J., et al. Soil Degradation Mapping in Drylands Using Unmanned Aerial Vehicle (UAV) Data. Soil Syst. 2019, 3, 33. Soil Syst. 4, 33. https://doi.org/10.3390/soilsystems4020033

Lucieer, A., Jong, S.M. de, Turner, D., 2014. Mapping landslide displacements using Structure from Motion (SfM) and image correlation of multi-temporal UAV photography. Prog. Phys. Geogr. Earth Environ. 38, 97–116. https://doi.org/10.1177/0309133313515293

Ludwig, J.A., Bastin, G.N., Chewings, V.H., Eager, R.W., Liedloff, A.C., 2007. Leakiness: A new index for monitoring the health of arid and semiarid landscapes using remotely sensed vegetation cover and elevation data. Ecol. Indic. 7, 442–454. https://doi.org/10.1016/j.ecolind.2006.05.001

Mighall, T.M., Foster, I.D.L., Rowntree, K.M., Boardman, J., 2012. Reconstructing recent land degradation in the semi-arid Karoo of South Africa: A palaeoecological study at Compassberg, Eastern Cape.

Mondal, A., Kundu, S., Chandniha, S.K., Shukla, R., Mishra, P.K., 2012. Comparison of support vector machine and maximum likelihood classification technique using satellite imagery. Int. J. Remote Sens. GIS 1, 116–123.

Moore, I.D., Gessler, P.E., Nielsen, G.A., Peterson, G.A., 1993. Soil Attribute Prediction Using Terrain Analysis. Soil Sci. Soc. Am. J. 57, 443–452. https://doi.org/10.2136/sssaj1993.03615995005700020026x

Morgan, R.P.C., 2005. Soil erosion and conservation, 3rd ed. ed. Blackwell Publishing, Malden, MA, USA.

Nakano, T., Kamiya, I., Tobita, M., Iwahashi, J., Nakajima, H., 2014. Landform monitoring in active volcano by UAV and SfM-MVS technique, in: ISPRS - International Archives of the

Photogrammetry, Remote Sensing and Spatial Information Sciences. Presented at the ISPRS Technical Commission VIII Symposium (Volume XL-8) - 09–12 December 2014, Hyderabad, India, Copernicus GmbH, pp. 71–75. https://doi.org/10.5194/isprsarchives-XL-8-71-2014

Neugirg, F., Stark, M., Kaiser, A., Vlacilova, M., Della Seta, M., Vergari, F., Schmidt, J., Becht, M., Haas, F., 2016. Erosion processes in calanchi in the Upper Orcia Valley, Southern Tuscany, Italy based on multitemporal high-resolution terrestrial LiDAR and UAV surveys. Geomorphology 269, 8–22. https://doi.org/10.1016/j.geomorph.2016.06.027

Nobajas, A., Waller, R.I., Robinson, Z.P., Sangonzalo, R., 2017. Too much of a good thing? the role of detailed UAV imagery in characterizing large-scale badland drainage characteristics in South-Eastern Spain. Int. J. Remote Sens. 1–17. https://doi.org/10.1080/01431161.2016.1274450

Nussbaum, M., Ettlin, L., Çöltekin, A., Suter, B., Egli, M., 2011. The relevance of scale in soil maps. Bull. BGS 32, 63–70.

Paterson, G., Turner, D., Wiese, L., van Zijl, G., Clarke, C., van Tol, J., 2015. Spatial soil information in South Africa: Situational analysis, limitations and challenges. South Afr. J. Sci. 111, 1–7. https://doi.org/10.17159/sajs.2015/20140178

Puigdefábregas, J., 2005. The role of vegetation patterns in structuring runoff and sediment fluxes in drylands: Vegetation and sediment fluxes. Earth Surf. Process. Landf. 30, 133–147. https://doi.org/10.1002/esp.1181

Rietkerk, M., Boerlijst, M.C., van Langevelde, F., HilleRisLambers, R., de Koppel, J. van, Kumar, L., Prins, H.H.T., de Roos, A.M., 2002. Self-Organization of Vegetation in Arid Ecosystems. Am. Nat. 160, 524–530. https://doi.org/10.1086/342078

Rietkerk, M., Ketner, P., Burger, J., Hoorens, B., Olff, H., 2000. Multiscale soil and vegetation patchiness along a gradient of herbivore impact in a semi-arid grazing system in West Africa. Plant Ecol. 148, 207–224. https://doi.org/10.1023/A:1009828432690

Rogers, R.D., Schumm, S.A., 1991. The effect of sparse vegetative cover on erosion and sediment yield. J. Hydrol. 123, 19–24. https://doi.org/10.1016/0022-1694(91)90065-P

Römkens, M.J., Helming, K., Prasad, S.N., 2002. Soil erosion under different rainfall intensities, surface roughness, and soil water regimes. Catena 46, 103–123.

Saco, P.M., Willgoose, G.R., Hancock, G.R., 2007. Eco-geomorphology of banded vegetation patterns in arid and semi-arid regions. Hydrol. Earth Syst. Sci. 11, 1717–1730. https://doi.org/10.5194/hess-11-1717-2007

Sanchez, P.A., Ahamed, S., Carré, F., Hartemink, A.E., Hempel, J., Huising, J., Lagacherie, P., McBratney, A.B., McKenzie, N.J., Mendonça-Santos, M. de L., Minasny, B., Montanarella, L., Okoth, P., Palm, C.A., Sachs, J.D., Shepherd, K.D., Vågen, T.-G., Vanlauwe, B., Walsh, M.G., Winowiecki, L.A., Zhang, G.-L., 2009. Digital Soil Map of the World. Science 325, 680–681. https://doi.org/10.1126/science.1175084

Schäuble, H., Marinoni, O., Hinderer, M., 2008. A GIS-based method to calculate flow accumulation by considering dams and their specific operation time. Comput. Geosci. 34, 635–646. https://doi.org/10.1016/j.cageo.2007.05.023

Schlesinger, W.H., Raikes, J.A., Hartley, A.E., Cross, A.F., 1996. On the Spatial Pattern of Soil Nutrients in Desert Ecosystems. Ecology 77, 364–374. https://doi.org/10.2307/2265615

Schlesinger, W.H., Reynolds, J.F., Cunningham, G.L., Huenneke, L.F., Jarrell, W.M., Virginia, R.A., Whitford, W.G., 1990. Biological Feedbacks in Global Desertification. Science 247, 1043–1048. https://doi.org/10.1126/science.247.4946.1043

Schwanghart, W., Groom, G., Kuhn, N.J., Heckrath, G., 2013. Flow network derivation from a high resolution DEM in a low relief, agrarian landscape. Earth Surf. Process. Landf. 38, 1576–1586. https://doi.org/10.1002/esp.3452

Smith, J.H., Stehman, S.V., Wickham, J.D., Yang, L., 2003. Effects of landscape characteristics on land-cover class accuracy. Remote Sens. Environ. 84, 342–349. https://doi.org/10.1016/S0034-4257(02)00126-8

Su, L., Chopping, M.J., Rango, A., Martonchik, J.V., Peters, D.P.C., 2007. Support vector machines for recognition of semi-arid vegetation types using MISR multi-angle imagery. Remote Sens. Environ., Multi-angle Imaging SpectroRadiometer (MISR) Special Issue 107, 299–311. https://doi.org/10.1016/j.rse.2006.05.023

Szuster, B.W., Chen, Q., Borger, M., 2011. A comparison of classification techniques to support land cover and land use analysis in tropical coastal zones. Appl. Geogr. 31, 525–532. https://doi.org/10.1016/j.apgeog.2010.11.007

Thompson, M., 1996. A standard land-cover classification scheme for remote-sensing applications in South Africa. South Afr. J. Sci. 92, 34–42.

Valentin, C., d'Herbès, J.M., Poesen, J., 1999. Soil and water components of banded vegetation patterns. CATENA 37, 1–24. https://doi.org/10.1016/S0341-8162(99)00053-3

Wang, R., Zhang, S., Pu, L., Yang, J., Yang, C., Chen, J., Guan, C., Wang, Q., Chen, D., Fu, B., Sang, X., 2016. Gully Erosion Mapping and Monitoring at Multiple Scales Based on Multi-Source Remote Sensing Data of the Sancha River Catchment, Northeast China. ISPRS Int. J. Geo-Inf. 5, 200. https://doi.org/10.3390/ijgi5110200

Weiss, A., 2001. Topographic position and landforms analysis, in: Poster Presentation, ESRI User Conference, San Diego, CA.

Wynn, T., Mostaghimi, S., 2006. The Effects of Vegetation and Soil Type on Streambank Erosion, Southwestern Virginia, Usa1. JAWRA J. Am. Water Resour. Assoc. 42, 69–82. https://doi.org/10.1111/j.1752-1688.2006.tb03824.x

Xie, Y., Sha, Z., Yu, M., 2008. Remote sensing imagery in vegetation mapping: a review. J. Plant Ecol. 1, 9–23. https://doi.org/10.1093/jpe/rtm005

CHAPTER 5

Synthesis and Outlook

5.1 SUMMARY OF PRIMARY RESULTS

The aim of this PhD-thesis was to assess the occurrence and potential relevance of small-scale soil patterns in a heterogeneous degraded semi-arid rangeland. By addressing this aim, this study intended to develop and test a methodological approach based on UAV imagery to map and quantify soil degradation. The following synthesis summarises the results of the studies and then discusses the major findings and limitations with reference to the questions raised in the introduction (Chapter 1).

Chapter 2 documented and described the spatial heterogeneity of an exemplary catchment in the Sneeuberg rangelands, which is characterised by erosion and deposition, based on field mapping, soil sampling and analysis. The field and laboratory work revealed that the patchiness of the soil properties was not reflected by the soil types depicted in the maps that are available for the Karoo. Degradation caused significant differences in soil nutrient content, which was greater in grass patches (TOC 1.10%, TN 0.10%) and mixed vegetation (TOC 0.93%, TN 0.08%) than on degraded areas (TOC 0.47%, TN 0.4%). The results also showed that depiction of eroded soil behind dams fosters the development of new, fertile soils on deep, fine-textured, nutrient-rich and moist sediments.

Chapter 3 examined whether UAVs can be used to assess the relevance of hot-spots of erosion, such as badlands, as sediment sources. Imagery for further generating DEMs and orthophotos were captured with a commercially available UAV. A workflow that enables the identification, mapping, and quantification of badland erosion volumes was developed. With this workflow, five badland and gully systems of different spatial extent and degrees of incision were identified using a high-resolution RGB-orthomosaic (resolution 3.12 x 3.12 cm per pixel). They comprised 21.6% (2.1 ha) of the studied area and a potential sediment volume of 7865 m^3. Best results were obtained for deeply incised badland systems that also have a low vegetation cover. An exact quantification of sediment sinks using a UAV was not possible, because it would rely on a high-resolution DEM before siltation as a comparison. The sediment volume was therefore estimated based on a potential reservoir shape and is approximately 30490 m^3. Hence, the sediment eroded from the badland areas accounts for 25% of the reservoir storage capacity.

Chapter 4 investigated the use of UAV imagery for soil degradation mapping in comparison to traditional field mapping. Two modelled maps, one based on vegetation cover, and one including additional topographic information, were produced. A major improvement of differentiation between degrees of degradation could be achieved when the orthomosaic was combined with the digital elevation model and a flow accumulation analysis. This approach classified 12% more as degraded than the conventional field mapping, which is attributed to the wider perspective of the UAV above the land surface. Even the small

commercial UAV thus proofed to be a valuable tool for rapid soil degradation assessment in a heterogeneous landscape, where field mapping is very time-consuming.

5.2 DISCUSSION OF THE RESEARCH QUESTIONS

5.2.1 IS LAND USE-INDUCED PATCHINESS OF SOIL AND VEGETATION A PREVALENT FEATURE IN THE KAROO LANDSCAPE?

The land cover and surface processes at the study site are highly variable and soil formation results from a complex pattern of processes (Chapter 2, Chapter 4). The vegetation, although not arranged in a typical dryland pattern, shows a heterogeneous patchwork of grasses interspersed with shrubs and bare patches. Vegetated areas are frequently disrupted by erosion, sometimes as severe as in badlands (Chapter 2, Chapter 4). Although the vegetation cover in the study area is largely within and above the expected natural cover of 50-70% (Esler et al., 2006), it does not provide good grazing for domestic livestock or game. Unpalatable grasses as *Merxmuellera distichia* or the shrub *Dicerothamnus rhinocerotis* (renosterbos) are frequent and probably replaced more palatable species as a consequence of overgrazing (Krug, 2004; Meadows and Watkeys, 1999). Currently, erosion may not only be prevented by shrub encroachment, but also the spread of non-palatable grasses (Bochet et al., 2006; Esler et al., 2006; Greene et al., 1994; van Oudenhoven et al., 2015).

A patchwork of grasses, shrubs, and bare soil occurs naturally due to the variability of surface soil properties (Chapter 2, Table 2-2). Besides rainfall, Nitrogen is considered the most limiting factor for plant growth in semi-arid areas (Snyman and du Preez, 2005). Although the nutrient contents are generally low, this pattern can also be observed in the study area, where areas with dense above-ground vegetation show greater nutrient contents. Such co-variances have also been reported by Schlesinger et al. (1996) and Dickie and Parsons (2012). Similar patterns emerge for SOC stocks, which are associated with differences in net primary production (NPP) (Smith, 2008). Soil texture showed less obvious patterns. Surface soil clay contents were lower than those of the underlying horizons throughout the study area (Chapter 2). Apparently, denudation and erosion of fine particles from the surface are not limited to obviously degraded areas, but appear to occur throughout the whole study area (Gabet and Dunne, 2003; Kuhn et al., 2012).

Besides the moderate vegetation cover, about 24% to 29% of the study area show clear signs of degradation (Chapter 4, Table 4-3) and an in-filled reservoir indicates that soil redistribution is happening in the Sneeuberg region. One sediment source of the infilling is denudation, which is indicated by many grasses growing on pedestals and frequent mound formation around shrubs (Bochet et al., 2000; Rostagno and del Valle, 1988) (Chapter 4, Figure 4-9). Severely degraded areas presumably act as sediment sources as well. Except from one, all of them are either directly or indirectly connected to the channel in the thalweg of the valley

by erosion rills (Chapter 2, 3 and 4) illustrating a high degree of hydraulic connectivity within the study area. Therefore, it is evident that all or most of the eroding areas acted as sources for the sediment trapped in the former reservoir. On these sediments, deep soils are forming, representing a new anthropogenic soil type. Dams have a high density (1 dam per km^2) in the Sneeuberg area (Boardman and Foster, 2011) and play a potentially relevant role in the ecosystem. The reservoirs are of small size and were mostly constructed for water storage in times of droughts or as check-dams (Keay-Bright and Boardman, 2006). Many are now silted-up and the estimated sediment volumes range from ca. 300 m^3 to about 323000 m^3 (Boardman and Foster, 2011). Based on the favourable conditions for plant establishment in silted-up reservoirs mentioned in Chapter 2, depositional areas immediately upstream of dams have the potential to act as C stores and facilitate C sequestration, as shown for check-dams in the Loess Plateau in China (Lü et al., 2012; Zhang et al., 2016). There, farmland used for maize cultivation has even been created on many check-dams (Xiang-zhou et al., 2004; Zhao et al., 2010). In the Sneeuberg region, with an average speculated storage potential of 20000 m^3, an average TOC content of 1%, and an average bulk density of 1160 kg m^{-3} a single dam stores potentially up to 232 t C. Considering that approximately 50 reservoirs are silted up in an area of appr. 100 km^2 (Boardman and Foster, 2011), about 11.6 kt C could be stored in those Sneeuberg reservoirs. In comparison about 52.20 kt C could be potentially stored in the A-horizons of the same area, if we assume an average A-horizon depth of 10 cm, an average TOC content of 1.0% (Chapter 2, Figure 2-3) and that approximately 45% of the area represent non-degraded vegetated valley bottoms. The estimated amount of C is equal to a carbon stock of 11.6 kg m^{-2}, a medium to high value compared to other studies in semi-arid areas (Table 5-1). The higher SOC-stocks could be attributed to the heterogeneous vegetation cover (Schlesinger et al., 1996) and the reduced SOC mineralisation due to water scarcity (Borken and Matzner, 2009). These C-stock estimates should be treated with some caution, because long-term C sequestration can only be achieved if the dams remain intact and are not breached and sediments eroded. Nevertheless, these considerations show that silted-up reservoirs can also increase the land productivity because they have a high potential for soil formation and C sequestration (Doetterl et al., 2012; Harden et al., 1999), both of accumulated C from the eroded sediments as well as photosynthetically captured CO_2, including translocation by plant roots into the deep sediment strata (Chapter 2). To confirm the biogeochemical relevance of newly formed soils behind dams, additional laboratory analyses, such as sediment fingerprinting (Valentin et al., 2005) are needed to identify their source areas and to describe the reservoir sediments and their characteristics in depth. Multivariate statistical techniques, such as regularised logistic regression could be used for the discrimination of soils and sediments (Reinwarth et al., 2017). Furthermore, pedogenic processes dominating the soil development and their biogeochemical implications should be investigated to improve our understanding of the anthropogenic soils forming behind dams.

Table 5-1 Estimated soil organic carbon (SOC) stocks for different semi-arid dryland systems. It should be noted, that a comparison of SOC-stocks is limited due to different measurement techniques used and variable soil depth that were sampled.

Study	Region	Ecosystem	Mean annual precipitation [mm]	Reference Depth [cm]	SOC Stock [kg C m^{-2}]
Denef et al. (2008)	Central Great Plains, Nebraska	Grassland	375	0-75	9.4
Denef et al. (2008)	Central Great Plains, Colorado	Grassland	570	0-75	5.4
Li et al. (2015)	Central Asia	Desert steppe	Not specified	0-100	4.1
Li et al. (2015)	Central Asia	Mountain steppe	Not specified	0-100	17.0
Manaye et al. (2019)	Endamekoni, Ethiopia	Dry forest	703	0-15	2.1-3
(Román-Sánchez et al. (2018)	Cordoba, Spain	Savannah	582	0-30	4.4
Wang et al. (2018)	New South Wales, Australia	Grassland and woodland	379	0-30	2.8
Yusuf et al. (2015)	Borana, Ethiopia	Rangeland	550	0-20	2.9
This study	Karoo, South Africa	Rangeland	500	0-10	11.6

5.2.2 HOW CAN REMOTE SENSING PRODUCTS REPRESENT THE HETEROGENEITY OF SOIL DEGRADATION IN DRYLANDS ACCURATELY?

One objective of the presented PhD-research aimed at developing a remote sensing approach for detecting and evaluating spatial soil patterns in a heterogeneous environment to improve the quality of soil maps (Chapter 4). Mapping of vegetation and soil degradation is challenging, which has led to the omission of their impacts from many global soil maps. The relevance of adequate soil information, e.g. for local soil management and the assessment of global biogeochemical cycles, underlines the need for closing this data gap. In this study, the underlying assumption was that vegetation cover can be used as a proxy for the soils' health status. Vegetation is commonly thought to be a significant controlling mechanism of land degradation in semi-arid environments (Dougill et al., 1998; Maestre and Cortina, 2002; Wainwright, 2009). Vegetation cover influences soil erosion rates significantly (Gyssels et al., 2005; Morgan, 2005), as plants intercept raindrops, enhance infiltration, and add additional surface roughness and organic components to the soil (Morgan, 2005). The results presented

in chapter 3 and 4 of the thesis show that UAV imagery provides a sufficient resolution to detect soil degradation patterns that are not detectable from satellite imagery and could only be mapped in the field with a significant effort. Major vegetation and degradation patterns from the conventional field mapping can be recognised on the orthophoto (Chapter 2, 4), and spatial patterns coincide with the classification of the soil samples from the field map. The orthophoto resolution is sufficient to identify small shrubs, grazed grasses, or even stones (< 10cm), although a differentiation between stones and grazed grasses with the supervised SVM classification was not possible due to the very similar RGB colour spectrum. Severely eroded areas, as important indicators for soil degradation are easily identifiable on orthomosaics due to the absence or reduced vegetation cover (Chapter 2, 3, 4). Transitional areas between severely degraded and vegetated areas are more difficult to assess, since they have higher vegetation coverage than badlands. Nevertheless, they are equally important because they also act as sediment source areas and could potentially develop into badlands over time. Apart from the absence of vegetation, terrain ruggedness turned out to be a good indicator for soil degradation (Chapter 4). This is plausible because the topography is both, captured by the UAV imagery, but also promotes flow concentration, promotes rill formation and consequently leads to higher sediment yields (Helming et al., 1998; Römkens et al., 2002). In addition to the major degradation features like erosion rills or badlands, the study area is characterised by a mosaic of small-scale sediment source and sink areas. However, it is not possible to identify the extent of denudation from UAV imagery without field knowledge. Small-scale degradation features, like shrubs on mounds are not identifiable because the view on the soil surface is shaded by plants. Concluding, digital mapping from UAV imagery can represent the landscapes' heterogeneity but most likely underestimates the area affected by soil degradation. This can be attributed to small-scale heterogeneity of land cover, a difficult distinction between bare soil ground cover and fading green tussock grasses, and shrubs inhibiting a clear view of the ground and its actual condition.

Besides the spatial extent of soil degradation, a volumetric quantification is important in order to assess sediment yields, but also for land management and evaluating restoration needs and activities. The high-resolution DEM derived from the UAV imagery enables a volume estimation of the badlands as sediment sources. Sediment sink bodies, such as silted-up reservoirs can be detected and estimated in their spatial extents but their sediment volumes are only rough estimates based on the potential reservoir shape and depth (Chapter 3). An accurate quantification of sediment sinks is only possible when images from the past are available for comparison.

5.3 GENERAL CONLUSIONS AND IMPLICATIONS FOR DRYLANDS

This PhD thesis aimed (i) to document the spatial heterogeneity of soils in a semi-arid rangeland and (ii) to develop a method for mapping and quantifying soil degradation using commercially available UAVs. The results of the landscape investigation show that the spatial variability of vegetation cover and soil characteristics is much higher than so far reflected by available soil data. Soil property patterns do not coincide with the vegetation cover, but show a high heterogeneity for soil nutrients and SOC. The implemented GIS-based UAV imagery analysis enabled the identification of soil degradation with similar accuracy than conventional field mapping. This illustrates that even conventional UAVs, capturing only the visible spectrum, offer a low-cost, fast, and comprehensive method to support land management and environmental sciences. High-resolution topographic information derived from a DEM, generated from UAV data, improved the degradation mapping greatly and enabled the estimation of badland erosion volumes. The limitations in distinguishing different degrees of degradation, illustrate that a combination with multispectral data could further reduce the uncertainties in degradation classification.

The lack of globally consistent information on the extent of soil degradation is a major challenge in assessing the current global C cycle and projecting future changes. Drylands have a significant potential for C sequestration due to their large spatial extent and their unsaturated C content (FAO, 2004). But SOC stocks and patterns are highly sensitive to climate change, as they are related to vegetation density and distribution. Especially silted-up dryland reservoirs should not be neglected as an important C storage, considering the wide distribution of dams and their reduced potential for leaching dissolved C compared to wet soils or regularly irrigated soils as a lack of limited water (Glenn et al., 1993). In addition, adequate management interventions that enhance plant production and slow down or reverse degradation processes in drylands will have positive effects on food security, biodiversity conservation and economic growth, particularly considering their vulnerability to increased climate change pressure. The heterogeneous pattern of dryland soil properties highlights the need for more knowledge on their properties, formation, patchiness, and role in soil-atmosphere interaction, as well as on effective simulation into global biogeochemical models. Local information gathered from UAV imagery can be used to upscale results from field mapping. As UAV imagery serves as a raw data for producing high-resolution DEMs, linkages between small-scale topography and soil characteristics can be determined. Thereby, the gap of missing soil degradation information on conventional soil maps is bridged and the uncertainty in rangeland soil and vegetation health assessment can be reduced.

5.4 OUTLOOK

Soil degradation is not induced by a single trigger, but a complex interaction of climate, land use and soil characteristics. Only when the spatial and temporal variations of these parameters can be linked to remote sensing products an explicit prediction of soil degradation is possible. This PhD research showed that UAV imagery serves as raw information for producing high-resolution DEMs and vegetation maps. The approaches developed in this study can now be combined with known spatial covariances within a landscape leading to soil degradation aimed at improving maps that reflect the actual soil condition at catchment scales.

The GIS-based UAV imagery analysis developed in this PhD project delivers a method that is low-cost, fast, comprehensive, and scale-invariant. Nevertheless, assessing the small-scale spatial heterogeneity has limitations, especially regarding low contrasts between vegetation and bare ground. Hence, future studies should include multispectral data to improve the classification. The study was conducted within a rather small study area with a limited amount of field samples. Although the study site is representative for the Sneeuberg region, comparison with other catchments in the area could validate the findings and provide better insights into the biogeochemical cycles in the Karoo rangelands.

Soil analysis in the depositional area was only based on samples from one particular depth (50 cm). More detailed soil analyses at various depths are required to assess the formation of anthropogenic soils in silted-up reservoirs and their relevance in biogeochemical cycles. Soil respiration measurements could give a first insight into biogeochemical activities of the deposited sediments.

Compared to conventional field mapping, the UAV-based degradation assessment approach is objective, repeatable, and systematic. For an extensive application, upscaling from local to regional scale while conserving as much small-scale information as possible is not only valuable for land management, but also to analyse temporal variations. By combining UAV imagery with satellite data an enormous amount of additional information becomes available that enables repeatable and systematic analysis on the spatial and temporal variability. With on-going technological and computational developments, such combined UAV-satellite remote sensing products will be crucial components for land cover change modelling. The next key area of research required for their development is the identification of explicitly defined local information in UAV and satellite imagery, in particular the upscaling between the two remote sensing systems.

5.5 REFERENCES

Andela, N., Liu, Y.Y., Van Dijk, A., De Jeu, R.A.M., McVicar, T.R., 2013. Global changes in dryland vegetation dynamics (1988–2008) assessed by satellite remote sensing: combining a new passive microwave vegetation density record with reflective greenness data. Biogeosci Discuss 10, 8749–8797.

Bai, Z.G., Dent, D.L., Olsson, L., Schaepman, M.E., 2008a. Proxy global assessment of land degradation. Soil Use Manag. 24, 223–234. https://doi.org/10.1111/j.1475-2743.2008.00169.x

Bai, Z.G., Dent, D.L., Olsson, L., Schaepman, M.E., 2008b. Global assessment of land degradation and improvement. 1. Identification by remote sensing. (No. Report 2008/1). ISRIC, Wageningen.

Bautista, S., Mayor, Á.G., Bourakhouadar, J., Bellot, J., 2007. Plant Spatial Pattern Predicts Hillslope Runoff and Erosion in a Semiarid Mediterranean Landscape. Ecosystems 10, 987–998. https://doi.org/10.1007/s10021-007-9074-3

Boardman, J., Foster, I.D.L., 2011. The potential significance of the breaching of small farm dams in the Sneeuberg region, South Africa. J. Soils Sediments 11, 1456–1465. https://doi.org/10.1007/s11368-011-0425-5

Bochet, E., Poesen, J., Rubio, J.L., 2006. Runoff and soil loss under individual plants of a semi-arid Mediterranean shrubland: influence of plant morphology and rainfall intensity. Earth Surf. Process. Landf. 31, 536–549. https://doi.org/10.1002/esp.1351

Bochet, E., Poesen, J., Rubio, J.L., 2000. Mound development as an interaction of individual plants with soil, water erosion and sedimentation processes on slopes. Earth Surf. Process. Landf. 25, 847–867. https://doi.org/10.1002/1096-9837(200008)25:8<847::AID-ESP103>3.0.CO;2-Q

Borken, W., Matzner, E., 2009. Reappraisal of drying and wetting effects on C and N mineralization and fluxes in soils. Glob. Change Biol. 15, 808–824. https://doi.org/10.1111/j.1365-2486.2008.01681.x

Cammeraat, L.H., Imeson, A.C., 1999. The evolution and significance of soil–vegetation patterns following land abandonment and fire in Spain. CATENA 37, 107–127. https://doi.org/10.1016/S0341-8162(98)00072-1

Denef, K., Stewart, C.E., Brenner, J., Paustian, K., 2008. Does long-term center-pivot irrigation increase soil carbon stocks in semi-arid agro-ecosystems? Geoderma 145, 121–129. https://doi.org/10.1016/j.geoderma.2008.03.002

Dickie, J.A., Parsons, A.J., 2012. Eco-geomorphological processes within grasslands, shrublands and badlans in the semi-arid Karro, South Africa. Land Degrad. Dev. 23, 534–547. https://doi.org/10.1002/ldr.2170

Doetterl, S., Six, J., Van Wesemael, B., Van Oost, K., 2012. Carbon cycling in eroding landscapes: geomorphic controls on soil organic C pool composition and C stabilization. Glob. Change Biol. 18, 2218–2232.

Dougill, A.J., Heathwaite, A.L., Thomas, D.S.G., 1998. Soil water movement and nutrient cycling in semi-arid rangeland: vegetation change and system resilience. Hydrol. Process. 12, 443–459. https://doi.org/10.1002/(SICI)1099-1085(19980315)12:3<443::AID-HYP582>3.3.CO;2-E

Esler, K.J., Milton, S.J., Dean, W.R.J. (Eds.), 2006. Karoo veld ecology and management, 1st ed. ed. Briza, Pretoria, South Africa.

FAO (Ed.), 2004. Carbon sequestration in dryland soils, World soil resources reports. FAO, Rome.

Gabet, E.J., Dunne, T., 2003. Sediment detachment by rain power: SEDIMENT DETACHMENT BY RAIN POWER. Water Resour. Res. 39, ESG 1-1-ESG 1-12. https://doi.org/10.1029/2001WR000656

Gerrard, A.J., 1981. Soils and landforms : an integration of geomorphology and pedology. G. Allen and Unwin, London.

Gessler, P.E., Chadwick, O.A., Chamran, F., Althouse, L., Holmes, K., 2000. Modeling Soil–Landscape and Ecosystem Properties Using Terrain Attributes. Soil Sci. Soc. Am. J. 64, 2046–2056. https://doi.org/10.2136/sssaj2000.6462046x

Glenn, E., Squires, V., Olsen, M., Frye, R., 1993. Potential for carbon sequestration in the drylands. Water. Air. Soil Pollut. 70, 341–355. https://doi.org/10.1007/BF01105006

Gomez, C., Viscarra Rossel, R.A., McBratney, A.B., 2008. Soil organic carbon prediction by hyperspectral remote sensing and field vis-NIR spectroscopy: An Australian case study. Geoderma 146, 403–411. https://doi.org/10.1016/j.geoderma.2008.06.011

Greene, R.S.B., Kinnell, P.I.A., Wood, J.T., 1994. Role of plant cover and stock trampling on runoff and soil-erosion from semi-arid wooded rangelands. Soil Res. 32, 953–973. https://doi.org/10.1071/sr9940953

Guo, L., Zhang, H., Shi, T., Chen, Y., Jiang, Q., Linderman, M., 2019. Prediction of soil organic carbon stock by laboratory spectral data and airborne hyperspectral images. Geoderma 337, 32–41. https://doi.org/10.1016/j.geoderma.2018.09.003

Gyssels, G., Poesen, J., Bochet, E., Li, Y., 2005. Impact of plant roots on the resistance of soils to erosion by water: a review. Prog. Phys. Geogr. Earth Environ. 29, 189–217. https://doi.org/10.1191/0309133305pp443ra

Harden, J.W., Sharpe, J.M., Parton, W.J., Ojima, D.S., Fries, T.L., Huntington, T.G., Dabney, S.M., 1999. Dynamic replacement and loss of soil carbon on eroding cropland. Glob. Biogeochem. Cycles 13, 885–901. https://doi.org/10.1029/1999GB900061

Helming, K., Römkens, M.J.M., Prasad, S.N., 1998. Surface Roughness Related Processes of Runoff and Soil Loss: A Flume Study. Soil Sci. Soc. Am. J. 62, 243–250. https://doi.org/10.2136/sssaj1998.03615995006200010031x

Hengl, T., Heuvelink, G.B.M., Stein, A., 2004. A generic framework for spatial prediction of soil variables based on regression-kriging. Geoderma 120, 75–93. https://doi.org/10.1016/j.geoderma.2003.08.018

Herbst, M., Diekkrüger, B., Vereecken, H., 2006. Geostatistical co-regionalization of soil hydraulic properties in a micro-scale catchment using terrain attributes. Geoderma 132, 206–221. https://doi.org/10.1016/j.geoderma.2005.05.008

Jenny, H., 1941. Factors of soil formation: a system of quantitative pedology. McGraw Hill, New York.

Keay-Bright, J., Boardman, J., 2006. Changes in the distribution of degraded land over time in the central Karoo, South Africa. Catena 67, 1–14. https://doi.org/10.1016/j.catena.2005.12.003

Krenz, J., Greenwood, P., Kuhn, N.J., 2019. Soil Degradation Mapping in Drylands Using Unmanned Aerial Vehicle (UAV) Data. Soil Syst. 3, 33. https://doi.org/10.3390/soilsystems3020033

Krug, C.B., 2004. Practical Guidelines for the Restoration of Renosterveld. University of Stellenbosch, Stellenbosch.

Kuhn, N.J., Armstrong, E.K., Ling, A.C., Connolly, K.L., Heckrath, G., 2012. Interrill erosion of carbon and phosphorus from conventionally and organically farmed Devon silt soils. CATENA, Experiments in Earth surface process research 91, 94–103. https://doi.org/10.1016/j.catena.2010.10.002

Land Degradation Assessment in Drylands. Manual for local level assessment of land degradation and sustainable land management, Part 2: Field methodology and tools, 2011. . FAO, Rome.

Li, C., Zhang, C., Luo, G., Chen, X., Maisupova, B., Madaminov, A.A., Han, Q., Djenbaev, B.M., 2015. Carbon stock and its responses to climate change in Central Asia. Glob. Change Biol. 21, 1951–1967. https://doi.org/10.1111/gcb.12846

Lü, Y., Sun, R., Fu, B., Wang, Y., 2012. Carbon retention by check dams: Regional scale estimation. Ecol. Eng. 44, 139–146. https://doi.org/10.1016/j.ecoleng.2012.03.020

Ludwig, J., Tongway, D., 1995. Spatial-Organization of Landscapes and Its Function in Semiarid Woodlands, Australia. Landsc. Ecol. 10, 51–63. https://doi.org/10.1007/BF00158553

Maestre, F.T., Cortina, J., 2002. Spatial patterns of surface soil properties and vegetation in a Mediterranean semi-arid steppe. Plant Soil 241, 279–291. https://doi.org/10.1023/A:1016172308462

Manaye, A., Negash, M., Alebachew, M., 2019. Effect of degraded land rehabilitation on carbon stocks and biodiversity in semi-arid region of Northern Ethiopia. For. Sci. Technol. 15, 70–79. https://doi.org/10.1080/21580103.2019.1592787

Meadows, M.E., Watkeys, M.K., 1999. Palaeoenvironments, in: Dean, W.R.J., Milton, S.J. (Eds.), The Karoo: Ecological Patterns and Processes. Cambridge University Press, Cambridge, pp. 27–41.

Minasny, B., McBratney, A.B., 2007. Spatial prediction of soil properties using EBLUP with the Matérn covariance function. Geoderma, Part of speciel issue: Pedometrics 2005, 140, 324–336. https://doi.org/10.1016/j.geoderma.2007.04.028

Mora-Vallejo, A., Claessens, L., Stoorvogel, J., Heuvelink, G.B.M., 2008. Small scale digital soil mapping in Southeastern Kenya. CATENA 76, 44–53. https://doi.org/10.1016/j.catena.2008.09.008

Morgan, R.P.C., 2005. Soil erosion and conservation, 3rd ed. ed. Blackwell Publishing, Malden, MA, USA.

Oldeman, L.R., 1988. Guidelines for general assessment of the status of human-induced soil degradation, Working Paper. ISRIC, Wageningen.

Petri, M., Biancalani, R., Lindeque, I., 2019. Guidelines for the national assessment and mapping of land degradation and conservation. FAO, Rome.

Pickup, G., Chewings, V.H., 1994. A grazing gradient approach to land degradation assessment in arid areas from remotely-sensed data. Int. J. Remote Sens. 15, 597–617. https://doi.org/10.1080/01431169408954099

Puigdefábregas, J., 2005. The role of vegetation patterns in structuring runoff and sediment fluxes in drylands: Vegetation and sediment fluxes. Earth Surf. Process. Landf. 30, 133–147. https://doi.org/10.1002/esp.1181

Reinwarth, B., Miller, J.K., Glotzbach, C., Rowntree, K.M., Baade, J., 2017. Applying regularized logistic regression (RLR) for the discrimination of sediment facies in reservoirs based on composite fingerprints. J. Soils Sediments 17, 1777–1795. https://doi.org/10.1007/s11368-016-1627-7

Román-Sánchez, A., Vanwalleghem, T., Peña, A., Laguna, A., Giráldez, J.V., 2018. Controls on soil carbon storage from topography and vegetation in a rocky, semi-arid landscapes. Geoderma 311, 159–166. https://doi.org/10.1016/j.geoderma.2016.10.013

Römkens, M.J.M., Helming, K., Prasad, S.N., 2002. Soil erosion under different rainfall intensities, surface roughness, and soil water regimes. CATENA 46, 103–123. https://doi.org/10.1016/S0341-8162(01)00161-8

Rostagno, C.M., del Valle, H.F., 1988. Mounds associated with shrubs in aridic soils of northeastern Patagonia: Characteristics and probable genesis. CATENA 15, 347–359. https://doi.org/10.1016/0341-8162(88)90056-2

Sauer, T., Ries, J.B., 2008. Vegetation cover and geomorphodynamics on abandoned fields in the Central Ebro Basin (Spain). Geomorphology, Dryland geomorphology and interacting processes 102, 267–277. https://doi.org/10.1016/j.geomorph.2008.05.006

Schlesinger, W.H., Raikes, J.A., Hartley, A.E., Cross, A.F., 1996. On the Spatial Pattern of Soil Nutrients in Desert Ecosystems. Ecology 77, 364–374. https://doi.org/10.2307/2265615

Schmidt, H., Karnieli, A., 2000. Remote sensing of the seasonal variability of vegetation in a semi-arid environment. J. Arid Environ. 45, 43–59. https://doi.org/10.1006/jare.1999.0607

Smith, P., 2008. Land use change and soil organic carbon dynamics. Nutr. Cycl. Agroecosystems 81, 169–178. https://doi.org/10.1007/s10705-007-9138-y

Snyman, H.A., du Preez, C.C., 2005. Rangeland degradation in a semi-arid South Africa—II: influence on soil quality. J. Arid Environ. 60, 483–507. https://doi.org/10.1016/j.jaridenv.2004.06.005

Stocking, M.A., Murnaghan, N. (Eds.), 2013. A Handbook for the Field Assessment of Land Degradation. Routledge, London.

Sumfleth, K., Duttmann, R., 2008. Prediction of soil property distribution in paddy soil landscapes using terrain data and satellite information as indicators. Ecol. Indic. 8, 485–501. https://doi.org/10.1016/j.ecolind.2007.05.005

Terra, J.A., Shaw, J.N., Reeves, D.W., Raper, R.L., Van Santen, E., Mask, P.L., 2004. Soil carbon relationships with terrain attributes, electrical conductivity, and a soil survey in a coastal plain landscape. Soil Sci. 169, 819–831.

Tian, F., Brandt, M., Liu, Y.Y., Verger, A., Tagesson, T., Diouf, A.A., Rasmussen, K., Mbow, C., Wang, Y., Fensholt, R., 2016. Remote sensing of vegetation dynamics in drylands: Evaluating vegetation optical depth (VOD) using AVHRR NDVI and in situ green biomass data over West African Sahel. Remote Sens. Environ. 177, 265–276. https://doi.org/10.1016/j.rse.2016.02.056

Valentin, C., Poesen, J., Li, Y., 2005. Gully erosion: Impacts, factors and control. CATENA, Gully Erosion: A Global Issue 63, 132–153. https://doi.org/10.1016/j.catena.2005.06.001

van Oudenhoven, A.P.E., Veerkamp, C.J., Alkemade, R., Leemans, R., 2015. Effects of different management regimes on soil erosion and surface runoff in semi-arid to sub-humid rangelands. J. Arid Environ. 121, 100–111. https://doi.org/10.1016/j.jaridenv.2015.05.015

Wainwright, J., 2009. Desert Ecogeomorphology, in: Parsons, A.J., Abrahams, A.D. (Eds.), Geomorphology of Desert Environments. Springer Netherlands, Dordrecht, pp. 21–66.

Wang, B., Waters, C., Orgill, S., Gray, J., Cowie, A., Clark, A., Liu, D.L., 2018. High resolution mapping of soil organic carbon stocks using remote sensing variables in the semi-arid rangelands of eastern Australia. Sci. Total Environ. 630, 367–378. https://doi.org/10.1016/j.scitotenv.2018.02.204

Wessels, K.J., Prince, S.D., Reshef, I., 2008. Mapping land degradation by comparison of vegetation production to spatially derived estimates of potential production. J. Arid Environ. 72, 1940–1949. https://doi.org/10.1016/j.jaridenv.2008.05.011

Xiang-zhou, X., Hong-wu, Z., Ouyang, Z., 2004. Development of check-dam systems in gullies on the Loess Plateau, China. Environ. Sci. Policy 7, 79–86. https://doi.org/10.1016/j.envsci.2003.12.002

Yusuf, H.M., Treydte, A.C., Sauerborn, J., 2015. Managing Semi-Arid Rangelands for Carbon Storage: Grazing and Woody Encroachment Effects on Soil Carbon and Nitrogen. PLoS ONE 10. https://doi.org/10.1371/journal.pone.0109063

Zhang, H., Liu, S., Yuan, W., Dong, W., Xia, J., Cao, Y., Jia, Y., 2016. Loess Plateau check dams can potentially sequester eroded soil organic carbon: Check Dams Increase Land Carbon Sink. J. Geophys. Res. Biogeosciences 121, 1449–1455. https://doi.org/10.1002/2016JG003348

Zhao, P., Shao, M., Melegy, A.A., 2010. Soil Water Distribution and Movement in Layered Soils of a Dam Farmland. Water Resour. Manag. 24, 3871–3883. https://doi.org/10.1007/s11269-010-9638-4

ACKNOWLEDGEMENTS

Working on this research topic has been challenging, rewarding, adventurous, difficult, enjoyable, and everything in between. There are many people I would like to thank, and who supported me on this journey.

First, I would like to thank Prof Dr. Nikolaus Kuhn, for giving me the chance to work on this complex topic and to discover a new research area, to develop myself and improve my research skills. My passion for South Africa started during my studies abroad in 2010. It was love at first sight and I am glad you gave me the opportunity to return and to conduct research in the beautiful Karoo. Finally, you did not make a wrong choice when you "hooked me up" with my flatmates.

I would also like to give my thanks to other colleagues for sharing your knowledge, perpetual support during field or lab work, fabulous mechanical skills, expanding my English dialect vocabulary, critical and stimulating discussions, organisational and administrational help, and many delicious cakes: Brigitte, Christoph, Claudia, Delia, Goswin, Hans-Rudi, Heike, Heleen, Lena, Lukas, Martina, Matthias, Phil, Robert, Rosi, Ruth, Sandra, Vincent, Wolfgang, and Yaxian. Not to forget about all the students that helped me during field work or entertained me during long office hours, in particular: Anouk, Christian, Gabriel, Marius, and Patrice.

I am lucky enough to have met colleagues who have become friends now. I would like to thank my former flatmates and PhD-buddies Brice and Vlad. You thrillseekers always took good care of my nutrition; being it Brice constantly providing organic vegetables or Vlad making the best salad sauce and delicious curries inspired by Kiran. In return, you never declined any desserts that I prepared, even in times of abundance when we had courgette ice cream. Thanks to the first floor Ex-Biogeography gang: Bibi, Chris, and Simon. You welcomed me so heart-warmingly and we spent innumerable nights at the Rhine or in your favourite bar, although I always declined your beer offers.

Lena, I am so grateful that you joined our first Karoo expedition and shared an office with me later, where we encouraged each other and always looked for the creative approach to master our tasks. There was no better office mate than you and I am happy to say that our friendship goes far beyond office walls.

During my doctoral studies I had the opportunity to visit several summer schools and conferences. Besides sharing research ideas, I was blessed to meet soul mates. Hulapalu and thank you Crazy Boys for all the fruitful and humorous discussions: Aayush, Chrystiann, Daniel and Thomas.

Dear EnvEuro gang, when I started my master studies, I could not imagine how many inspiring people I will meet. Spatially, we are far apart now but our hearts and minds will always be bound up together. I am looking forward to our upcoming IPCC meeting and the next adventures in the woods of Austria, Bulgaria, Germany, Hungary, Spain, Sweden, and Switzerland or wherever we drift next. Magdakeba, my best travel and hiking buddy: Panda mlima!

I feel deeply indebted to my wonderful friends from home who supported me regardless of me moving places and countries over and over again. I am happy for the few hours of fun we spent together more or less regularly, for your visits and our friendship: Arne, Ken, Mandy, Robert, Steffi, and Tabea. I hope I can further feed you with interesting travel destinations. Thank you Johann for all your support and achieving the impossible in the kitchen, on the bike or by foot, who cares?!

I would like to thank my mum who always believed in me and my skills. You, sparked my interest in science, raised me as a person who is not afraid of any challenge and always supported me along the way. Thank you!

Finally, thank you apostle Petrus, that you gave us a cold, cloudy, and rainy spring that did not distract me too much from writing my thesis in the final stage and protected me from working in sauna office. Now, turn the summer on.